THE UNIVERSITY OF ASTON IN BIRMINGHAM

STUDIES OF THE SHELLSIDE PERFORMANCE OF SHELL-AND-TUBE HEAT EXCHANGERS

A thesis submitted for the degree of

Doctor of Philosophy

by

Martin James Noel Wills

1984

THE UNIVERSITY OF ASTON IN BIRMINGHAM

STUDIES OF THE SHELLSIDE PERFORMANCE OF SHELL-AND-TUBE HEAT EXCHANGERS

A thesis submitted for the degree of

Doctor of Philosophy

by

Martin James Noel Wills

1984

Summary

Accurate prediction of shellside pressure drop in a baffled shell-and-tube heat exchanger is very difficult because of the complicated shellside geometry. Ideally, all the shellside fluid should be alternately deflected across the tube bundle as it traverses from inlet to outlet. In practice, up to 60% of the shellside fluid may bypass the tube bundle or leak through the baffles. This short-circuiting of the main flow reduces the efficiency of the exchanger.

Of the various shellside methods, it is shown that only the multi-stream methods, which attempt to obtain the shellside flow distribution, predict the pressure drop with any degree of accuracy, the various predictions ranging from -30% to +70%, generally overpredicting.

It is shown that the inaccuracies are mainly due to the manner in which baffle leakage is modelled. The present multi-stream methods do not allow for interactions of the various flowstreams, and yet is is shown that three main effects are identified, a) there is a strong interaction between the main crossflow and the baffle leakage streams, enhancing the crossflow pressure drop, b) there is a further short-circuit not considered previously i.e. leakage in the window, and c) the crossflow does not penetrate as far, on average, as previously supposed.

Models are developed for each of these three effects, along with a new windowflow pressure drop model, and it is shown that the effect of baffle leakage in the window is the most significant. These models developed to allow for various interactions, lead to an improved multi-stream method, named the **"STREAM-INTERACTION"** method. The overall method is shown to be consistently more accurate than previous methods, with virtually all the available shellside data being predicted to within ±30% and over 60% being within ±20%. The method is, thus, strongly recommended for use as a design method.

KEY WORDS: Heat Exchanger, Shellside, Pressure Drop,

AUTHOR

The author graduated from the University of Aston in Birmingham in 1979 with an honours degree in Chemical Engineering.

The author was subsequently employed by the University of Aston in Birmingham as a Research Assistant until the end of 1982, and did the research leading to this thesis, at U.K.A.E.A. Harwell for the Heat Transfer and Fluid Flow Service (H.T.F.S.). The author now has a position at U.K.A.E.A. Harwell, working for H.T.F.S., and is actively engaged on research and development of computer programs and design methods for shell-and-tube heat exchangers, using much of the valuable knowledge gained in this work.

ACKNOWLEDGEMENTS

I would like to express my gratitude to:

My dear wife, Jean, who spent many hours typing this thesis,

The Heat Transfer and Fluid Flow Service for funding this work,

Dr B. Gay and Dr J. Jenkins for their supervision,

and finally, I would like to especially thank

Mr D. Johnston of AERE Harwell for his many hours of useful discussions which undoubtedly led to many of the ideas in this work.

CONTENTS

Page

LIST OF TABLES

Page

LIST OF FIGURES

1.0 INTRODUCTION

This chapter describes a shell-and-tube heat exchanger. It outlines the shellside flow distribution and associated problems with predicting the flow distribution and pressure drop. The effect of baffles are especially considered, and they are singled out as the most important aspect of the exchanger geometry to influence the shellside flow distribution and pressure drop.

1.1 Shell-and-Tube Heat Exchangers

Heat transfer between process streams is a common requirement in many industrial plants as heat is an expensive commodity and it is desirable to recover/use as much heat as is economically feasible.

The most common form of equipment to perform this process is a shell-and-tube heat exchanger which consists of an array of tubes (the bundle) enclosed by a cylindrical case (the shell). One process stream flows through the tubes and the other flows in the space around the tubes enclosed by the shell (Figure 1.1.). Heat is transferred through the walls of the tubes as the process streams flow from inlet to outlet.

FIGURE 1.1 : A SHELL-AND-TUBE HEAT EXCHANGER

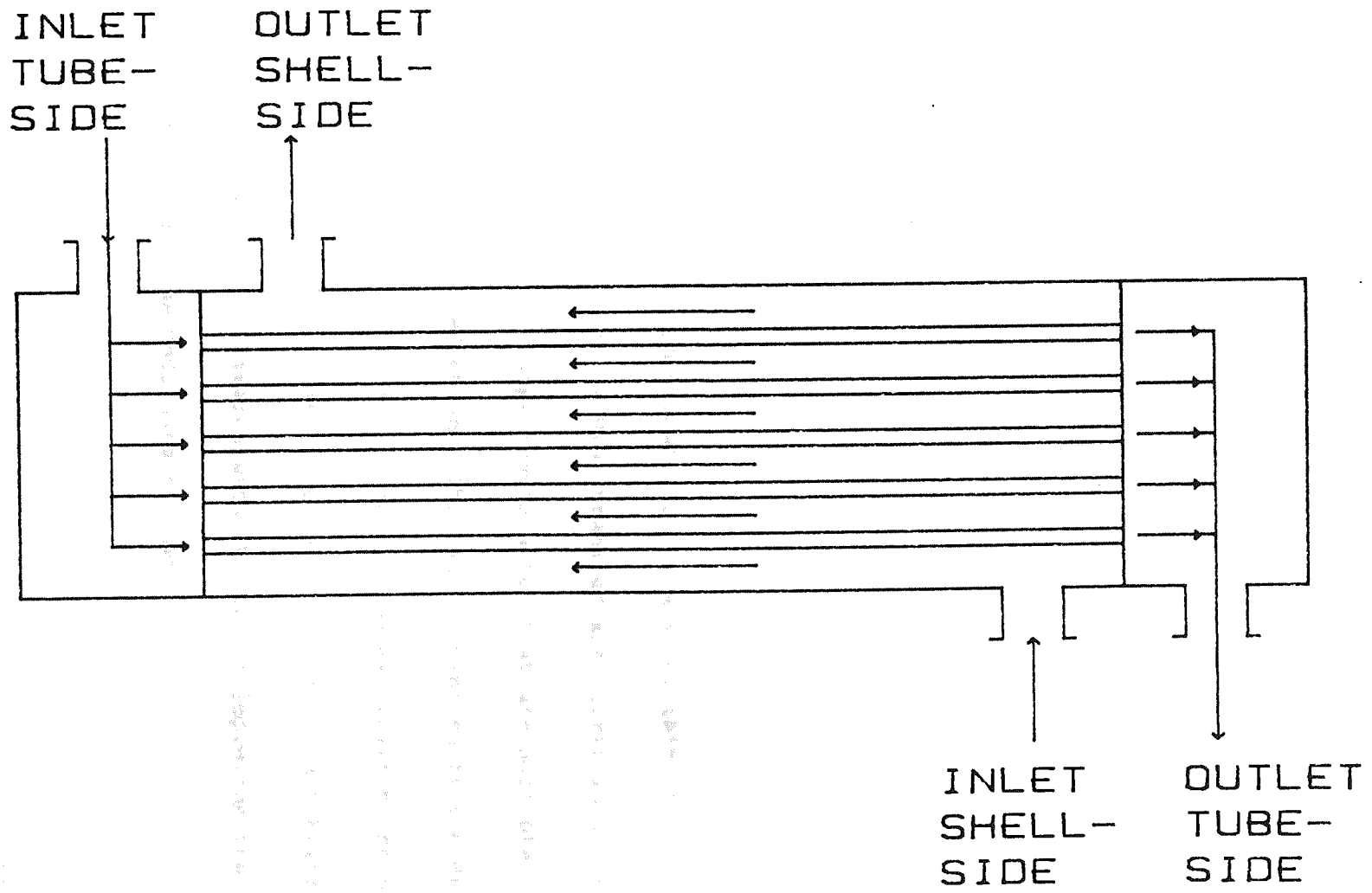

The mechanics of tubeside flow are relatively well understood and deisgners may refer to standard texts e.g. Rosenhow and Hartnett (1973), Perry and Chilton (1963), Coulson and Richardson (1970), Kern (1950), to name a few. However, this is not so for shellside flow where the mechanics are only understood in a limited manner and so any investigation into shell-and-tube heat exchangers must necessarily consider shellside flow in as much detail as possible.

At the outset of this investigation it is realised that shellside pressure drop is much more sensitive to flow distribution than the heat transfer since pressure drop is proportional to flowrate squared a pproximately whereas heat transfer is only proportional to flowrate to the 0.6 power approximately. Because of this, the prediction methods for shellside heat transfer are fairly good, or at least, do not suffer the large inaccuracies that are possible in shellside pressure drop prediction. This was recognised by the Heat Transfer and Fluid Flow (HTFS) at the Atomic Energy Research Establishment, Harwell, and the National Engineering Laboratory (NEL), East Kilbride, who generously funded this research with the aim of improving the shellside pressure drop methods used by them.

1.2 Shellside Geometry and its Effect on Flow Distribution

The flow distribution on the shellside of an exchanger is very complex and depends on many factors such as

1) tube bundle layout and shell/bundle clearance,

2) number of tubeside passes,

3) baffle cut and baffle pitch, and

4) baffle tolerances.

to name but a few. Many other complications can occur e.g. sealing strips, finned tubes, fouling layers and so on. The shape of an exchanger largely influences the flow distribution and a complete study of all the various factors is practically impossible within the scope of a three year research project. However, certain phenomena can be studied in isloation (and with other effects where possible)in an attempt to build a realistic picture of shellside flow.

It is presupposed here that shellside heat transfer is important in governing the overall heat transfer for the remainder of this thesis and that it is desirable to predict the shellside pressure drop accurately.

FIGURE 1.2 : A BAFFLED SHELL-AND-TUBE EXCHANGER

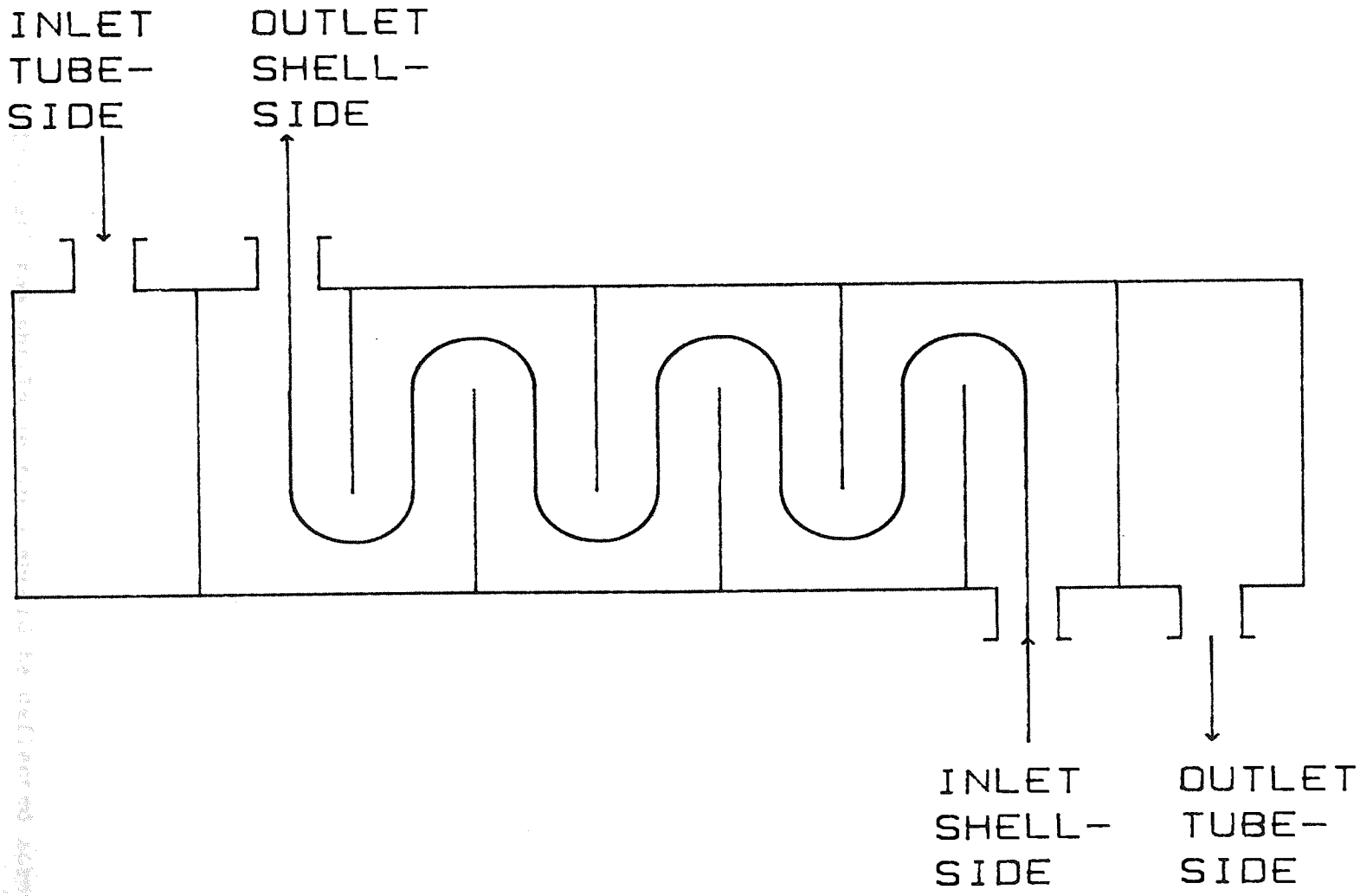

The rate of heat transfer is significantly increased by the introduction of baffles (Figure 1.2) which perform three functions:-

1) They force the shellside fluid to flow across the bundle rather than axially along the tubes, increasing the effective path length.

2) The shellside velocity is increased promoting turbulence and hence heat transfer.

3) They act as tube supports preventing the tubes from vibrating which can lead to tubes fracturing.

The introduction of baffles increases heat transfer but at the expense of increased pressure drop in the exchanger. (If the shellside is not the dominant heat transfer resistance then addition of baffles may only serve to increase the shellside pressure drop with very little gain overall to the heat transfer). Clearly the gain in heat transfer has to be offset against the increase in pressure drop.

Ideally, all the shellside fluid should be deflected across the tube bundle to give the maximum heat transfer.

In reality, this does not happen and only a fraction of the fluid flows in the desired manner. There are two main reasons for this:-

1) Much of the fluid bypasses the bundle altogether and tries to flow in the gap between the bundle and shell which has to exist in order to be able to insert the bundle into the shell. For certain types of heat exchanger duty it is necessary to remove the bundle for cleaning which can lead to very large clearances (over 10 cms in a commercial exchanger) and hence a very large portion of the shellside fluid may flow through this path. This bypassing is often reduced by the introduction of sealing strips which block the gap between the bundle and the shell and force the fluid into the tube bundle (Figure 1.3). There is some doubt about the true effectiveness of these sealing strips. In this present work it is contended that the increase in heat transfer is not offset against the resultant increase in pressure drop unless the strips are placed close enough together to prevent a number of bypass streams being formed in series. If bundle bypassing is a serious problem, then it is believed that one should consider alternative baffle arrangements such as rod baffles (Small (1979)) or even different types of exchangers altogether such as plate heat exchangers.

FIGURE 1.3 : THE USE OF SEALING STRIPS TO BLOCK THE BYPASS LANES

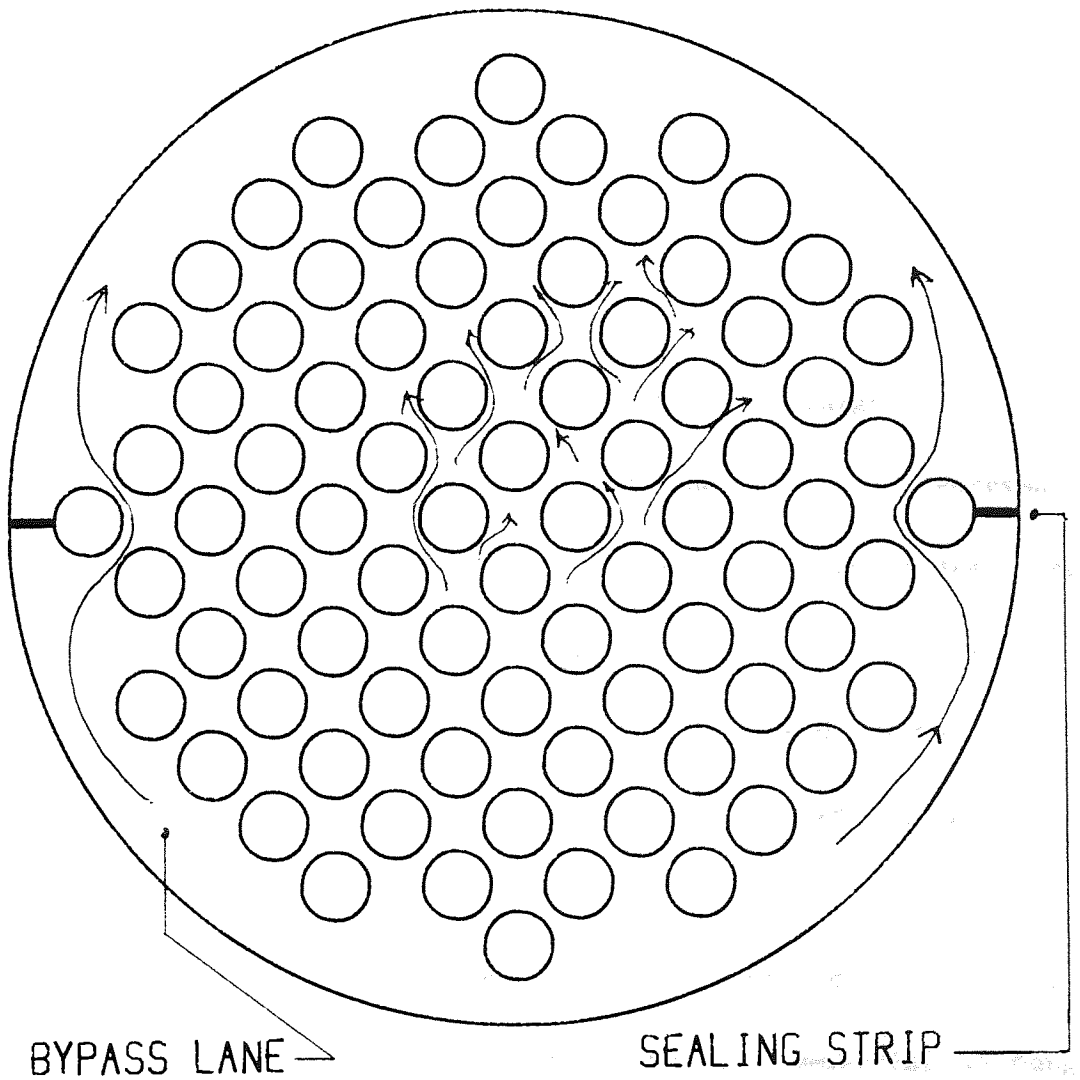

2) There is a necessary tolerance between the baffles and the shell (Figure 1.4) in order to be able to insert the fully assembled bundle into the shell. Similarly there is a necessary tolerance between the tubes and the baffle (Figure 1.5). Shellside fluid can preferentially leak through these tolerances from baffle space to baffle space rather than flowing between the baffles as desired.

The shell-baffle leakage is probably the more serious in the sense that this stream does not directly contact with the tube-bundle and hence can be a serious loss of efficiency. However, it should be realised that although the tube-baffle leakage must be in intimate contact with the tubes, this stream is usually the much larger of the two streams, especially in larger exchangers and hence may still represent a significant loss of efficiency. From the point of view of designing an exchanger certain assumptions are required about the effectiveness of these leakage streams in heat transfer but no attempt is made in this work to study this as it is clearly a subject in its own right.

Bundle bypassing and baffle leakage can represent considerable losses in efficiency of the exchanger. The crossflow in a commercial exchanger may only be 30-60% of the total flow which means an exchanger needs to be considerably larger than is theoretically possible. Again this is offset by the fact that larger exchangers usually have lower pressure drops.

FIGURE 1.4 : SHELL-BAFFLE LEAKAGE

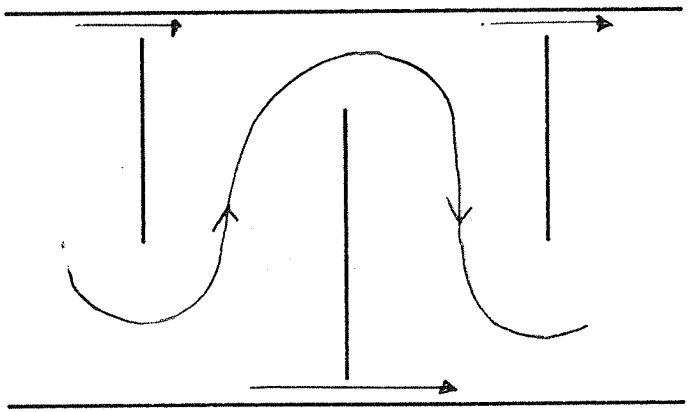

SHELL-
BAFFLE
LEAKAGE

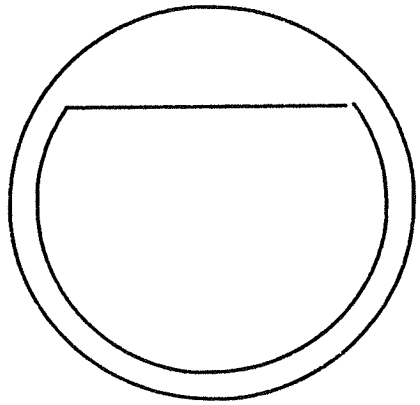

SHELL-
BAFFLE
TOLERANCE

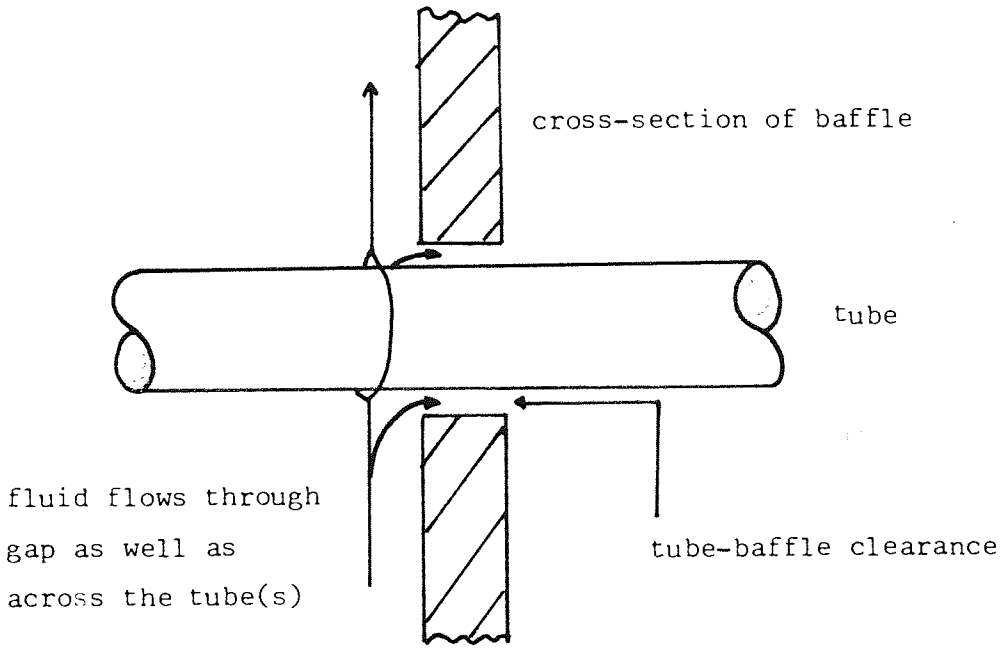

Figure 1.5 : TUBE-BAFFLE LEAKAGE

An excellent diagram showing the major flowpaths in an exchanger is given by Tinker (1951) in Figure 1.6.

There are additional complications which may occur and some are briefly described below:-

1) Fouling can block baffle leakage paths causing the pressure drop to rise sharply and the heat transfer to be reduced markedly.

2) There is a possibility of internal bypass lanes caused by multiple tube pass arrangements which are often used to increase the tubeside heat transfer coefficient.

3) Sometimes exchangers are designed with no tubes in the window region to prevent tubes having too long an unsupported length which could give rise to vibration problems.

4) The shellside pressure drop may be so limited to make it necessary to consider other baffle types than the standard 'single-segmental' baffles which are most often used e.g. 'double-segmental' baffles (Figure 1.7).

FIGURE 1.6 : THE FLOW MODEL OF TINKER

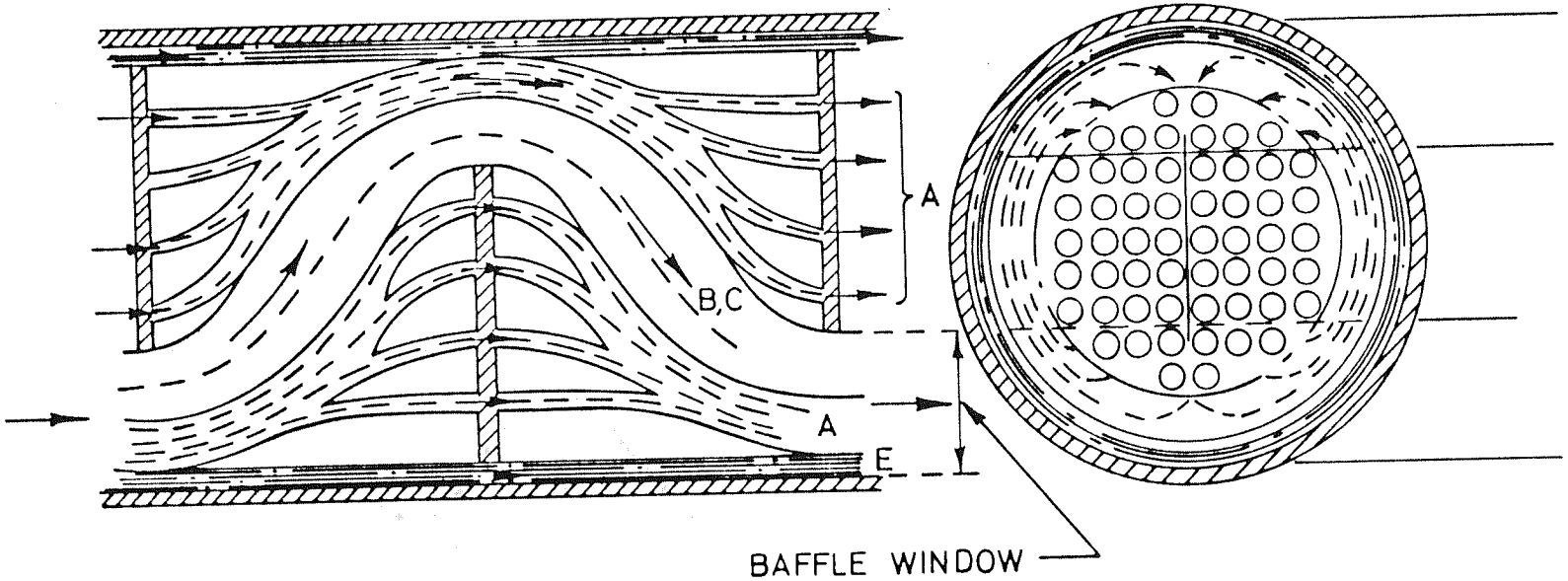

FLOW-STREAMS

A = TUBE/BAFFLE LEAKAGE

B = CROSSFLOW

C = CROSSFLOW BYPASS

E = SHELL/BAFFLE LEAKAGE

FIGURE 1.7 : A BAFFLED SHELL-AND-TUBE EXCHANGER
(DOUBLE SEGMENTAL BAFFLES)

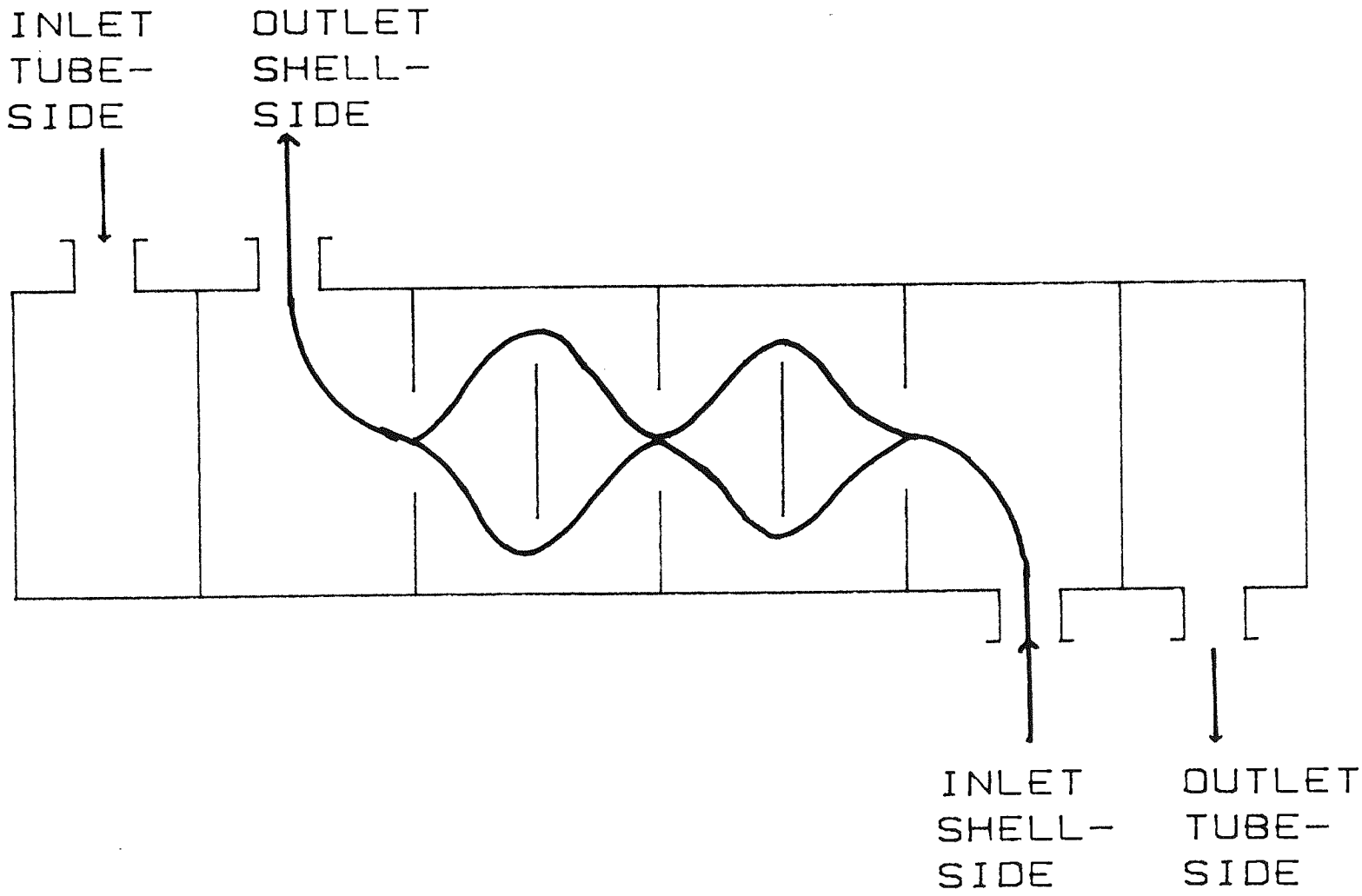

The list is virtually inexhaustive with such effects as nozzle sizes, tube bundle optimum layout, whether to design exchangers in "trains" or "networks". In this work, it was decided to consider the simplest baffled geometry possible which is representative of a commercial exchanger. Furthermore, only single-phase effects are considered (two-phase applications e.g. condensers, add a whole new dimension of uncertainties).

Only clean single-segmental single-phase exchangers with plain tubes and full tube bundles are considered i.e. the "E" shell (T.E.M.A. (1958)). The major variables to be considered stem predominantly from the baffle geometry:-

1) effect of baffle cut,

2) effect of baffle pitch,

3) effect of baffle leakage,

and also

4) effect of bundle bypassing.

1.3 Objective of Thesis

The objective of this thesis is to study the effect of shellside geometry (in particular the baffle geometry) on shellside flow distribution and to develop a reliable prediction method for shellside pressure drop which can be used with confidence by commercial heat exchanger designers.

2.0 REVIEW OF PREVIOUS SHELLSIDE PRESSURE DROP PREDICTION METHODS

In this chapter, the two main types of method for estimating shellside pressure drop are reviewed, outlining their advantages and disadvantages. The review ranging from very simplistic to very complicated methods, shows the influence of computers in the development of shellside methods.

2.1 Model Types In Shellside Pressure Drop Prediction

The calculation of shellside pressure drop has been investigated by a number of researchers and many different methods have been proposed. They fall broadly into two categories

1) single-stream models , and

2) multi-stream models .

Single-stream models treat the shellside flow in an analogous manner to pipe flow and may or may not apply correction factors for the effects of baffle leakage and bundle bypassing.

Multi-stream models calculate the shellside pressure drop by calculating the flow distribution, in an analogous manner to piping network methods.

There is a third type of model which treats the shellside as a porous medium and attempt to solve the Navier-Stokes equations using finite difference/element techniques. This type of model does enable one to predict effects that the first two cannot easily do, but these methods are extremely complicated and require extensive computation. Even with today's high speed computers, the time taken is still impractical especially when the uncertainties in shellside flow are considered. From an engineer's viewpoint only single-stream and multi-stream models are considered, as they enable relatively simple solutions.

2.2 The Development of Shellside Pressure Drop Prediction Methods

The development of shellside pressure drop prediction methods has been largely influenced by the availability of computers. It has been long since recognised that the number of independent variables on the shellside is large, and hence a full analysis of shellside flow is impossible. Consequently early research tended to treat shell-and-tube exchangers as 'black-boxes' and ignored the shellside flow to a large extent although fairly basic attempts were made to correlate some of the more major geometric aspects such as baffle spacing. By the late 1940's and early 1950's it was realised that such an approach was inadequate and hence later researchers attempted to model the shellside flow. By the 1960's access to powerful computers meant that it was possible to consider the multi-stream models to obtain the shellside pressure drop.

Virtually all the subsequent developments have been based on multi-stream models. Figure 2.1 gives the chronological order in which the models have been published (although not necessarily their original development). From this chart is is seen that the development of shellside models has not been a linear path but rather the development of two main paths with the emphasis going in different directions. Prior to 1942 there was no attempt to calculate shellside pressure drop other than assumming that 'ideal tube-bank' correlations* applied to the whole exchanger.

One of the earliest developments was that of Short (1942) who considered the individual components of pressure drop in a semi-analytical manner. He considered crossflow and windowflow separately but di not take the effects of baffle leakage into account. During the 1940's it was realised that the effects of baffle leakage and bundle-bypassing had great influence on the design of exchangers. The first to deal with this problem was Tinker (1948) presenting the first multi-stream method. The extremely valuable contribution that he made to the understanding of shellside flow cannot be over-emphasised. Examining the time-chart it is seen that future developments of the multi-stream methods did not occur until the 1960's with the advent of high speed computers.

---

*An 'ideal tube-bank' is a rectangular bank of tubes with no bypassing e.e. all the shellside flow is in crossflow.

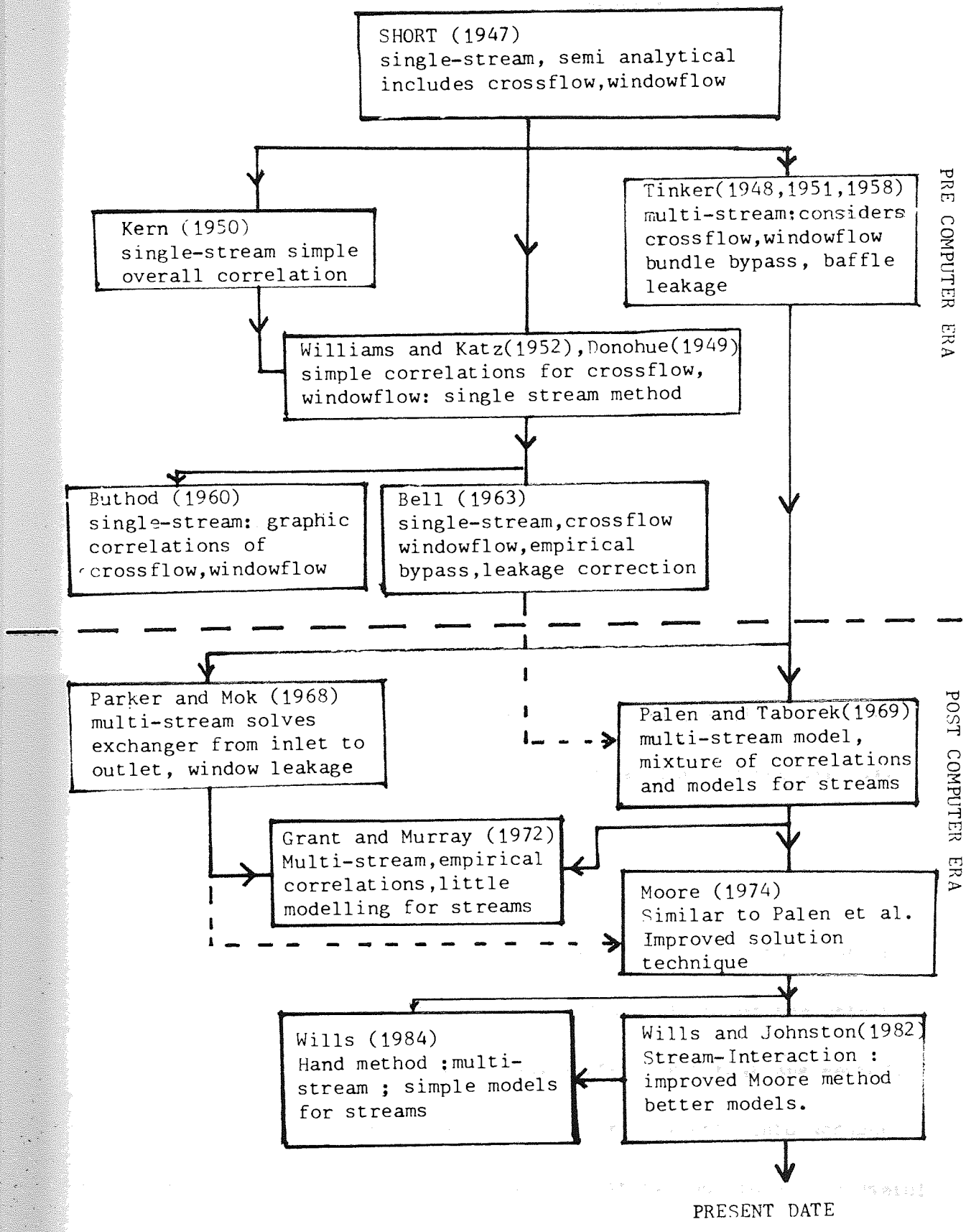

Figure 2.1 : THE DEVELOPMENT OF SHELLSIDE PRESSURE DROP PREDICTION METHODS

Unfortunately for Tinker, his method was never to achieve popularity because it was extremely lengthy and in any case, the methods used were rather suspect because of the lack of adequate data to develop reliable correlations for each flowstream.

Also during the 1940's with the expanding chemical industries, there was a greater need to be able to predict shellside pressure drop, which led to the development of the single-stream models which had the great advantage of simplicity. Kern (1950) published his well-known correlation based on actual heat exchangers in service. The correlation treated the shellside flow in a manner analogous to pipe flow.

Williams, Katz and also Donohue (1952) developed similar types of correlations although they treated the crossflow and the windowflow separately.

By the mid 1950's it was realised that these simple correlations were hopelessly inadequate because they did not allow for the effects of bypassing or baffle leakage. It was self-evident that any method, to be reliable would have to take both of these effects into account. Only the model of Tinker could do this, but it was not in a form useful to engineers. The American Society of Mechanical Engineers (ASME) embarked on an ambitious project at Delaware University along with other organisations, to study shellside flow with the eventual aim of developing an accurate method for use by engineers.

The 'Co-operative Research Program' or, the 'Delaware Research Program' as it is often referred to, continued for 12 years gaining much valuable data on many aspects of shellside flow. Bell (1960) recognised Tinker's model and its inherent difficulties and developed his well known method by assuming an exchanger to be as series of ideal banks connected by turnaround zones (windows) and applying empirical correction factors for the effect of baffle leakage and bundle bypassing. The advantage of this approach was that the method could be expressed semi-graphically and hence was relatively easy to use. Taborek (1983) has recently modified this method improving some of the correlations but, in essence, the method is still the same.

Although Bell's method represented the last of the single-stream models, it is widely used to date by many designers as, at present, it is the only reasonably accurate method available in the public domain. All subsequent developments of shellside models have remained proprietary to organisations such as HTFS, or HTRI*.

Also worth mentioning, is the method of Buthod (1960), essentially the same as Williams, Katz, and Donohue, but rather more comprehensive. The advantage of this method was that it was almost entirely graphical which was very important in the late 1950's and early 1960's.

---

* Heat Transfer Research, Incorporated, Alhambra, California U.S.A.

Although Buthods's method never achieved popularity it does illustrate that the needs of engineers were being seriously considered.

Whitley (1961) compared Kern's, Williams, Katz and Donohue's, Buthod's and Bell's model with field data concluding that Bell's model was the most accurate because it allowed for bypassing and baffle leakage. Ultimately the other methods became obsolete with Bell's model becoming the industry standard.

By the late 1960's, the advent of high speed computers meant engineers were designing exchangers using extensive computer programs and it was realised that these programs were often of limited use because of the uncertainties especially on the shellside, involved in heat exchanger design. By now, the cost of fundamental research was so high, companies were jointly contributing to continue research in shell-and-tube heat exchangers leading to the development of HTFS in the U.K. and HTRI in the U.S.A. The unfortunate side effect of these "clubs" is that virtually all shellside work since 1969 has remained proprietary being published in qualitative form only.

Palen and Taborek (1969) examined the Bell method and realised that it was not possible to extend it any further without resorting to a very lengthy and prohibitive research programme.

It was clear that there was a need to model the flow in detail and so they explored the potential of Tinker's model. It seems ironic that it took over 20 years of detailed investigation of shellside flow before the full potential of Tinker's model was explored and yet Tinker had developed his ideas on minimal knowledge of shellside flow.

Palen and Taborek produced the first useful model based on Tinker's model i.e. the "STREAM-ANALYSIS METHOD" which as its name suggests analyses each flowpath separately. Subsequent developments have been by Parker and Mok (1968) who attempted to solve the pressure drop across the whole exchanger, by Grant and Murray (1972), the "DIVIDED-FLOW METHOD" and Moore (1979), the latter two methods being proprietary to HTFS.

Also shown in the chart are the developments as a result of this work. As a result of insight gained in this work, a new method has been developed for ESDU (1983) by Wills (1984) which is a simplified method based on Tinker's model, which is very accurate and yet simple enough to be used as a hand-method. The bulk of this thesis is concerned with the development of the "STREAM-INTERACTION" model which is believed to be the most accurate method available to HTFS.

3.0 A DETAILED EXAMINATION OF SHELLSIDE PRESSURE DROP PREDICTION METHODS

This chapter examines the most commonly used methods for shellside pressure drop prediction (both past and present) in detail to identify their individual strengths and weaknesses. A framework is identified for a reliable method, and also areas for future research are identified.

3.1 Single-Stream Methods

As shown in chapter 2, the methods can be split into two main categories:-

1) single-stream methods,

and

2) multi-stream methods.

The single-stream methods are mainly of historic interest and are discussed first. The methods are presented in order of increasing complexity, rather than in chronological order. A summary of the main features of these methods is given in table 3.1. Sections 3.1.1 to 3.1.5 outline the main equations of the methods with section 3.2 discussing the features of these methods in more detail.

3.1.1 Kern (1950)

Kern treated shellside flow in a manner analogous to flow in a pipe.

TABLE 3.1: SUMMARY OF MAIN FEATURES OF SINGLE-STREAM METHODS

METHOD / FEATURE	SHORT	KERN	WILLIAMS KATZ DONOHUE	BUTHOD	BELL
EASE OF USE	FAIRLY EASY	VERY EASY	VERY EASY	QUITE EASY	QUITE EASY BUT LENGTHY
TOTAL PRESSURE DROP	YES	YES	YES	YES	YES
CROSSFLOW PRESSURE DROP	YES	NO	YES	YES	YES
WINDOWFLOW PRESSURE DROP	YES	NO	YES	YES	YES
BYPASSING CORRECTION	NO	NO	NO	NO	YES
BAFFLE-LEAKAGE CORRECTION	NO	NO	NO	NO	YES
END-SPACE CORRECTION	NO	NO	NO	NO	YES
GENERAL RELIABILITY	VERY POOR	VERY POOR	POOR	POOR	MODERATE
RECOMMENDATION AS A DESIGN METHOD	NO	NO	NO	NO	YES (WITH CAUTION)
POSSIBLE FUTURE EXTENSION	NONE	NONE	NONE	NONE	LIMITED WITHOUT EXTRA EXPERIMENTS

He gave the shellside pressure drop as

$$\Delta p_T = \frac{f_T \dot{m}_T^2 D_s}{\rho D_e S_g} (N_B + 1) \qquad (3.1)$$

where the friction is obtained from a friction factor versus Reynolds Number chart (similar to the Fanning friction factor for flow in a pipe.)

3.1.2 Williams, Katz (1952), and Donohue (1949)

Donohue presented a correlation for the windowflow pressure drop (per baffle space) as

$$\Delta p_w = 1.087 \times 10^{-3} \frac{\dot{m}_w^2}{S_g} \qquad (3.2)$$

Williams and Katz used the above to obtain a crossflow relationship by subtracting the total windowflow pressure drop from the total pressure drop, correlating the crossflow pressure drop using

$$\Delta p_c = 2 f_c N_c \frac{\dot{m}_c^2}{\rho} \phi_s \qquad (3.3)$$

where the friction factor is also obtained from a friction factor versus Reynolds Number chart.

The total shellside pressure drop is then given by

$$\Delta p_T = (N_B + 1)\Delta p_c + N_B \Delta p_w \qquad (3.4)$$

3.1.3 Buthod (1960)

This method is similar to Williams, Katz, and Donohue's method given above. The key equations are

$$\Delta p_w = 1.67 \times 10^{-3} \frac{\dot{m}_w^2}{\rho} \tag{3.5}$$

and

$$\Delta p_c = \frac{F A N_c}{\rho} \tag{3.6}$$

where F and A are obtained from graphical charts as a function of the mass velocity, $\dot{m}_c$. The total pressure drop is then given by

$$\Delta p_T = (N_B + 1)\Delta p_c + N_B \Delta p_w \tag{3.7}$$

3.1.4 Short (1942)

This is probably the earliest shellside pressure drop prediction method to be developed. Short's equations were

$$\Delta p_w = \left((0.42 - 0.45 \frac{S_w}{S_s})^2 + (1 - \frac{S_w}{S_s})^2 + \left(\frac{D_c}{\sqrt{D_c^2 + 3.53 \times 10^{-3}}}\right)\right) \frac{\rho v_w^2}{2} \tag{3.8}$$

and

$$\Delta p_c = 2.5\left(\frac{P_t - D_0}{D_0}\right)\left(1 - \frac{S_m}{S_p}\right)^2 \left(\frac{S_w}{S_m}\right)^2 N_c \frac{\rho v_w^2}{2} \tag{3.9}$$

and the total pressure drop is given by

$$\Delta p_T = (N_B + 1)\Delta p_c + N_B \Delta p_w \tag{3.10}$$

3.1.5 Bell (1960)

This is the most comprehensive of the single-stream methods, taking baffle leakage and bundle bypassing into account. Only the main equations for turbulent flow are presented here. His method treats the exchanger as a series of ideal tube-banks connected by turnaround zones (window zones). The pressure drop is calculated for both of these, assuming all the fluid flows through them, applying correction factors for baffle leakage and bundle bypassing as shown below. The ideal crossflow pressure drop is given by

$$\Delta p'_c = \frac{4 f_c N_c \dot{m}_c^2}{2 \rho \phi_s} \tag{3.11}$$

and the ideal windowflow pressure drop is given by

$$\Delta p'_w = (2 + 0.6 N_{tw}) \frac{\rho v_z^2}{2} \tag{3.12}$$

where the geometric mean velocity, v_z, is given by

$$v_z = \sqrt{v_c v_w} \tag{3.13}$$

The actual crossflow pressure drop is then given as

$$\Delta p_c = \Delta p'_c R_b R_L \tag{3.14}$$

and the windowflow pressure drop as

$$\Delta p_w = \Delta p'_w R_L \tag{3.15}$$

Bell also defines a correction factor for the end-spaces where the fluid enters or leaves the shell. At the inlet (or outlet) the number of rows crossed by the shellside fluid is greater than in a baffle space in the middle of the exchanger (a mid-space). A later modification by Taborek (1983) also allows for the fact that the inlet or outlet end-space is usually larger than a mid-space. Bell assumes that there is bundle bypassing but no baffle leakage in the end-spaces i.e.

$$\Delta p_e = \Delta p'_c \, R_b \, R_e \qquad (3.16)$$

Finally the total pressure drop is given by

$$\Delta p_T = 2\Delta p_e + (N_B - 1)\Delta p_c + N_B \Delta p_w \qquad (3.17)$$

R_b and R_L are either obtained graphically, or from curve fits, with the expression for R_e being an analytical expression.

3.2 Discussion of the Single-Stream Methods

Of all the methods, only the Bell method is still widely used today. Whitley (1961) has shown that this is the most reliable for his field data, with the methods of Kern, Williams, Katz and Donohue, and of Buthod giving very unreliable predictions, overpredicting by up to a factor of 10 in some cases. The main reason for the improved reliability of the Bell method is due to the use of correction factors for baffle leakage and bypassing.

It is useful to note that all the researchers, except Kern, have generally correlated crossflow pressure drop in the ideal tube-bank form i.e.

$$\Delta p_c = \frac{4 f_c N_c \dot{m}_c^2}{2 \rho} \qquad (3.18)$$

although the definitions for N_c and f_c vary. Many other researchers e.g. Bergelin (1954), Boucher and Lapple (1948), Grimison (1937), Moore (1974), Butterworth (1979), ESDU (1979) have correlated crossflow pressure drop in ideal tube-banks and it is not intended to study this aspect in any further detail in this work.

The situation is radically different for windowflow pressure drop with Short and Bell both making semi-analytical analyses, with Buthod and Donohue obtaining very simple but clearly inadequate empirical correlations. It is already clear that there is a need to devise a rational method for windowflow pressure drop based on sound correlations or physical modelling.

It is immediately evident that the single stream methods do not offer much hope of success in being able to predict accurately shellside pressure drop. The remainder of this chapter describes the multi-stream methods in detail and shows how any reliable method must allow for baffle leakage and bypassing.

3.3 Multi-Stream Methods

Of all the multi-stream methods, only that of Tinker (1951) is in the open literature, all the others being proprietary. The methods are presented here, paying attention to the correlations and/or methods used to obtain the pressure drop, rather than the actual solution procedures. However, the solution procedures are an important aspect of these methods and the solution procedures of four of the methods are given in Appendix 1, showing the contrast in the techniques used. In order to understand multi-stream methods, a discussion of the main features is given.

3.3.1 Pressure Drop and Mass Balance Relationships

Consider a simple flowstream model consisting of five streams:-

1) crossflow,

2) bypass,

3) windowflow,

4) shell/baffle leakage,

and

5) tube/baffle leakage,

as shown schematically in Figure 3.1. The model is analogous to an electrical resistance network, with pressure drop equivalent to voltage,

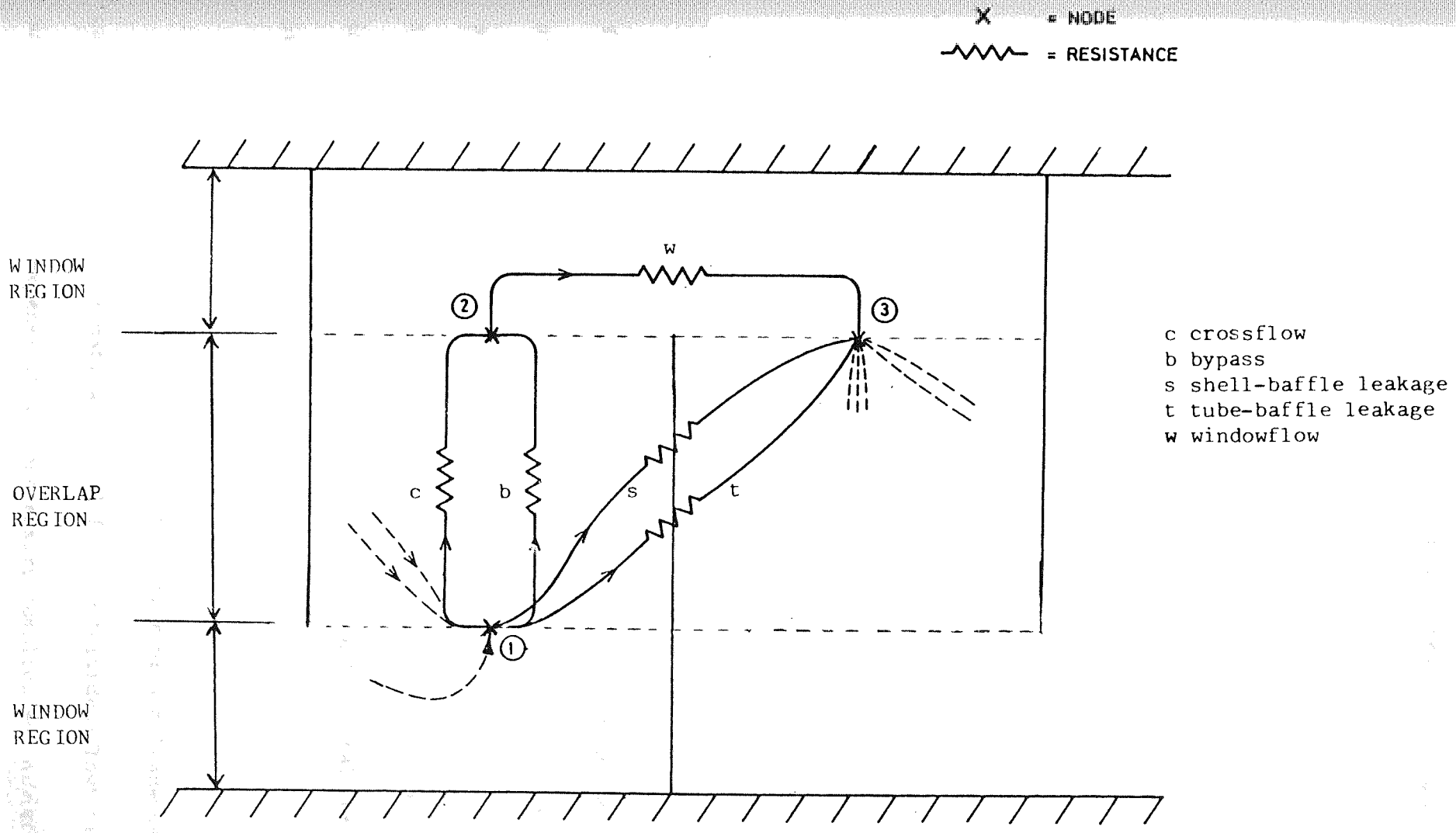

Figure 3.1 : A SIMPLE FLOWSTREAM MODEL

flowrate equivalent to current, and the hydraulic resistance equivalent to electrical resistance, excepting the hydraulic resistance is a function of the flowrate necessitating iterative solutions. It is possible to define a set of equations to solve for the pressure drop per baffle-space i.e.

$$\Delta p_c = \Delta p_b \tag{3.18}$$

$$\Delta p_s = \Delta p_t = \Delta p_p \tag{3.19}$$

$$\Delta p_p = \Delta p_c + \Delta p_w \tag{3.20}$$

$$\dot{M}_T = \dot{M}_c + \dot{M}_b + \dot{M}_s + \dot{M}_t \tag{3.21}$$

$$\dot{M}_w = \dot{M}_T - \dot{M}_s - \dot{M}_t \tag{3.22}$$

Also defining

$$\Delta p_i = f\{\dot{M}_i\} \tag{3.23}$$

for each of the five streams leads to a set of 10 equations with 10 unknowns and hence a solution can be obtained for the flowsplit and the pressure drop per baffle space. This pressure drop is then multiplied by the number of mid-spaces, adding on the end-space pressure drops and also, the nozzle pressure drops, if appropriate, giving the total shellside pressure drop.

From Appendix 1, it is seen that the number of simultaneous equations can be reduced quite dramatically to 2 for the 'Divided-Flow' method, but this is at the expense of an unnecessary complicated numerical solution

procedure for the resultant non-linear simultaneous equations. Of all the procedures, the method of Moore is the most efficient, requiring only a few relatively simple calculations. A simplified iteration scheme is shown below.

A simple relationship for the pressure drop as a function of flowrate is defined

$$\Delta p_i = n_i \dot{M}_i^2 \tag{3.24}$$

where

$$n_i = f(\dot{M}_i) \tag{3.25}$$

and substituting these into equations 3.18 to 3.22 gives

$$\dot{M}_w = \frac{\dot{M}_T}{1 + (n_s^{-\frac{1}{2}} + n_t^{-\frac{1}{2}})((n_c^{-\frac{1}{2}} + n_b^{-\frac{1}{2}})^{-2} + n_w)^{\frac{1}{2}}} \tag{3.26}$$

$$\Delta p_w = n_w \dot{M}_w^2 \tag{3.27}$$

$$\Delta p_c = (n_c^{-\frac{1}{2}} + n_b^{-\frac{1}{2}})^{-2} \dot{M}_w^2 \tag{3.28}$$

$$\dot{M}_c = \left(\frac{\Delta p_c}{n_c}\right)^{\frac{1}{2}} \tag{3.29}$$

$$\dot{M}_b = \left(\frac{\Delta p_c}{n_b}\right)^{\frac{1}{2}} \tag{3.30}$$

$$\dot{M}_s = \left(\frac{\Delta p_p}{n_s}\right)^{\frac{1}{2}} \tag{3.31}$$

$$\dot{M}_t = \left(\frac{\Delta p_p}{n_t}\right)^{\frac{1}{2}} \text{, or alternatively from the mass balance} \tag{3.32}$$

$$\dot{M}_t = \dot{M}_T - \dot{M}_w - \dot{M}_s \tag{3.33}$$

the iteration scheme is then:-

1) guess n_s, n_t, n_c, n_b

2) calculate $\dot{M}_w$, n_w

3) calculate Δp_c, Δp_w, Δp_p. Check if the iteration has converged.

If so then stop, otherwise continue from step 4

4) calculate the new flowsplit, $\dot{M}_c$, $\dot{M}_b$, $\dot{M}_s$, $\dot{M}_t$

5) re-evaluate n_s, n_t, n_c, n_b and continue from step 2

Rosenhow and Hartnett (1973) state " It is possible by means of complex reiterative programs for high-speed computers to improve prediction methods markedly, but no such program is now in the literature". The above analysis shows that the method does not need to be complicated.

Ultimately, the success of any multi-stream model depends on the accuracy of the pressure drop/mass flowrate relationships used and the assumptions used to develop the multi-stream methods. Sections 3.3.2 to 3.3.6 outline the basic pressure drop/mass flowrate relationships of the four known multi-stream methods. A fifth method by Parker and Mok (1968) is also included, as their method takes a slightly different

approach to the above type of procedure, solving for the whole exchanger, rather than just a single baffle-space.

3.3.2 Tinker (1948, 1958)

Tinker initially presented his method in 1948 which used the scheme given in Appendix 1. The method was never a success primarily because of the difficulties in understanding the method. There were two main reasons for this:-

1) the style of Tinker was very hard to understand because of a poor and rather incomplete presentation, especially the explanation of many of the assumptions he used in deriving the equations, making them virtually impossible to follow.

2) Even assuming the equations were understood, the method was exceptionally lengthy, and hence was not used.

In 1958 Tinker republished a simplified version of the 1948 method which was semi-graphical. This simplified method calculated the crossflow fraction and then, calculated the crossflow and windowflow pressure drops summing these along the length of the exchanger to obtain the total pressure drop. There was no iteration involved in this later

method as Tinker made many gross simplications based purely on guesswork, as no shellside data of suitable form were yet available.

It is not intended to show this method in any detail, except for a few key equations to illustrate why even this simpler method was never popular. The crossflow fraction is calculated by

$$F_c = (a + N_p\sqrt{\frac{D_s}{P_t}})^{-1} \tag{3.34}$$

where Tinker introduces the rating number (N_p) which is a function of geometry, determined by

$$N_p = (\frac{D_s}{D_t})^{-\frac{1}{2}} (\frac{D_s}{D_t}-1)^{\frac{3}{2}} (\frac{P_t}{P_t-D_0})^{\frac{3}{2}} + 1.18(\frac{2t_s}{D_s})(\frac{D_s}{D_t})^{\frac{1}{2}}(\frac{D_s}{L_b})(\frac{P_t}{P_t-D_0})(1-0.01P_d) \tag{3.35}$$

and the baffle space pressure drop is given by

$$\Delta p_p = 0.355\ C_c\ S\ \frac{f_c}{\phi}\ (\frac{F_c\ M_T}{10^5\ A})^2\ (1 + \frac{Y}{S}) \tag{3.36}$$

where $S = D_s/P_t$, $Y = \frac{4.08}{C_c}(\frac{144\ L_b\ C_a}{C_2\ D_s})^{0.35}$ (3.37)

and C_c, C_a, C_2 are also functions of flowrate and geometry.

Even examining the above equations which are for inline triangular tube layouts, it is clear why Tinker's method never became popular, being extremely difficult to understand. In one sense, it is because of Tinker that the multi-stream methods were not developed until the advent of

computers, as the exchanger industry wanted a reasonable method which was simple to use, and easily understood. Naturally, Tinker's method was superseded by the Bell method described in Section 3.1.5. It was not until the late 1960's that Tinker's ideas were taken seriously by Palen and Taborek whose method is described in the next section.

3.3.3 Palen and Taborek (1969)

Palen and Taborek developed the first truly iterative flowstream method in the mid 1960's based on the ideas of Tinker (extending it to include a pass-partition lane). Unfortunately the cost of developing the 'STREAM-ANALYSIS' has meant that this method has remained proprietary to members of HTRI. The method was published in qualitative form in 1969 outlining the iteration technique and the form of the correlations used for the pressure drop/mass flowrate equations for each of the flowstreams. These are briefly described below in terms of the velocity heads where

$$\Delta p_i = C\, K_i \frac{\dot{M}_i^2}{A_i^2} \qquad (3.38)$$

It is most likely that $C = \frac{1}{2}\rho$, being the usual form. The various K values are given for each stream.

Crossflow

The crossflow K value is obtained in the usual ideal tube-bank form i.e.

$$K_c = 4\, f_c\, N_c \qquad (3.39)$$

Bypass

This was correlated from data obtained from commercial sized bundles (almost certainly rectangular bundles with bypass lanes present). The spread of bypass clearances represented a typical spread found in industry. The form of the correlation is similar to the crossflow being

$$K_b = 4\ f_b\ N_b\ \phi_b \qquad (3.40)$$

where ϕ_b takes into account the difference of viscosity between the crossflow and the bypass stream. It is implied by Palen and Taborek that the friction factor relationships for the bypass were deduced rather than explicitly measured. To measure bypass flowrate is actually a difficult operation. Instead the bypass friction factor is deduced from ideal tube-bank correlations and the measured pressure drop from the bundles with bypassing present. From the measured pressure drop, the crossflow portion of the flowrate can be estimated and hence the bypass flowrate can be estimated. From the measured pressure drop and the calculated bypass flowrate, the bypass friction factor is then obtained. Of course, it is assumed that the bypass and crossflow paths do not affect each other. Appendix 3 shows the analysis for obtaining the bypass friction factor.

Windowflow

This is perhaps the most doubtful of the relationships developed as Palen and Taborek attempted to produce a semi-analytical model for

the windowflow pressure drop but still had to rely on an empirical correction factor. It is known that the model has been changed but details are not known, except that their new model allows for windowflow bypass and has probably dispensed with the empirical correction factor. However, in the original formulation, Palen and Taborek defined the window losses as

$$K_w = 4\ f_w\ N_w\ F_r + 2\theta \qquad (3.41)$$

The first term accounts for the frictional losses in the window and the second accounts for the turning losses. The form of the first term strongly suggests that frictional losses in the axial direction are ignored but the crossflow-in-the-window losses are not. Also the form of the term θ is not known except that it varies from 0 to 1 as the baffle spacing varies from very large to very small compared to the shell diameter.

Shell-baffle Leakage

This was correlated as two parts using data from orifice measurements. The two parts were

1) Frictional losses, and

2) geometric losses, as

$$K_s = K_{gs} + 4\ f_s \frac{B_t}{t_s} \phi_s \qquad (3.42)$$

The second term accounts for the frictional losses through the orifice, and the first term allows for the expansion/contraction losses. K_{gs} is effectively a discharge coefficient, correlated as a function of the orifice geometry i.e.

$$K_{gs} = f \{ B_t, t_s \} \tag{3.43}$$

Tube-baffle Leakage

The form is identical to the shell/baffle leakage (although not numerically the same) i.e.

$$K_t = K_{gt} + 4 f_t \frac{B_t}{t_t} \phi_t \tag{3.44}$$

Pass-Partition Flow

This is correlated in a manner similar to the crossflow and the bypass as

$$K_a = (4 f_a N_a + 4 f_{tr} N_{tr}) \phi_a \tag{3.45}$$

the first term accounting for the losses in the inline pass-partition and the second term allows for the tie-rods that may obstruct the flow in the lane.

Appendix 1 gives details of the iteration technique used by Palen and Taborek in the 'STREAM-ANALYSIS' method which combined with the equations above gives the shellside pressure drop and flow distribution.

3.3.4 Grant and Murray (1972)

This method, the 'DIVIDED-FLOW' method is also based on the method of Tinker but is actually simpler in one respect, as Grant and Murray made no attempt to model the flow in any of the flowstreams, relying solely on correlations of experimental data. This may not be considered to be the best approach and yet it is fairly reasonable as Grant and Murray realised that the key point was that if the correlations used were applicable over a wide range, then it was unlikely that the overall method would be extrapolated outside its range. Of course, the counter argument to this is that correlations are not usually applicable over a wide range. This is reflected in some of the correlations used, because of lack of adequate data. However the correlations used probably represent the best from the point of view of HTFS, and as such remain proprietary to HTFS. The form of the correlations is given below, again in terms of the velocity heads lost.

Crossflow

The correlations is in the usual form of an ideal tube-bank,

$$K_c = 4\ f_c\ N_c \qquad (3.46)$$

Bypass

Again this is in the same form as Palen and Taborek i.e.

$$K_b = 4\ f_b\ N_b \qquad (3.47)$$

Windowflow

Rather than attempt to model the pressure drop, Grant and Murray found they could accurately correlate the available windowflow pressure drop by using the ratio of the windowflow to crossflow areas as the correlating parameter i.e.

$$K_w = f\left\{\frac{A_w}{A_{cl}}\right\} \qquad (3.48)$$

In turbulent flow this expression is independent of flowrate. Of course this expression implicitly allows for the frictional losses in the window, including the crossflow-in-the-window losses. Hence the crossflow equations only account for the frictional losses between the baffle overlap region.

Shell-Baffle Leakage

This was simply defined as the friction factor, obtained by correlating the data of Bell (1958) in terms of Reynolds Number i.e.

$$K_s = f_s \qquad (3.49)$$

Tube-Baffle Leakage

This was obtained similarly as above as

$$K_t = f_t \qquad (3.50)$$

Pass-Partition Flow

This was obtained in a similar manner to Palen and Taborek except that the tierods are ignored i.e.

$$K_a = 4\, f_a\, N_a \qquad (3.51)$$

Although Grant and Murray's correlations are rather simple in form, the method becomes unnecessarily complicated because of the manner in which the friction factors were obtained. The friction factor for any stream is defined by

$$f_i = a_i \, Re_i^{b_i} \quad \text{where } i = c, b, s, t. \tag{3.52}$$

Because Grant and Murray did not choose the Reynolds Number definitions very well, they ended up having to produce many separate correlations, resulting in unwieldy 'look-up' tables for the values of a_i and b_i. For example the crossflow Reynolds number was defined as

$$Re_c = \frac{M_c \, D_0}{\eta \, A_c} \tag{3.53}$$

Had Grant and Murray chosen the tube gap as the correlating parameter in the Reynolds number definitions, then the many different curves for the various pitch-diameter ratios would have been reduced to one for each type of tube layout. Choosing the tube diameter meant that there were many separate curves, one for each pitch-diameter ratio. The whole approach of Grant and Murray meant that a potentially simple method became unnecessarily cumbersome.

Examining the method in detail shows the Grant and Murray method to be really a correlation imposed on the framework of a multi-stream model and as such must be regarded with a certain amount of caution, and yet is is clearly preferable to the single-stream correlations which do

not calculate the flow distribution. Also the method does give reasonable results but limitations inherent in its concept mean that it cannot be significantly improved without resorting to either new and better correlations, should any data become available or to resort to mathematical modelling.

3.3.5 Moore (1974)

The method of Moore (proprietary to HTFS) is essentially similar to the method of Palen and Taborek, although the correlations are obtained from different sources. Moore uses a rather simpler solution technique than Palen and Taborek (Appendix 1), and hence the method is very quick. The main equations are given below.

Crossflow

This is obtained in the usual ideal tube-bank form i.e.

$$K_c = 4\ f_c\ N_c \qquad (3.54)$$

where

$$f_c = a\ Re_c^b \qquad (3.55)$$

and the crossflow Reynolds number is defined with the inter-tube gap as the characteristic length,

$$Re_c = \frac{\dot{M}_c\ (P_t - D_o)}{\eta\ A_c} \qquad (3.56)$$

Using this characteristic length has meant that it enables many curves for different tube pitch/diameter ratios to be correlated by a single line, reducing the number of curves to just 4 for turbulent flow (one for each common tube layout).

Bypass

Moore correlates crossflow bypass in the usual form i.e.

$$K_b = 4\ f_b\ N_b \tag{3.57}$$

where

$$f_b = a\ Re^b$$

The Reynolds number is based on an effective hydraulic diameter of the bypass lane,

$$Re_b = \frac{\dot{M}_b\ D_e}{\eta A_b} \tag{3.59}$$

and

$$D_e = \frac{4\ A_b}{2\ (t'_b + 2L_b)} \tag{3.60}$$

where

$$t'_b = t_b - \left(\frac{P_t - D_0}{2}\right) \tag{3.61}$$

The term t'_b is used because it is assumed that the flow is still in crossflow until a distance of half of the inter-tube gap outside the tube bundle, in accordance with the suggestion of Bell (1963). There is no real evidence to suggest that this is actually true but since bypass

friction factors are deduced by the method in Appendix 3, then the definition is merely an arbitrary one in any case.

Windowflow

Moore produced a hybrid version of the Bell method and the method of Palen and Taborek,

$$K_w = (4\ f_w \frac{L_b}{D_w} + 2\sin(\alpha)) \frac{A_w}{A_c} \qquad (3.62)$$

where the term in brackets is similar to the method of Palen and Taborek. The first part allows for axial frictional losses and the second allows for the turning losses as the fluid turns through 180°. It will be noted here that crossflow-in-the-window losses are not included directly. Instead, these losses are taken into account by the crossflow equation, N_c being larger than the number of tube rows in the overlap region. Moore assumes that the crossflow extends to the centroids of the windows.

The second term is actually very similar to the Θ term of Palen and Taborek, $\sin(\alpha)$ having a value of 1 when the baffle spacing is very small compared with the shell diameter.

For reasons rather difficult to understand, Moore multiplies the term in brackets by the ratio of the windowflow to the crossflow area. This has the effect of converting the velocity term ($\Delta p_w = K_w \rho v_w^2/2$) to the geometric mean velocity in a manner similar to Bell. It is apparent

that Moore attempted to get the best of both worlds in his equation.

Another significant variation in his method is that he treated the window as two regions, windowflow through the tubed region, and windowflow bypass as the flow between the edge of the shell and the tubed region. It is debatable whether there is any great advantage in doing this as he used the same equations to describe the pressure drop/mass flowrate relationships. The same could be achieved by assuming only one stream to obtain the pressure drop and merely proportioning the flow in ratio of the areas.

Shell-Baffle Leakage

Moore correlated the data of Bell in a similar manner to Palen and Taborek,

$$K_s = a \left(\frac{B_t}{t_s}\right)^b + 4 f_s \left(\frac{B_t}{t_s}\right) \qquad (3.63)$$

Tube-Baffle Leakage

The same form of equation as equation 3.63 is used for the tube-baffle leakage stream,

$$K_t = a \left(\frac{B_t}{t_t}\right)^b + 4 f_t \left(\frac{B_t}{t_t}\right) \qquad (3.64)$$

where

$$f_t = a \left(\frac{2 \dot{M}_i t_i}{\eta A_i}\right)^b \quad \text{for } i = s, t \qquad (3.65)$$

Pass-Partition Flow

Moore does not include an inline pass-partition lane in his model but it is a simple matter to do so.

Overall Moore's method is quite an elegant method using simple relationships for the pressure drop/mass flowrate relationships combined with an efficient solution technique. Because of this, the method has the potential to be extended further.

3.3.6 Parker and Mok (1968)

This method is a multi-stream method but is is a departure from the baffle-space methods described in Section 3.3.2 to 3.3.5. Parker and Mok attempt to solve the flow distribution across the whole exchanger as they realised that total flow enters the exchanger and distributes itself in the exchanger and recombines only at the exit. Implicit in their method is that conditions of total flow never exist at a nodal point in a mid-space as assumed by the baffle-space methods.

For an exchanger with N_B baffles, Parker and Mok define the following pressure drop relationships, with reference to Figure 3.2

$$\Delta p_T = (N_B + 1)\,\Delta p_c + N_B\,\Delta p_w \qquad (3.66)$$

Figure 3.2 : THE FLOW MODEL OF PARKER AND MOK (1968)

A similar equation is defined for the bypass and the windowflow path,

$$\Delta p_T = (N_B + 1)\,\Delta p_b + N_B\,\Delta p_w \qquad (3.67)$$

They consider the leakage to be as two sets of parallel streams i.e. leakage in the overlap (o) and leakage in the window (w),

$$\Delta p_T = N_B\,\Delta p_{so} \qquad (3.68)$$

$$\Delta p_T = N_B\,\Delta p_{to} \qquad (3.69)$$

$$\Delta p_T = \frac{N_B}{2}\,(\Delta p_{tw} + \Delta p_w) \qquad (3.70)$$

$$\Delta p_T = \frac{N_B}{2}\,(\Delta p_{tw} + \Delta p_w) \qquad (3.71)$$

Equations 3.68 and 3.69 arise because there is leakage passing through a baffle in every mid-space and equations 3.70 and 3.71 arise because leakage only passes through a baffle every two baffle-spaces.

The following mass balances apply:-

$$\dot{M}_T = \dot{M}_w + \dot{M}_{so} + \dot{M}_{to} + \dot{M}_{sw} + \dot{M}_{tw} \qquad (3.72)$$

and

$$\dot{M}_w = \dot{M}_c + \dot{M}_b + \dot{M}_{sw} + \dot{M}_{tw} \qquad (3.73)$$

In principle, defining

$$\Delta p_i = K_i \frac{\dot{M}_i^2}{2\rho A_i^2} \qquad \text{for each path} \tag{3.74}$$

will lead to a solution for Δp_T.

No details are given for the K values, except for a few rather limited graphs. No method is given either for the solution procedure. The key point about this method is that it does seem to allow for baffle leakage in a more rational manner than the baffle-space methods. This has great bearing on the research in chapter 7 where baffle leakage in the window is considered. If the above equations are examined in more detail, it becomes apparent that the equations given above are not correct with equations 3.68 to 3.71 requiring the addition of one crossflow pressure drop (or actually an end-space pressure drop if the method is to be more rigorous).

3.4 Discussion of The Multi-Stream Methods

The multi-stream methods are summarised in Table 3.2 and are compared with the single-stream methods in Table 3.3. Palen and Taborek (1969) concluded the method of Tinker was not very accurate,

TABLE 3.2: SUMMARY OF MAIN FEATURES OF MULTI-STREAM METHODS

METHOD / FEATURE	TINKER	PALEN*, TABOREK	PARKER*, MOK	GRANT, MURRAY	MOORE
TYPE OF METHOD	BAFFLE-SPACE	BAFFLE-SPACE	OVERALL	BAFFLE-SPACE	BAFFLE-SPACE
POTENTIAL HAND METHOD	NO	NO	NO	NO	YEST BUT LENGTHY
BAFFLE LEAKAGE IN WINDOW	YES	NO	YES	NO	NO
END-SPACES	NO	YES	NO	YES	YES
CROSSFLOW EXTENT	CENTROID OF WINDOW	CENTROID OF WINDOW	BAFFLE OVERLAP REGION ONLY	BAFFLE OVERLAP REGION ONLY	CENTROID OF WINDOW
INTERACTIONS BETWEEN STREAMS	NO	NO	YES	NO	NO
RELATIVE RELIABILITY	MODERATE	NOT KNOWN ASSUMED MODERATE-GOOD	NOT KNOWN ASSUMED MODERATE-GOOD	MODERATE-GOOD	MODERATE-GOOD
RECOMMENDED AS A DESIGN METHOD	NO	ASSUMED YES	? MAYBE	YES	YES

* These are not known in detail but, as far as is known, the main features are correctly given.

TABLE 3.3: COMPARISON OF SINGLE-STREAM AND MULTI-STREAM METHODS

METHOD / FEATURE	SINGLE-STREAM	MULTI-STREAM
EASE OF USE	HAND METHOD	COMPUTER SOLUTION
ACCURACY	POOR-MODERATE	MODERATE-GOOD
MODEL TYPE	PIPE-FLOW	PIPING NETWORK
POSSIBLE FUTURE EXTENSION	NO	YES
RECOMMENDED DESIGN METHOD	NO	YES

tending to underpredict severely by up to 60% in some cases. The Bell method, being the best single-stream method, fares reasonably well with predictions of Palen and Taborek's data varying from -50% to + 100%, with the values usually being conservative. However, the Bell method does fail in rather too many cases for safety. Their own method, the 'STREAM-ANALYSIS' method gives fairly good predicitions ranging from -30% to + 50%. This is not as good as it may seem because their method did use empirical correction factors, which inevitably will have used their data, and hence good agreement is to be expected. Contrast this with the HTFS methods of Grant and Murray, and of Moore who avoided the use of empirical correction factors. They found they could get good agreement of no-leakage data ($\pm$ 30%) but tended to overpredict the leakage data by up to 60-70%, suggesting the treatment of leakage was inadequate.

No attempt is made to discuss the end-spaces in detail, this being a subject for future work in its own right.

Perhaps one of the main points to be seen, in this examination is that all the researchers agreed on how to correlate crossflow and bypass pressure drop, and even baffle leakage (although not necessarily how to allow for the leakage) but all differed in allowing for the windowflow

pressure drop. Three important questions arise:-

1) How should the windowflow pressure drop be modelled?

2) What is the effect of the frictional losses in the window?

3) What is the effect of leakage in the window?

Clearly each of these questions must be addressed, in order to develop a reliable pressure drop prediction method.

One implicit assumption in the multi-stream methods is that the streams do not interact with each other i.e. the pressure drop in any path is only dependent on the flowrate in that path. It is difficult to see how this assumption can be true in such a complex flow situation. This also needs to be examined in further detail.

The model of Parker and Mok seems suited to be able to solve some of these questions but unfortunately it is not suited for use in design programs because the method attempts to solve for the whole exchanger at the same time, whereas the design programs require a local method as the heat transfer calculations are performed in increments along the shell, requiring knowledge of the local pressure gradient which can be easily obtained by the baffle-space methods. To use the Parker and Mok method would mean considerable iteration between the heat transfer

calculations and the pressure drop calculations which would prove too prohibitive, even for todays high-speed computers.

Since this work is funded by HTFS, then ultimately it is to the two HTFS methods that attention is focussed. As discussed earlier, the Grant and Murray method is rather limited, and is unnecessarily complicated. For this reason, the method of Moore offers the best scope for development of a more accurate shellside pressure drop prediction method. The next section describes the type of method that is sought after in this work.

3.5 Desired Features of a Shellside Pressure Drop Method

After examining the shellside pressure drop methods in detail, the following features are deemed to be necessary for a reliable prediction method:-

1) The method will be a multi-stream method with six (or possibly seven) streams consisting of

   a) crossflow,

   b) bypass,

   c) pass-partition flow,

   d) windowflow,

   e) shell-baffle leakage,

   f) tube-baffle leakage,

and possibly

g) windowflow bypass.

2) The method will contain a reliable windowflow pressure drop model.

3) The method will allow for interaction between various streams.

4) The method will allow for the leakage in the window.

5) It will use the method of Moore as the starting point for the new method.

The remainder of this thesis is concerned with the development of the 'STREAM-INTERACTION' method which helps to resolve many of the questions raised in this chapter.

4.0 THE INTERACTION BETWEEN CROSSFLOW AND BAFFLE LEAKAGE

This chapter outlines the discovery of a strong interaction between the crossflow stream and the baffle leakage stream and the subsequent development of a model to predict this effect.

4.1 The No-Interaction Assumption of Multi-Stream Models

One of the main features in the multi-stream models is that the pressure drop between any two points is constant regardless of flowpath taken. In solving for the flow distribution, as shown in Chapter 3, relevant pressure drop/mass flowrate relationships are applied to each flowstream. These relationships are obtained from either theoretical considerations or from empirical correlations.

One implicit assumption of these models is that each flowstream can be treated individually i.e. the pressure drop in an individual flowstream is only dependent on the flowrate in that path. The major flowstream in an exchanger is the crossflow stream but in a practical exchanger there is, also axial baffle leakage which flows normal to the crossflow. It is difficult to visualise how the crossflow pressure drop can only be dependent on the magnitude of the crossflow stream. Intuitively, it is realised the crossflow pressure drop must also be a function of the leakage flowrate, as there must be momentum changes due

to the flowstreams intersecting at right angles. It is hypothesised that the crossflow pressure drop with leakage present must be greater when there is no baffle leakage present, for the same crossflow flowrate.

4.2 Experimental Evidence of Crossflow/Leakage Interaction

HTFS has obtained much valuable data from a model exchanger at UKAEA Winfrith. The model was a copy of the model used by Bergelin (1954) consisting of 80 tubes as shown in figure 4.1. Pressure drop measurements have been taken by Macbeth covering a range of baffle pitches and baffle cuts under conditions of no-leakage and leakage. Baffle leakage was eliminated by making special baffles which consisted of two baffle halves sandwiching a thin rubber sheet which gave a tight seal when the tubes were inserted as in Figure 4.2. Despite the quantity of data from Macbeth (1973) there were only three corresponding datasets with baffle leakage present/not present. Of these, the exchanger with the smallest baffle cut (18.4%) was chosen as it had the smallest baffle leakage area in the window zone and it was believed that this set was the one most likely to exhibit the effect of crossflow/leakage interaction, should it exist.

Table 4.1 gives the recorded pressure drops for the chosen non-leakage and leakage geometries (all other parameters being the same) for a range of flowrates. These data are plotted in Figure 4.3 and, from this figure, two important points can be noted:-

FIGURE 4.1 : LAYOUT OF WINFRITH MODEL EXCHANGER

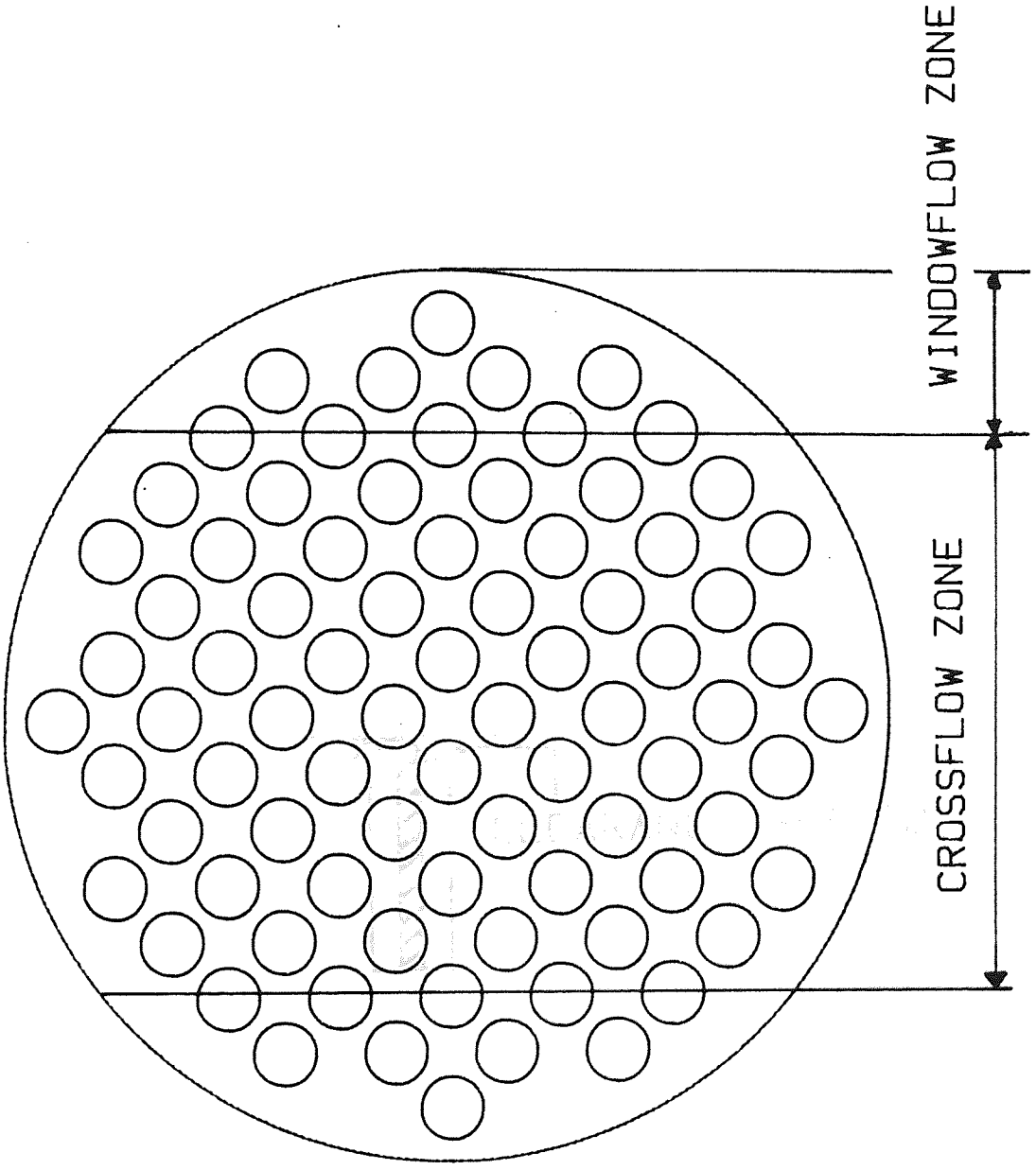

FIGURE 4.2 : SPECIAL NO-LEAKAGE BAFFLES

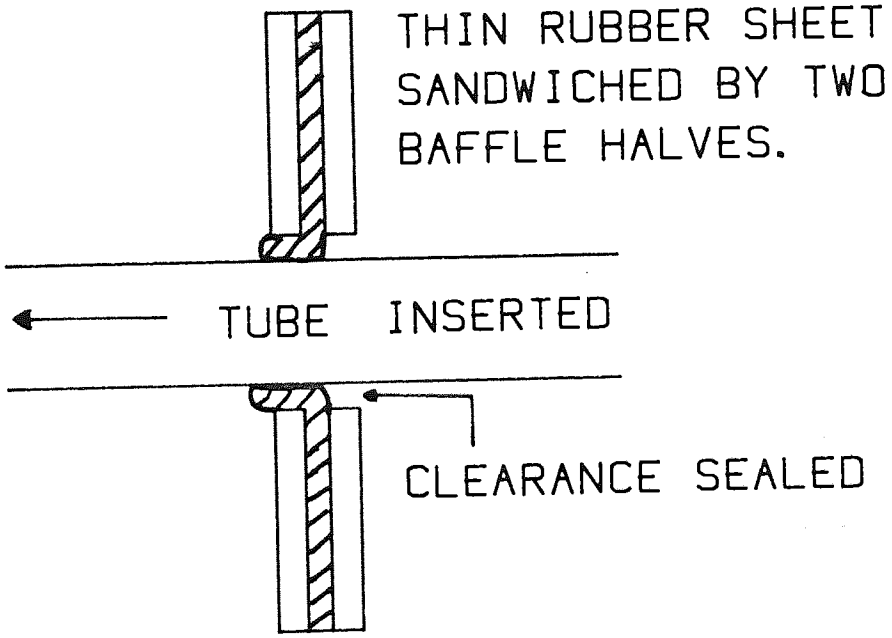

TABLE 4.1: EXPERIMENTAL PRESSURE DROPS FOR 18.4% BAFFLE CUT EXCHANGER

FLOWRATE Kg/s	NO-LEAKAGE N/m^2		LEAKAGE N/m^2	
M_T	Δp_c	Δp_w	Δp_c	Δp_w
0.63	280.6	356.2	68.9	46.1
1.11	741.5	1041.2	163.6	132.0
1.58	1298.6	2142.2	288.9	227.9
2.37	2387.1	4483.6	582.0	477.0
3.17	3952.2	8269.8	1034.5	868.1
3.96	5546.4	12603.9	-	-
4.74	-	-	2126.4	1878.1
4.83	7414.5	17971.8	-	-
6.32	-	-	3586.9	3312.9
7.90	-	-	5380.3	5218.4

FIGURE 4.3 : EXPERIMENTAL EVIDENCE OF CROSSFLOW/LEAKAGE INTERACTION

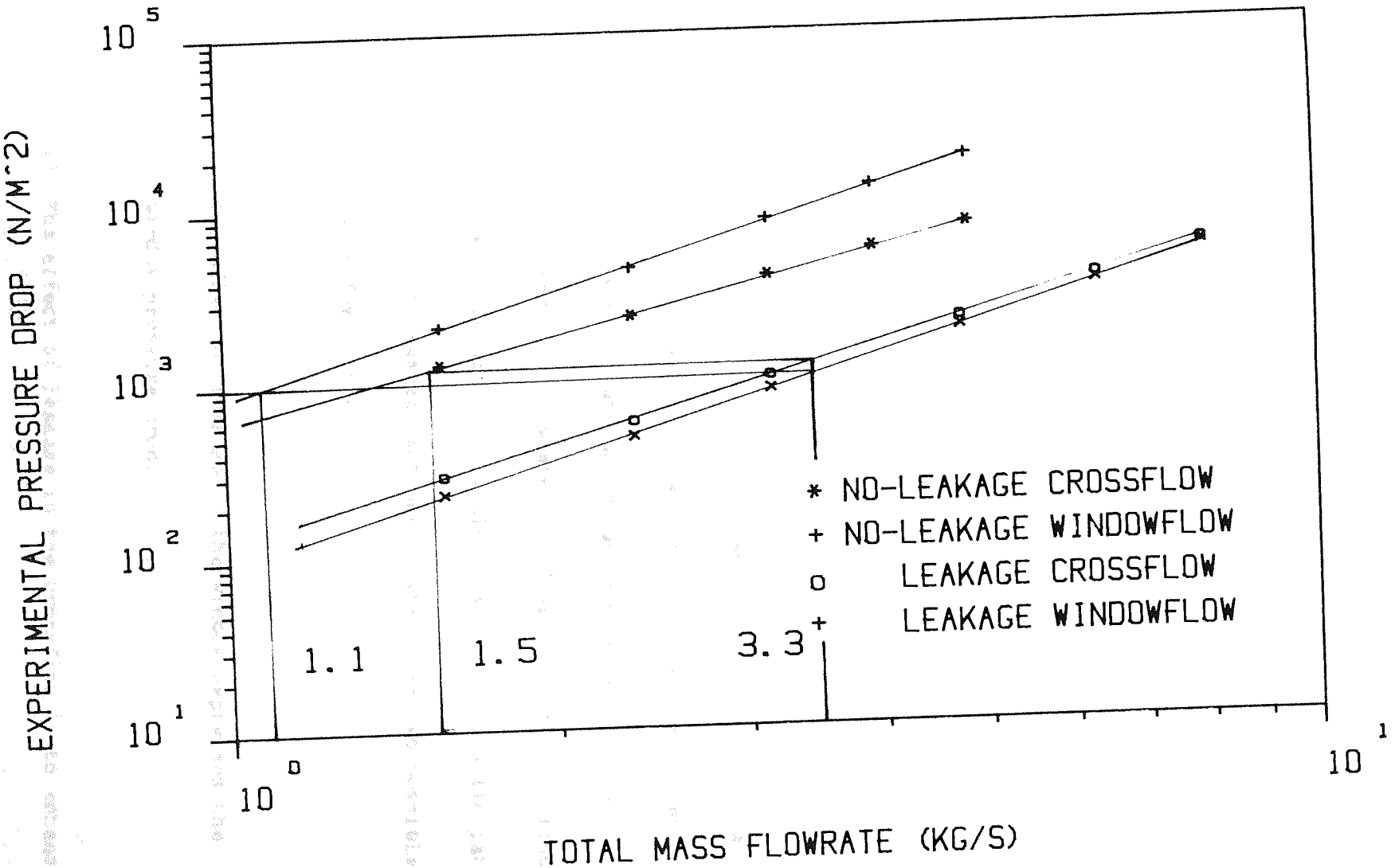

1) The flowrate to give a pressure drop of 1000 N/m^2 in the window zone for the leakage case is 3.3 kg/s whereas the flowrate for the no-leakage case is 1.1 kg/s. From this it is apparent that approximately two-thirds of the flow in the leakage case must pass through the baffle as leakage rather than flowing through the window region. It is assumed here that the maximum flowrate in the window is 1.1 kg/s for the leakage case.

2) For the crossflow, a flowrate of 3.3 kg/s for the leakage case corresponds to a pressure drop of 1156N/m^2 which in turn corresponds to a crossflow flowrate for the exchanger with no-leakage of 1.5 kg/s. There is immediately a paradoxical situation since the crossflow flowrate cannot be bigger than the window flowrate which has been established as 1.1 kg/s above. Apparently a flowrate of 1.1 kg/s in the crossflow is giving a pressure drop that would be expected of a flowrate of 1.5 kg/s in the leakage exchanger. There are two possible explanations for this:-

(i) The effect of leakage in the window depresses the window pressure drop.

(ii) The effect of leakage in the crossflow is to enhance the crossflow pressure drop.

Explanation (i) is not very plausible as it implies momentum recovery as the leakage and the window streams mix which is highly improbable. Explanation (ii) is much more likely i.e. there is an effect of mixing as the leakage enters the crossflow leading to extra momentum losses.

For the case shown, it is evident that the effect of crossflow/leakage interaction exists and is a strong effect. An estimate of the magnitude of the effect can be obtained by considering the apparent leakage crossflow flowrate is 1.5 kg/s but the probable maximum crossflow flowrate in the leakage case is 1.1 kg/s, and that the crossflow pressure drop is approximately proportional to flowrate to the power of 1.8, then

$$F_L = \left(\frac{1.5}{1.1}\right)^{1.8} = 1.75 \qquad (4.1)$$

i.e. for the case chosen the enhancement is 75%

The data is further examined as only one point value is examined above. The results of this examination are shown in Table 4.2. In order to achieve this table a number of steps were required, these being

1) the no-leakage window pressure drop is correlated against the window flowrate giving

$$\Delta p_w = 886.36\ \dot{M}_w^{1.936} \qquad (4.2)$$

TABLE 4.2: COMPARISON OF CROSSFLOW PRESSURE DROP WITH AND WITHOUT BAFFLE LEAKAGE FOR 18.4% CUT EXCHANGER

TOTAL FLOWRATE FOR LEAKAGE CASE (Kg/s)	ESTIMATED CROSSFLOW FLOWRATE (Kg/s)	EQUIVALENT NO-LEAKAGE CROSSFLOW DROP* (N/m^2)	LEAKAGE CROSSFLOW PRESSURE DROP N/m^2
0.63	0.22	54.0	68.9
1.11	0.37	124.0	163.6
1.58	0.50	200.8	288.9
2.37	0.73	367.9	582.0
3.17	0.99	599.0	1034.5
4.74	1.47	1127.5	2126.4
6.32	1.98	1815.8	3586.9
7.90	2.50	2637.0	5380.3

* The equivalent no-leakage pressure drop is the pressure drop that would occur if the crossflow flowrate is the estimated flowrate and there is no baffle leakage.

2) a similar correlation is obtained for the no-leakage pressure drop

$$\Delta p_c = 608.65\ \dot{M}_c^{1.604} \qquad (4.3)$$

Equations 4.2 and 4.3 are accurate to ± 2% and ± 3% respectively.

3) The flowrate in the window for the leakage case is estimated from the windowflow pressure drop using equation 4.2, assuming that the equation is valid when the fraction of leakage is very small.

4) The crossflow flowrate is assumed to be equal to the window flowrate for the leakage case. This is a conservative assumption as generally $\dot{M}_c$ is less than M_w.

5) Using equation 4.3, the no-leakage pressure drops can be estimated at the flowrates estimated for the leakage case i.e. for any given crossflow flowrate, the leakage and the equivalent no-leakage pressure drop may be compared.

The results of this analysis are shown in Figure 4.4. These results are quite remarkable, showing the effect of crossflow/leakage interaction to be a very strong effect enhancing the crossflow pressure

FIGURE 4.4 : COMPARISON OF NO-LEAKAGE AND LEAKAGE CROSSFLOW PRESSURE DROP

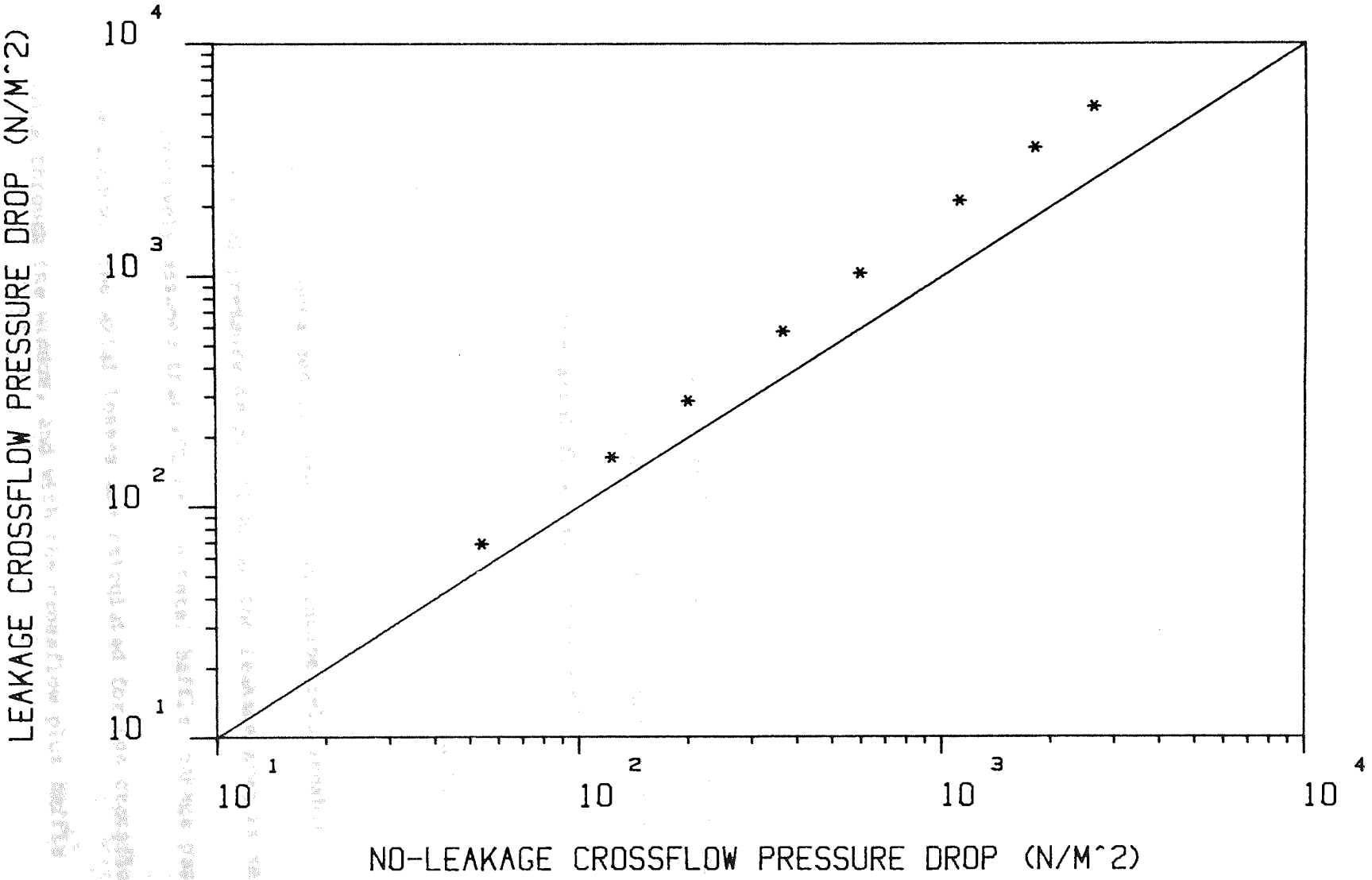

drop by up to a factor of 2. It is important to bear in mind that these comparisons depend very much on the assumptions made, namely

1) the effect of baffle leakage in the window is negligible

2) and the crossflow flowrate equals the window flowrate.

The second assumption is fairly easy to justify as it must necessarily be conservative. Repeating the above analysis with $\mathring{M}_c < \mathring{M}_w$ would only make the effect appear even stronger.

In order to justify assumption 1 it is necessary to be able to predict the effect of the leakage in the window. It is reasonable to assume the leakage only undergoes axial frictional losses as it is not turned in the window like the crossflow. For the exchanger chosen, the frictional losses for the axial flow can be estimated as

$$\Delta p_{ax} = 134\ \mathring{M}_w^2 \qquad (4.5)$$

The above equation was obtained by assuming an intube relationship applies for the axial pressure drop. Although the leakage area is small, it is conservatively assumed that 20% of the total baffle leakage passes through the window. The axial losses are calculated for the crossflow only flowing through the window, and with the crossflow plus baffle

leakage flowing through the window. The difference in these two values is the effect of the leakage on the windowflow pressure drop. From Table 4.3 it is seen that when this value is compared with the total windowflow pressure drop, the effect is at most 16%. This in turn means a maximum error of about 9% in the windowflow flowrate (and subsequently the crossflow flowrate). Even allowing for this margin of error in the crossflow flowrate, such large differences between the leakage crossflow pressure drop and the no-leakage pressure drop cannot be directly accounted for.

Overall it is concluded that the effect of crossflow/leakage interaction does exist and appears to be a very strong effect. It is thus necessary to be able to predict this effect in order to ensure accurate prediction of shellside pressure drop.

4.3 The Development of a Crossflow/Leakage Interaction Model

4.3.1 The Prediction of Crossflow Pressure Drop with no Baffle Leakage Using the Permeability Concept

It is convenient to use the permeability concept as described by Butterworth (1977). Consider the flow through a rectangular tube bank (Figure 4.5) as flow in a porous medium. The equations governing the flow assuming steady state and neglecting gravitational effects can be written

TABLE 4.3: THE EFFECT OF BAFFLE LEAKAGE ON WINDOWFLOW PRESSURE DROP

$\dot{M}_T$	$\dot{M}_c$	$\dot{M}_L$	$\dot{M}_{Lw}$	Δp_1	Δp_2	Δp_w	$\frac{\Delta p_2 - \Delta p_1}{\Delta p_w}$
1.58	0.50	1.08	0.22	33.5	69.5	227.9	0.158
2.37	0.73	1.64	0.33	71.4	131.3	477.0	0.166
3.16	0.99	2.17	0.43	131.3	270.2	868.1	0.160
4.74	1.47	3.27	0.65	289.6	602.2	1878.1	0.166
6.32	1.98	4.34	0.87	525.3	1088.4	3312.9	0.170
7.90	2.50	5.40	1.08	837.5	1717.4	5218.4	0.169

Δp_1 = axial pressure drop of crossflow only

Δp_2 = axial pressure drop of crossflow and leakage

$\dot{M}_{Lw}$ ias assumed to be $\dot{M}_L/5$

FIGURE 4.5: IDEAL TUBE BANK

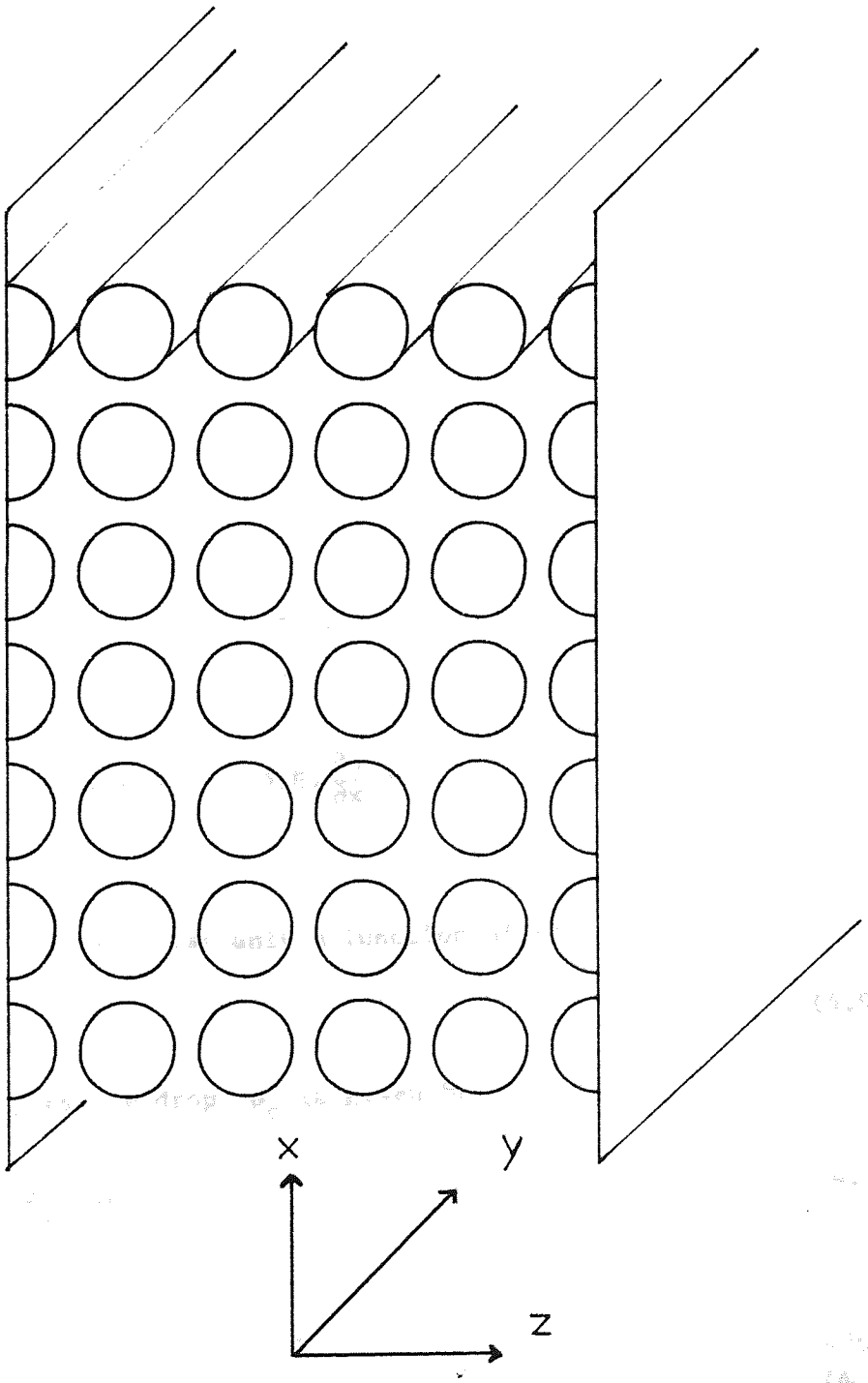

in terms of superficial velocities as

$$\frac{\rho}{\varepsilon}\left(u\frac{\partial u}{\partial x} + v\frac{\partial u}{\partial y}\right) = -\eta\bar{R}_x u - \frac{\partial p}{\partial x} \tag{4.6}$$

$$\frac{\rho}{\varepsilon}\left(u\frac{\partial v}{\partial x} + v\frac{\partial v}{\partial y}\right) = -\eta\bar{R}_y v - \frac{\partial p}{\partial y} \tag{4.7}$$

where $\bar{R}_x$, $\bar{R}_y$ are mean resistances incorporating second order effects etc.

The z direction is not considered as there is no flow in the z direction.

The x is the crossflow, the y direction the baffle leakage flow.

The mass continuity equation is

$$\frac{\partial u}{\partial x} + \frac{\partial v}{\partial y} = 0 \tag{4.8}$$

In the case where there is no baffle leakage, there is no bulk flow or pressure gradient in the y direction making equation 4.7 redundant as $v = 0$ and hence $\frac{\partial v}{\partial x} = 0, \frac{\partial v}{\partial y} = 0$.

As $\frac{\partial v}{\partial y} = 0$, then from equation 4.8, $\frac{\partial u}{\partial x} = 0$.

Equation 4.6 reduces to (as only a function of x)

$$\frac{dp}{dx} = -\eta\bar{R}_x u \tag{4.9}$$

The crossflow pressure drop p_c is given by

$$\int_{p_1}^{p_2} dp = -\int_0^L \bar{R}_x u \, dx \tag{4.10a}$$

$$p_2 - p_1 = -\bar{R}_x u L \tag{4.10b}$$

or $\Delta p_c = \eta \bar{R}_x u L$ (4.11)

It can be seen that the above equation can be expressed in the more usual friction factor form where $\bar{R}_x$ contains physical property, geometric and process parameters.

4.3.2. The Prediction of Crossflow Pressure Drop with Baffle Leakage Using the Permeability Concept

Now consider a more complex flow situtation where there is baffle leakage in the y direction. The equations governing the flow are as equations 4.6 and 4.7. A full solution is only possible by numerical techniques but a few assumptions are made enabling an analytical solution to be obtained.

1) Assume the crossflow velocity, u, is constant in the direction of flow, i.e.

$u \neq f(x)$

hence

$$\frac{\partial u}{\partial x} = 0$$

from equation 4.8 then $\frac{\partial v}{\partial y} = 0$.

2) Assume the velocity profile of the leakage is constant in the x axis. This is reasonable as the axial leakage profile will be influenced by the upstream and downstream conditions. The

leakage only travels in one direction whereas the crossflow alternately crosses the leakage stream. It is assumed that this has the effect of "averaging" out the leakage velocity profile. Hence

$$\frac{\partial v}{\partial x} = 0 \text{ or } v = \text{constant}$$

Equation 4.7 reduces to

$$\frac{\rho}{\varepsilon}(v \frac{\partial u}{\partial y}) = -\eta \bar{R}_x u - \frac{\partial p}{\partial x} \tag{4.12}$$

rearranging and integrating gives

$$u = \frac{\Delta p_c}{\eta \bar{R}_x L} (1 - \exp(\frac{-y\varepsilon\eta \bar{R}_x}{\rho v})) \tag{4.13}$$

The above equation shows that the local velocity u is a function of the leakage velocity v.

The average velocity, $\bar{u}$, can be obtained by integrating equation 4.13 using

$$\bar{u} = \frac{\int_0^{L_B} u \, dy}{\int_0^{L_B} dy} \tag{4.14}$$

hence

$$\bar{u} = \frac{1}{L_B} (\frac{\Delta p_c}{\eta \bar{R}_x L}) \int_0^{L_B} (1 - \exp(\frac{-\varepsilon\eta \bar{R}_x y}{\rho v})) \, dy \tag{4.15}$$

integrating, rearranging and isolating gives

$$\Delta p_c = \frac{\eta \bar{u} \bar{R}_x L}{1 - (\frac{\rho v}{\varepsilon\eta \bar{R}_x L_B})(1 - \exp(\frac{-\varepsilon\eta \bar{R}_x L_B}{\rho v}))} \tag{4.16}$$

The average velocity is easily calculated being

$$\bar{u} = \frac{\dot{M}_c}{\rho A_c} \tag{4.17}$$

Equation 4.16 is interesting as it means the crossflow pressure drop can be calculated knowing the superficial leakage velocity v and the average crossflow velocity, $\bar{u}$.

Comparing equation 4.16 and equation 4.11 noting $u = \bar{u}$ for equation 4.11, then it is seen that equation 4.11 is a trivial solution of equation 4.16 when $v = 0$.

Unfortunately equation 4.16 is not easy to use without obtaining a representative value of $\bar{R}_x$.

4.3.3. The Calculation of the Mean Crossflow Resistance, $\bar{R}_x$.

For an ideal tube bank where u is a constant, the resistance $\bar{R}_x$ can be written as

$$\bar{R}_x = m \bar{u}^n \qquad (4.18)$$

where m, n are constants.

The above equation only applies to the local conditions (R_x, u where $R_x = f(y)$, $u = f(y)$) when baffle leakage is present i.e.

$$R_x = m u^n \qquad (4.19)$$

The mean resistance, $\bar{R}_x$, is given by

$$\bar{R}_x = \frac{\int_0^{L_B} R_x \, dy}{\int_0^{L_B} dy} \tag{4.20}$$

or

$$\bar{R}_x = \frac{\int_0^{L_B} m \, u^n \, dy}{\int_0^{L_B} dy} \tag{4.21}$$

substituting 4.13 into 4.21 gives

$$\bar{R}_x = \frac{m\int_0^{L_B} \left(\frac{\Delta p_c}{\eta \bar{R}_x L}\left(1 - \exp\left(\frac{-\varepsilon\eta\bar{R}_x y}{\rho v}\right)\right)\right)^n dy}{\int_0^{L_B} dy} \tag{4.22}$$

Using equation 4.22 and equation 4.16 one could obtain Δp_c and $\bar{R}_x$ (the solution is simultaneous as Δp_c is needed to evaluate $\bar{R}_x$ and vice versa). Furthermore no analytical solution can be obtained for equation 4.22 as n is a non-integer value between zero and unity and also $\bar{R}_x$ appears on both sides of the equation. Appendix 4 gives a numerical procedure which could be used but it is realised that the procedure is very lengthy and considering the assumptions in this model, is unsuitable for use in a design method.

However, if one examines equation 4.19 realising that the exponent n usually varies between 0.8 and 0.9, i.e. $n \simeq 1$. Equation 4.21 then becomes

$$\bar{R}_x = \frac{\int_0^{L_B} m \, u \, dy}{\int_0^{L_B} dy} \tag{4.23}$$

or

$$\bar{R}_x = m\,\bar{u} \tag{4.24}$$

It is realised that equation 4.24 is a simplification but considering the errors involved by not allowing for baffle leakage (giving a factor of 2 difference in the pressure drop) it is considered a reasonable assumption. The advantage of this simplification is that equation 4.24 may be substituted directly into equation 4.16 giving

$$\Delta p_c = \frac{\eta\, m\, \bar{u}^2 L}{1 - \left(\frac{\rho v}{m\varepsilon\eta\bar{u}L_B}\right)\left(1 - \exp\left(\frac{-m\varepsilon\eta\bar{u}L_B}{\rho v}\right)\right)} \tag{4.25}$$

It is convenient to define a crossflow/leakage interaction factor, F_L, such that

$$\Delta p_{c_{leakage}} = \Delta p_{c_{no\text{-}leakage}} \cdot F_L \tag{4.26}$$

leading to

$$F_L = \left(1 - \left(\frac{\rho v}{m\varepsilon\eta\bar{u}L_B}\right)\left(1 - \exp\left(\frac{-m\varepsilon\eta\bar{u}L_B}{\rho v}\right)\right)\right)^{-1} \tag{4.27}$$

It is easy to see how equation 4.27 is incorporated into a multi-stream model since $\bar{u}$, v are calculated (or can be calculated) as part of the normal solution procedure.

4.4 Validation of the Crossflow/Leakage Interaction Model

4.4.1 The model has been developed from the flow equations assuming a rectangular tube bundle. In a real exchanger the bundle is circular.

Also bundle bypassing occurs and it is reasonable to assume the shell-baffle leakage interacts with the bypass stream only and the tube-baffle leakage interacts with the crossflow stream only. This means the solution of the crossflow pressure drop is iterative, there being two parallel flowstreams. A flow diagram showing the necessary procedure is given in Figure 4.6

In order to be able to predict the effect of interaction it is necessary to be able to predict the baffle leakage flowsplit. This is done using the equations of Grant (1972). The same exchanger used to identify the experimental effect i.e. the 18.4% baffle cut exchanger, is used to validate the crossflow/leakage interaction model.

4.4.2 Two ideal relationships are required for the pressure drops in the crossflow and the bypass stream which are

$$\Delta p_c = \eta \bar{u} \bar{R}_c L \quad \text{(Butterworth (1979))} \tag{4.28}$$

and

$$\Delta p_b = 4 f_b N_b \frac{\rho \bar{u}_b^2}{2} \quad \text{(Russell and Wills (1983))} \tag{4.29}$$

As

$$\dot{M}_{cr} = \dot{M}_c + M_b \tag{4.30}$$

Using equations 4.30, 4.28 and 4.29 the crossflow pressure drop can be obtained as

$$\Delta p_c = \Delta p_b \tag{4.31}$$

FIGURE 4.6 : ITERATION SCHEME FOR THE CROSSFLOW PRESSURE DROP

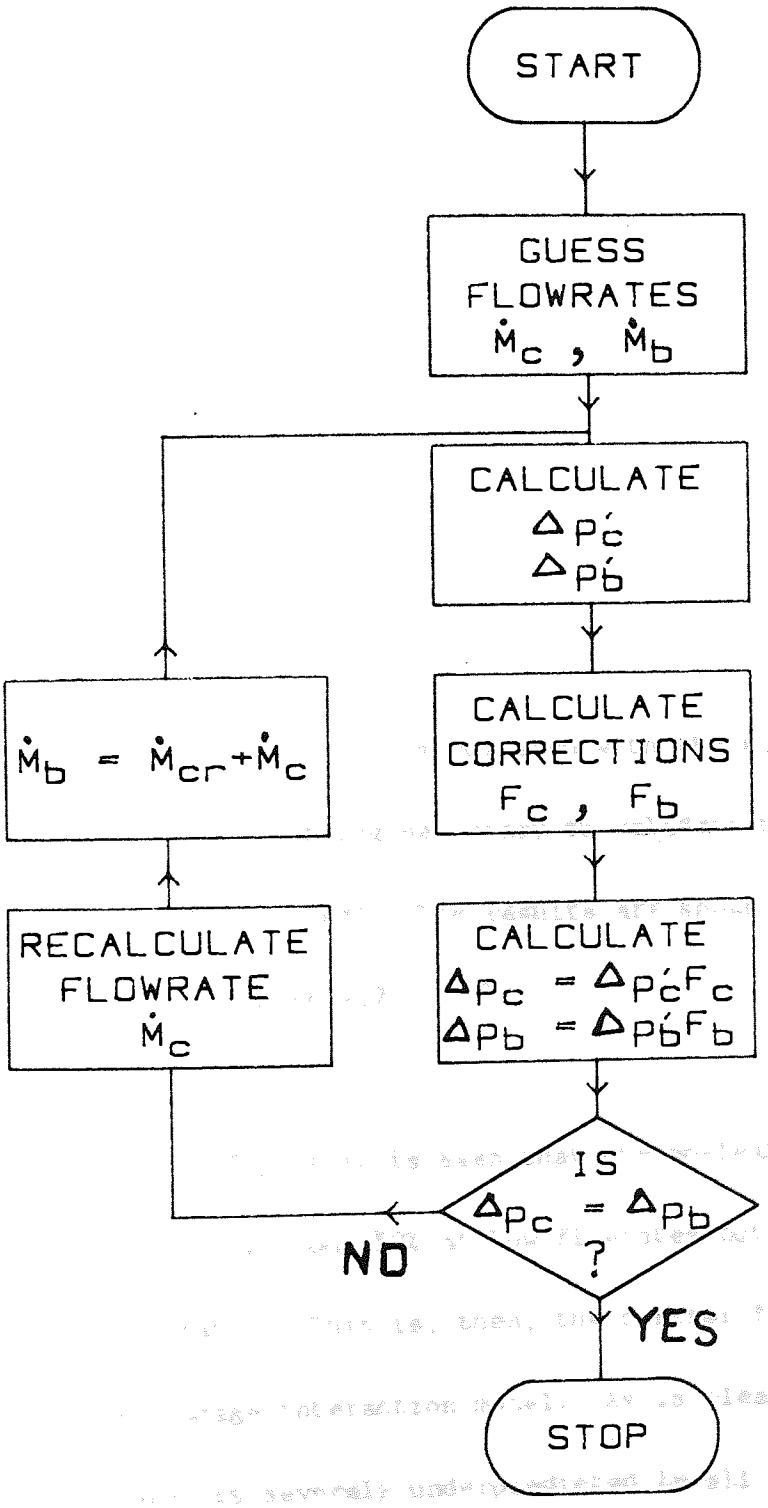

To allow for the effect of crossflow/leakage interaction equations 4.28 and 4.29 are modified using

$$\Delta p_c = F_{Lc}\, \eta \bar{u}_c\, \bar{R}_c L \tag{4.32}$$

$$\Delta p_b = F_{Lb}\, \eta \bar{u}_b\, \bar{R}_b L \tag{4.33}$$

where the bypass equation is expressed in a different form. Since F_{Lc}, F_{Lb} depend on $\dot{M}_c$ and $\dot{M}_b$ it is necessary to evaluate F_{Lc} and F_{Lb} within the iteration scheme.

4.4.3 The pressure drop is predicted for the exchanger with and without the effect of crossflow leakage interaction and also the no-interaction pressure drop is compared with the equivalent no-leakage pressure drop (this being necessary to validate the accuracy of the correlations being used). The results are shown in Table 4.4 and are plotted in Figure 4.7

From this figure it is seen that the no-leakage pressure drop is underpredicted by about 50% at low flowrates but gives reasonable results at high flowrates. This is, then, the control for evaluating the crossflow/leakage interaction model. As is clearly seen the leakage pressure drop is severely underpredicted in all cases if the effect of

TABLE 4.4: PREDICTIONS OF CROSSFLOW PRESSURE DROP WITH AND WITHOUT THE EFFECT OF CROSSFLOW/LEAKAGE INTERACTION

CROSSFLOW FLOWRATE (kg/s)	NO LEAKAGE*			LEAKAGE			
	EXPERIMENTAL PRESSURE DROP (N/m^2)	PREDICTED PRESSURE DROP (N/m^2)	PREDICTED EXPERIMENTAL RATIO -	EXPERIMENTAL PRESSURE DROP (N/m^2)	PREDICTED PRESSURE DROP (N/m^2)		PREDICTED EXPERIMENTAL RATIO	
					No-Interaction	Interaction	No-Interaction	Interaction
0.22	54.0	23.6	0.437	68.9	23.6	37.1	0.343	0.538
0.37	124.0	67.1	0.541	163.6	67.1	106.4	0.410	0.650
0.50	200.8	122.4	0.610	288.9	122.4	197.5	0.424	0.684
0.73	367.9	261.1	0.710	582.0	261.1	424.9	0.449	0.730
0.99	5990.0	480.2	0.802	1034.5	480.2	777.2	0.464	0.751
1.47	1127.5	1058.9	0.939	2126.4	1058.9	1719.0	0.498	0.808
1.98	1815.8	1921.0	0.945	3586.9	1921.0	3108.6	0.536	0.867
2.50	2637.0	3062.4	1.161	5380.3	3062.4	4940.1	0.569	0.919

*Equivalent values.

FIGURE 4.7 : COMPARISON OF CROSSFLOW PRESSURE DROP PREDICTIONS

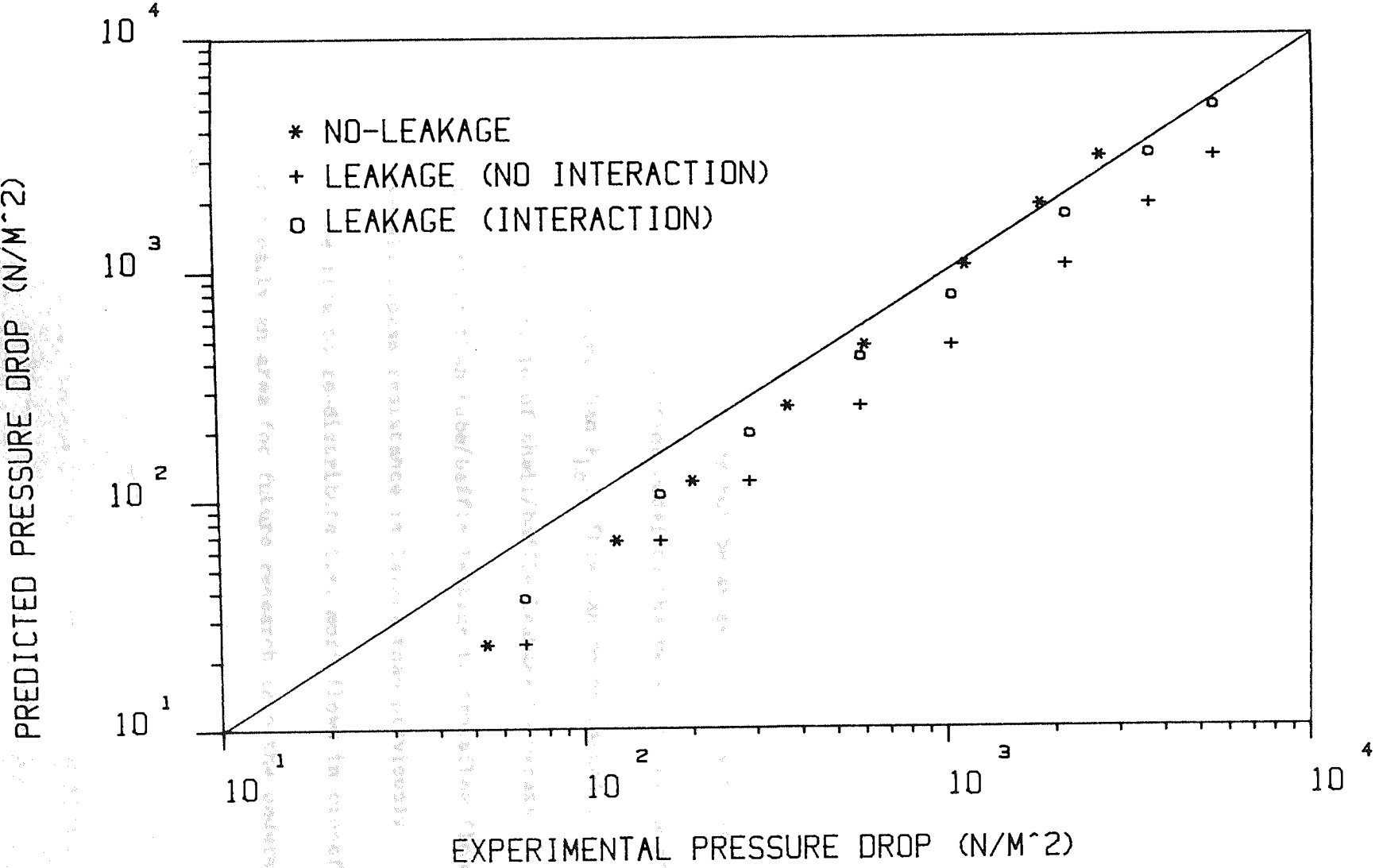

crossflow/leakage interaction is not taken into account. When the effect is included the predictions are similar to the no-leakage control i.e. about 50% low at low flowrates and fairly reasonable at high flowrates.

Since the leakage predictions give results of a similar magnitude to the no-leakage predictions when the model for crossflow leakage interaction is included, it is concluded that the model for crossflow/leakage interaction is an improvement over the models which do not allow for crossflow/leakage interaction.

One striking possibility to arise from this model is that the effect of bypassing in an exchanger may not be as severe as is often supposed. In applying the interaction model to the bypass it is found that F_{Lb} is usually much larger than F_{Lc}. This can be explained in physical terms because the ratio of shell/baffle leakage to bypass flowrates is usually larger than tube/baffle leakage to crossflow flowrates. As a result the overall bypass resistance is larger than previously supposed, causing the flow to re-distribute i.e. more flows in crossflow. This of course, is clearly an area for future research into the understanding of shellside flow.

5.0 THE PENETRATION OF CROSSFLOW INTO THE WINDOW ZONE

This chapter describes a model to account for the crossflow effects in the window zone. The model is based on simple considerations of the resistances to flow in the axial and crossflow directions. It is shown that the average penetration is always less than 50%.

5.1 Crossflow-in-the-Window

As shown in Chapter 3, a crucial factor in shellside pressure drop is the effect of crossflow-in-the-window. In the overlap region the fluid is in crossflow and then it is turned through 180^{o} in the window region to pass through the next overlap region. Clearly the shellside fluid cannot instantly change direction but is gradually turned by the shellside geometry. The crossflow diminishes in the window from the crossflow flowrate at the baffle edge to zero at the shell where crossflow ceases to exist.

There are two main ways of allowing for the crossflow-in-the-window, one being implicit and the other explicit. The first approach is to allow for the crossflow-in-the-window effects empirically as in the windowflow pressure drop correlation of Grant and Murray (1972) or, secondly, defining a crossflow extent which is larger than the overlap region, as per Tinker (1951), Donohue (1949), Moore (1974) and many others.

The second approach has been adopted by the majority of research workers with the simple assumption that "on average" the crossflow flows to the centroids of the window region. This approach is considered in this work to be the best approach but the assumption of crossflow flowing to the centroid "on average" is believed to be an overestimate.

Consider an "idealised window zone" as in Figure 5.1. Fluid flowing along path A-F has to travel further than B-E which, in turn, has to travel further than path C-D. Ultimately the pressure drop along the path A-E will be greater than C-D. Since the pressure drops along the paths will be approximately the same, then the mass of fluid travelling along path C-D will be larger than the mass of fluid flowing along A-E, which means ultimately a non-linear velocity profile in the plane of the baffle cut. This means the fluid's centre of gravity in the window is nearer the baffle edge than the centroid of the window. The next section describes a model for predicting this centre of gravity i.e. the true average penetration of the crossflow-into-the-window zone.

5.2 The Development of a Model to Predict the Average Penetration of the Crossflow-in-the-Window

First consider the models which assume, that the crossflow flows on average to the centroid of the windows by considering an ideal exchanger with a rectangular window. The total crossflow flowrate is $\dot{M}_{cr}$ at the

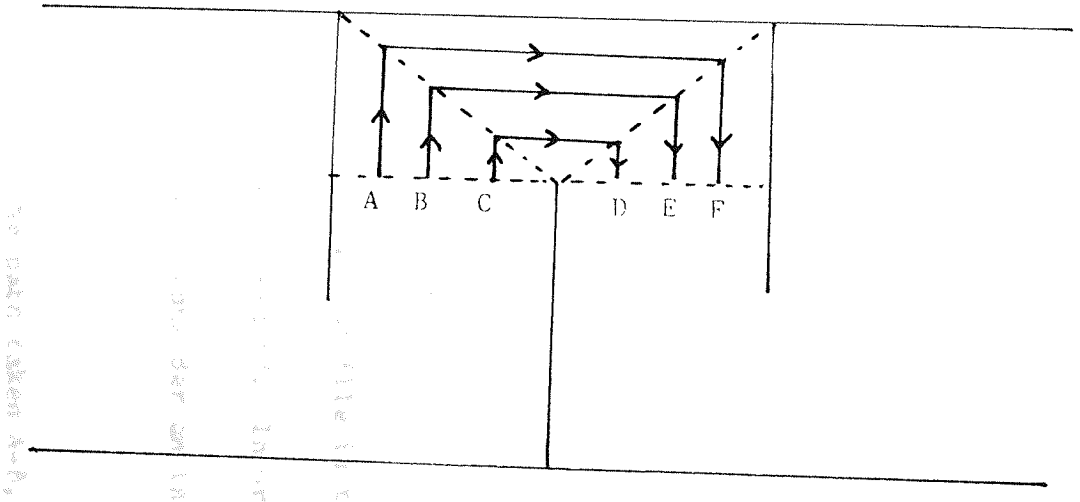

Figure 5.1 : AN IDEALISED WINDOWFLOW ZONE

baffle-edge as in Figure 5.2, and is zero at the edge of the shell. Assuming a flat velocity profile in the window means that the fluid flows to the centroid on average. However, as shown in Section 5.1, this is unlikely.

However, let us first examine this case where it is assumed that the fluid flows to the centroid. The crossflow flowrate boundary conditions are

$$\mathring{M}_x = \mathring{M}_{cr} \text{ at } x = 0 \tag{5.1}$$

$$\mathring{M}_x = 0 \quad \text{at } x = h \tag{5.2}$$

Because it is assumed that the windowflow velocity profile is flat in the axial direction then

$$\frac{d\mathring{M}_x}{dx} = c \tag{5.3}$$

integrating gives

$$\mathring{M}_x = \mathring{M}_{cr} \left(1 - \frac{x}{h}\right) \tag{5.4}$$

However the velocity profile is thought not to be flat and hence the above equation is invalid. In order to predict the velocity profile, it is necessary to consider an infinite window as in Figure 5.3.

Consider the path taken A-B, B-C, C-D at a position x where $0 < x < \infty$

For path A-B and path C-D

$$\frac{d}{dx}(\Delta p_x) = -4 \frac{f_x}{P_x} \frac{\rho u_x^2}{2} \tag{5.5}$$

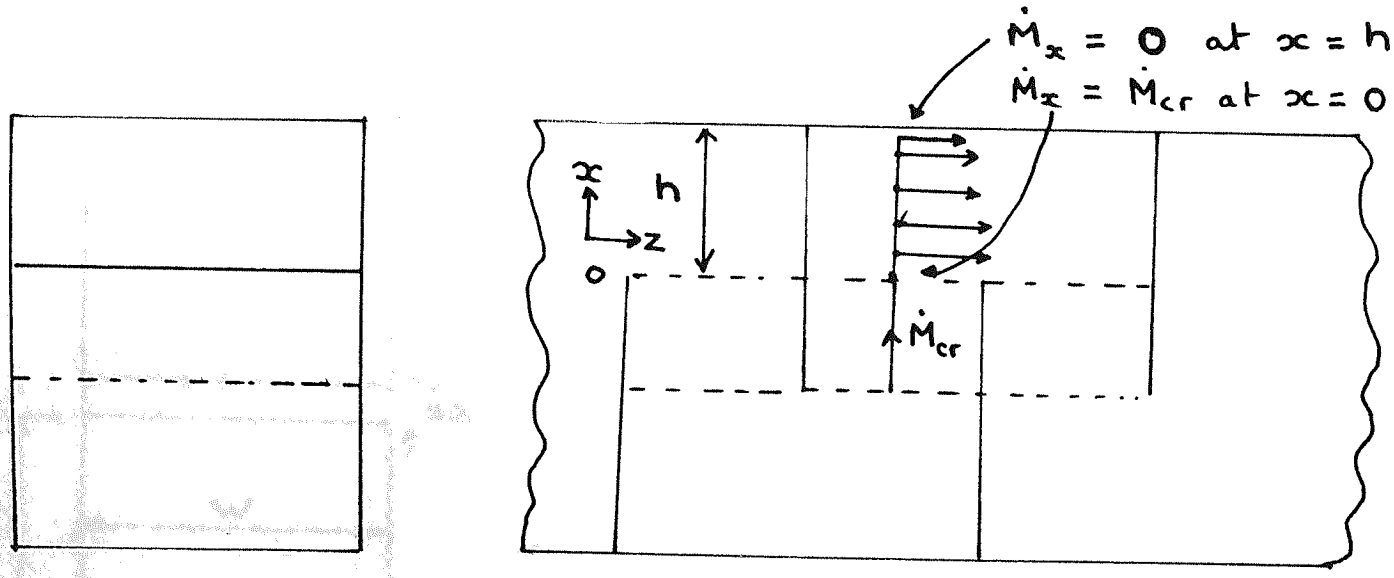

Figure 5.2 : AN EXCHANGER WITH A RECTANGULAR WINDOW

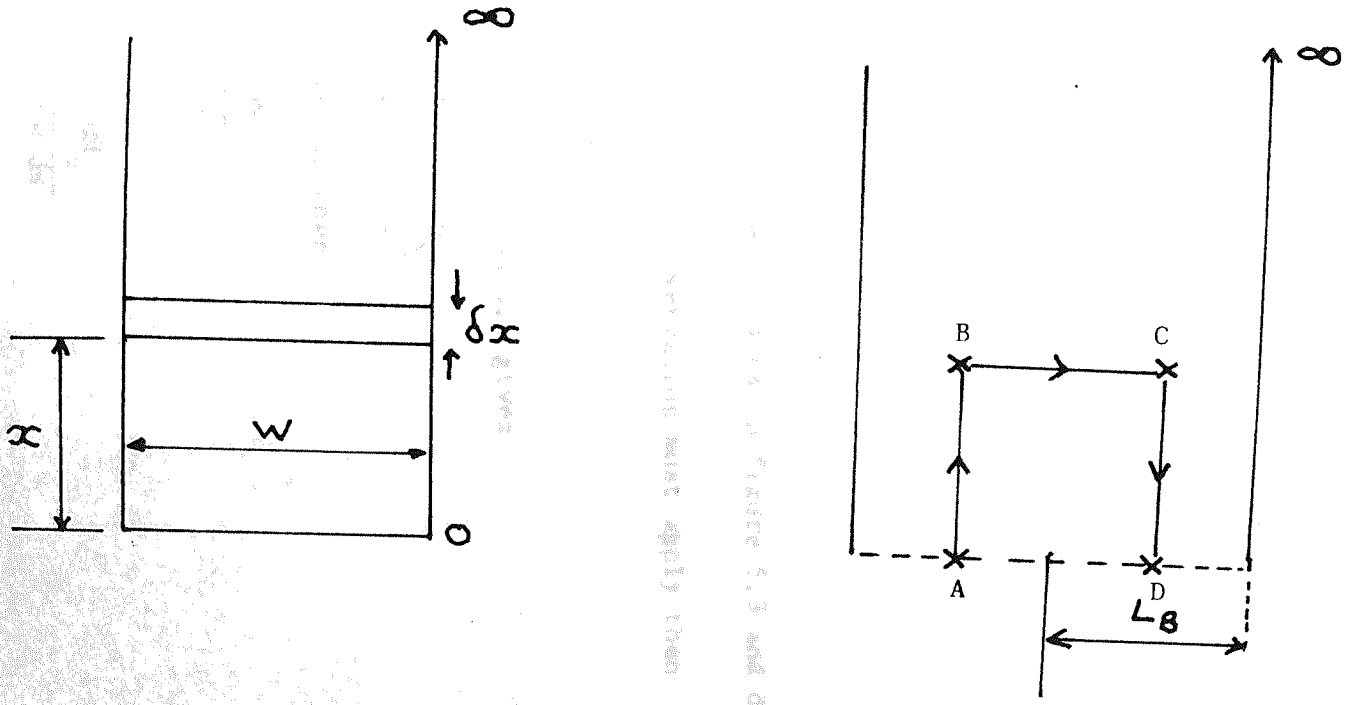

Figure 5.3 : AN EXCHANGER WITH AN INFINITE WINDOW

As the exchanger is assumed to be rectangular then the velocity u_x at any position x is

$$u_x = \frac{\dot{M}_x}{\rho\, w\, L_B} \tag{5.6}$$

and hence from 5.5 and 5.6

$$\frac{d}{dx}(\Delta p_x) = -\,4\,\frac{f_x}{2\,P_x\,L_B\,w^2}\,\frac{\rho u_x^2}{2} \tag{5.7}$$

For path B–C, the pressure gradient is given by

$$\frac{d}{dz}(\Delta p_z) = -\,4\frac{f_z}{D_e}\,\frac{\rho u_z^2}{2} \tag{5.8}$$

As u_z is a function of x only, then integrating equation 5.8 gives

$$\Delta p_z = 4\,\frac{f_z\,L_B}{D_e}\,\frac{\rho u_z^2}{2} \tag{5.9}$$

The axial velocity is given by

$$u_z = \frac{d\dot{M}_z}{\rho\, w\, dx} \tag{5.10}$$

where wdx is the elemental area in figure 5.3 and $d\dot{M}_z$ is the elemental flowrate. Since mass conservation must apply then

$$\dot{M}_z = \dot{M}_{cr} - \dot{M}_x \tag{5.11}$$

Differentiating equation 5.1 gives

$$\frac{d\dot{M}_z}{dx} = \frac{d\dot{M}_{cr}}{dx} - \frac{d\dot{M}_x}{dx} \tag{5.12}$$

As $\dot{M}_{cr}$ is constant then

$$\frac{d\dot{M}_z}{dx} = -\,\frac{d\dot{M}_x}{dx} \tag{5.13}$$

and hence

$$u_z = -\,\frac{d\dot{M}_x}{\rho\, w\, dx} \tag{5.14}$$

and equation 5.9 becomes

$$\Delta p_z = - 4 \frac{f_x L_B}{2 D_e \rho w^2} \left(\frac{d\dot{M}_x}{dx}\right)^2 \qquad (5.15)$$

The pressure drop between points A-D is

$$\Delta p_w = 2\Delta p_x + \Delta p_z + \Delta p_\phi \qquad (5.16)$$

where Δp_ϕ is the pressure drop due to the geometric shape of the window. It is assumed here that the geometric pressure drop is a function of the shape of the window and not a function of the position x, and hence

$$\frac{d}{dx}(\Delta p_\phi) = 0 \qquad (5.17)$$

Differentiating equation 5.16 and substituting equation 5.17 gives

$$\frac{d}{dx}(\Delta p_w) = \frac{d}{dx}(2\Delta p_x) + \frac{d}{dx}(\Delta p_z) \qquad (5.18)$$

As the pressure drop from A to D is constant regardless of how far the fluid flows in the x direction then

$$\frac{d}{dx}(\Delta p_w) = 0 \qquad (5.19)$$

and hence

$$2 \frac{4 f_x}{2 P_x \rho L_B^2 w^2} \dot{M}_x^2 + \frac{d}{dx}\left(\frac{4 f_z L_b}{2 \rho D_e w^2}\right)\left(\frac{d\dot{M}_x}{dx}\right)^2 = 0 \qquad (5.20)$$

i.e.

$$A \dot{M}_x^2 + \frac{d}{dx}\left(B\left(\frac{d\dot{M}_x}{dx}\right)^2\right) = 0 \qquad (5.21)$$

A solution is

$$\dot{M}_x = C \exp(ax) \qquad (5.22)$$

The solution of the differential equation is then

$$A \dot{M}_x^2 + 2 B a^3 \dot{M}_x^2 = 0 \qquad (5.23)$$

i.e.

$$(A + 2 B a^3) \dot{M}_x^2 = 0 \qquad (5.24)$$

Since $\dot{M}_x \neq 0$ then

$$a = \sqrt[3]{\frac{A}{2\ B}} \tag{5.25}$$

Using the boundary condition,

$$\dot{M}_x = \dot{M}_{cr} \text{ at } x = 0 \tag{5.26}$$

then

$$\dot{M}_x = \dot{M}_{cr} \exp(-ax) \tag{5.27}$$

or

$$\dot{M}_x = \dot{M}_{cr} \exp\left(-\frac{1}{L_B} \sqrt[3]{\frac{f_x\ D_e}{f_z\ P_x}}\ x\right) \tag{5.28}$$

Equation 5.28 gives the velocity profile for an exchanger with an infinite window, the velocity profile being due to frictional effects. Of course, in a real exchanger the window is not infinite, and in a real exchanger it is assumed that equation 5.28 and equation 5.4 may be combined, the exponential decay of the crossflow due to friction being imposed on the geometric decay i.e.

$$\dot{M}_x = \dot{M}_{cr} \left(1 - \frac{x}{h}\right) \exp\left(-\frac{1}{L_B} \sqrt[3]{\frac{f_x\ D_e}{f_z\ P_x}}\ x\right) \tag{5.29}$$

The fractional penetration is defined as the position at which $\dot{M}_x = \dot{M}_{cr}/2$. As the fractional penetration, f, = x/h then

$$\frac{\dot{M}_{cr}}{2} = \dot{M}_{cr}(1 - f) \exp\left(-\frac{h}{L_B} \sqrt[3]{\frac{f_x\ D_e}{f_z\ P_x}}\ f\right) \tag{5.30}$$

or

$$f = 1 - \left(2 \exp\left(-\frac{h}{L_B} \sqrt[3]{\frac{f_x\ D_e}{f_z\ P_x}}\ f\right)\right)^{-1} \tag{5.31}$$

This equation is transcendental and can only be solved interatively. However, it is useful to consider the limits of f.

Consider 5.31 as

$$f = 1 - (2 \exp(-jf))^{-1} \text{ where j is positive} \tag{5.32}$$

As $j \to 0$, $f \to 0.5$ (but $j > 0$) and as $j \to \infty$, $f \to 0$ (cannot be negative) i.e. $0 < f < 0.5$ showing that the average fractional penetration is not to the centroid of the window.

The above analysis was developed for a rectangular bundle and a similar analysis could be performed for a circular bundle but the solution becomes very unwieldy. Fortunately, the crossflow area is nearly constant in the window as tubes are removed as one progresses to the edge of the shell, and so it is reasonable to apply the above analysis to a circular bundle.

This model cannot be directly tested, but it is used as part of the windowflow pressure drop model developed in Chapter 6 and it is shown that application of this model significantly improves the predictions of windowflow pressure drop.

6. A MODEL FOR WINDOWFLOW PRESSURE DROP

This chapter describes the development of a model to predict windowflow pressure drop. The model is compared with existing models known in detail against, both, openly available and proprietary data. The model is shown to be as accurate as the best available empirical correlation without resorting to any empirical correlations of windowflow pressure drop data itself.

6.1 The Development of A Mechanistic Windowflow Pressure Drop Model

In order to simplify the task of developing a model, it is necessary to consider the simpler case where there is no baffle leakage present. Chapter 7 allows for the effect of leakage in the window zone.

Many factors influence windowflow pressure drop but they can be divided into two main categories:-

1) frictional effects,

and

2) geometric effects.

The frictional effects occur because of the form drag on the shellside fluid as it flows along and/or across the tubes. The geometric effects occur

because of the general shape of the window zone, being largely influenced by the baffle geometry.

Taking the frictional effects first, then these will be of two types:-

1) axial frictional losses as the fluid flows along the tubes, and

2) crossflow losses as the fluid flows normal to the tubes.

In practice it is expected that the true flow will be a combination of both of the above effects but it is convenient to consider the two effects separately. In chapter 5, a model has been presented to allow for the crossflow losses. Comparison of the magnitude of these losses with the expected axial losses has strongly indicated that the axial portion of the frictional losses may be safely ignored when developing a windowflow pressure drop model. Consequently the two streams may be considered as one stream i.e. windowflow and windowflow bypass may be treated as one stream.

Taking the geometric losses next, it is contended that the number of separate effects that need to be considered can be reduced to a minimum of three, these being,

1) Momentum losses as the shellside fluid turns through 180^{o} as it makes repeated crosspasses of the exchanger.

2) Expansion losses as the fluid flows from a smaller crossflow area to a larger windowflow area (or vice versa).

3) Contraction losses as the fluid flows from a larger crossflow area to a smaller windowflow area (or vice versa).

It is speculated here that non-ideal effects, such as recirculation of the fluid in the window are fairly small in comparison to the above three effects.

When considering the geometric effects, previous workers e.g. Palen and Taborek (1969), Bell (1963), Moore (1979), have all included effects for the turning losses, but none of them have taken the changing area of the flow area, as the fluid flows through the window, into account. This may be because it is generally recognised by designers that the flow area should not alter significantly in any case (hence minimising the contraction/ expansion losses). However, in practice, this 'rule of thumb' is often violated with the crossflow area being significantly different to the windowflow area, especially when shellside pressure drop, itself, is an important criterion.

Sections 6.2 to 6.4 describe the proposed models for the three effects mentioned above, with section 6.5 describing the validation of the windowflow pressure drop model with experimental data, and finally,

section 6.6 discusses the results of the validation, along with the predictions of the other methods known in detail.

6.2 Turning Losses in the Window

In order to develop a model for the turning losses, it is necessary to consider a uniform pipe with a smooth 90^{o} bend. The pressure drop is given by

$$\Delta p_{turning} = f \{ Eu \} \frac{\rho v^2}{2} \tag{6.1}$$

where the Euler number (Eu) is defined by

$$Eu = \Delta p/(\rho v^2/2) \tag{6.2}$$

for a 90^{o} bend, the generally accepted value for $f \{ Eu \}$ is 1 e.g. Coulson and Richardson (1970) give $f \{ Eu \} \simeq 0.8 - 1.$ and hence a mean value of 1 is reasonable. Clearly for two successive 90^{o} bends (i.e. a 180^{o} bend) the pressure drop is then

$$\Delta p = 2 \frac{\rho v^2}{2} \tag{6.3}$$

It is suggested in this work that the turning losses in the window can be approximated by

$$\Delta p_{turning} = \frac{\rho v_w^2}{2} + \frac{\rho v_{cr}^2}{2} \tag{6.4}$$

where the above equation allows for the fact that the downstream velocity in the first 90^{o} bend is v_w and v_{cr} for the second 90^{o} bend. The velocity v_w refers to all the flow in the plane of the window (including windowflow bypass)and v_{cr} refers to all the flow in the plane of crossflow including bypass. Now the window velocity may be related to the crossflow by

$$\dot{M}_w = \rho A_{cr} v_{cr} = \rho A_w v_w \tag{6.5}$$

and therefore

$$\Delta p_{turning} = (1 + (\frac{A_w}{A_{cr}})^2) \frac{\rho v_w^2}{2} \quad (6.6)$$

When $A_w = A_{cr}$ then

$$\Delta p_{turning} = 2 \frac{\rho v_w^2}{2} \quad (6.7)$$

Compare this with the Bell method which gives

$$\Delta p_w = (2 + 0.6\ N_{tw}) \frac{\rho v_z^2}{2} \quad (6.8)$$

If $A_w = A_{cr}$ then $v_z = v_w$ and hence

$$\Delta p_w = (2 + 0.6\ N_{tw}) \frac{\rho v_w^2}{2} \quad (6.9)$$

where the first term (2) in the brackets are the turning losses. Thus equation 6.6 is consistent with other methods when $A_w = A_{cr}$.

6.3 Expansion Losses in the Window

In order to allow for the expansion losses, it is assumed that the momentum losses due to expansion are not recovered. It is assumed that the expansion losses can be treated by analogy to a sudden expansion in two pipes of different diameter.

Holland (1973) gives the sudden expansion losses as fluid flows from a pipe of diameter d_1 to a larger pipe of diameter d_2 as

$$\Delta p = (1 - (d_1/d_2)^2)^2 \frac{\rho v^2}{2} \quad (6.10)$$

where v is the velocity in the smaller pipe.

In a shell-and-tube exchanger, the window area (A_w) may be greater or smaller than the crossflow area (A_c). When $A_w < A_{cr}$ the expansion loss is given by anology as

$$\Delta p_{expansion} = (1 - \frac{A_w}{A_{cr}})^2 \frac{\rho v_w^2}{2} \qquad (6.11)$$

and when $A_w > A_{cr}$

$$\Delta p_{expansion} = (1 - \frac{A_{cr}}{A_w})^2 \frac{\rho v_{cr}^2}{2} \qquad (6.12)$$

However from equation 6.5 it is seen that when $A_{cr} > A_w$

$$\Delta p_{expansion} = (1 - \frac{A_{cr}}{A_w})^2 (\frac{A_w}{A_{cr}})^2 \frac{\rho v_w^2}{2} \qquad (6.13)$$

or

$$\Delta p_{expansion} = (1 - \frac{A_w}{A_{cr}})^2 \frac{\rho v_w^2}{2} \qquad (6.14)$$

which is identical to equation 6.11 i.e. equation 6.11 may be used if the windowflow area is greater or smaller than the crossflow area.

When $A_w = A_{cr}$ then $\Delta p_{expansion} = 0$ as is expected because there is no overall change in velocity as the fluid flows through the window (although there will be local changes of course).

6.4 Contraction Losses in the Window

The contraction losses are also treated in the same manner as the expansion losses i.e. a sudden contraction. Holland (1973) gives the contraction losses as

$$\Delta p_{contraction} = K \frac{\rho v^2}{2} \qquad (6.15)$$

where $K = 0.4\ (1.25 - (\frac{d_1}{d_2})^2)$ for $(\frac{d_1}{d_2})^2 < 0.715$ (6.16)

or $K = 0.75\ (1 - (\frac{d_1}{d_2})^2)$ for $0.715 < (\frac{d_1}{d_2})^2 \leqslant 1$ (6.17)

By analogy then the contraction losses for the window are given by

$$\Delta p_{contraction} = a\ (b - \frac{A_w}{A_{cr}})\ \frac{\rho v_w^2}{2} \quad (6.18)$$

where $a = 0.4$, $b = 1.25$ for $A_w/A_{cr} < 0.715$ (6.19a)

or $a = 0.75, b = 1.0$ for $0.715 < A_w/A_{cr} < 1.0$ (6.19b)

The expression above applies when $A_w < A_{cr}$. The expression is slightly different when $A_w > A_{cr}$. The equation can be shown as

$$\Delta p_{contraction} = a\ (b(\frac{A_w}{A_{cr}})^2 - \frac{A_w}{A_{cr}})\ \frac{\rho v_w^2}{2} \quad (6.20)$$

where $a = 0.4$, $b = 1.25$ for $A_{cr}/A_w < 0.715$ (6.21a)

or $a = 0.75, b = 1.0$ for $0.715 < A_{cr}/A_w \leq 1.0$ (6.21b)

Again when $A_w = A_{cr}$ then $\Delta p_{contraction} = 0$ as expected i.e. no contraction losses.

6.5 The Validation of the Windowflow Pressure Drop Model

The full expression for windowflow pressure drop is given as

$$\Delta p_w = \Delta p_{turning} + \Delta p_{expansion} + \Delta p_{contraction} + \Delta p_{crossflow\text{-}in\text{-}the\text{-}window} \quad (6.22)$$

where the first three terms are given by the expression in Sections 6.2 to 6.4. The crossflow-in-the-window losses are given by the crossflow

(and bypass) equations of Moore (1979), except that the penetration of the crossflow-in-the window is given by the equations in Chapter 5.

There are two suitable sources of experimental data, i.e. no-leakage windowflow pressure drop versus mass flowrate measurements, these being,

1) data of Brown (1956)

and

2) data of Macbeth (1973).

The latter set of data is proprietary to HTFS. The data, in both sets of data, comes from small model exchangers with a wide range of baffle geometries being used. There is, unfortunately, no comparable data for full-scale exchangers. Fortunately, the range of windowflow/crossflow ratios covered in the tests by Brown and Macbeth is sufficiently wide to encompass the range likely to be encountered in commercial exchangers. Of course, it is not possible to predict any possible problems due to scale-up of the model but it is felt that the form of the model presented will not suffer from this problem.

The model developed in this work is also compared with four other models, others being either very unreliable by their nature or their being unknown in detail e.g. Palen and Taborek (1969). The four models are:-

1) Bell

$$\Delta p_w = (2 + 0.6\, N_{tw}) \frac{A_w}{A_{cl}} \quad \frac{\dot{M}_w^2}{2\, \rho\, A_w^2} \tag{6.23}$$

2) Ishigai

$$\Delta p_w = (2.5 + 0.2 \frac{H}{L}) \frac{\dot{M}_w^2}{2\, \rho\, A_w^2} \tag{6.24}$$

3) Grant and Murray

$$\Delta p_w = f\left(\frac{A_w}{A_{cl}}\right) \frac{\dot{M}_w^2}{2\, \rho\, A_w^2} \tag{6.25}$$

and finally

4) Moore

$$\Delta p_w = (4 f_c \frac{L}{D_e} + 2 \sin(\alpha)) \frac{A_w}{A_{cl}} \frac{\dot{M}_w^2}{2\, \rho\, A_w^2} + \Delta p^*_{c\text{-}in\text{-}w} \tag{6.26}$$

*Fractional penetration of 0.5 assumed.

Figures 6.1 to 6.5 give the predictions of the above 5 models (including the model developed in this work) for the data obtained by Macbeth (1973) at Winfrith. The initial comparisons for these data, by the model developed here, assume a fractional penetration of 0.5.

Figures 6.6 (a) and 6.6 (b) show the effects of allowing for a variable crossflow penetration as shown in Chapter 5 and finally Figure 6.7 shows the predictions of the Macbeth data and the data of Brown (1956).

The results are also given in tabular form in tables 6.1 to 6.3

* A model by Ishigai is included which was developed in preference to Bell's model. However, since the model was developed from data with no tubes in the window, its application to actual exchanger data is very doubtful.

FIGURE 6.1 PREDICTIONS OF MACBETH WINDOWFLOW PRESSURE DROP DATA : BELL METHOD

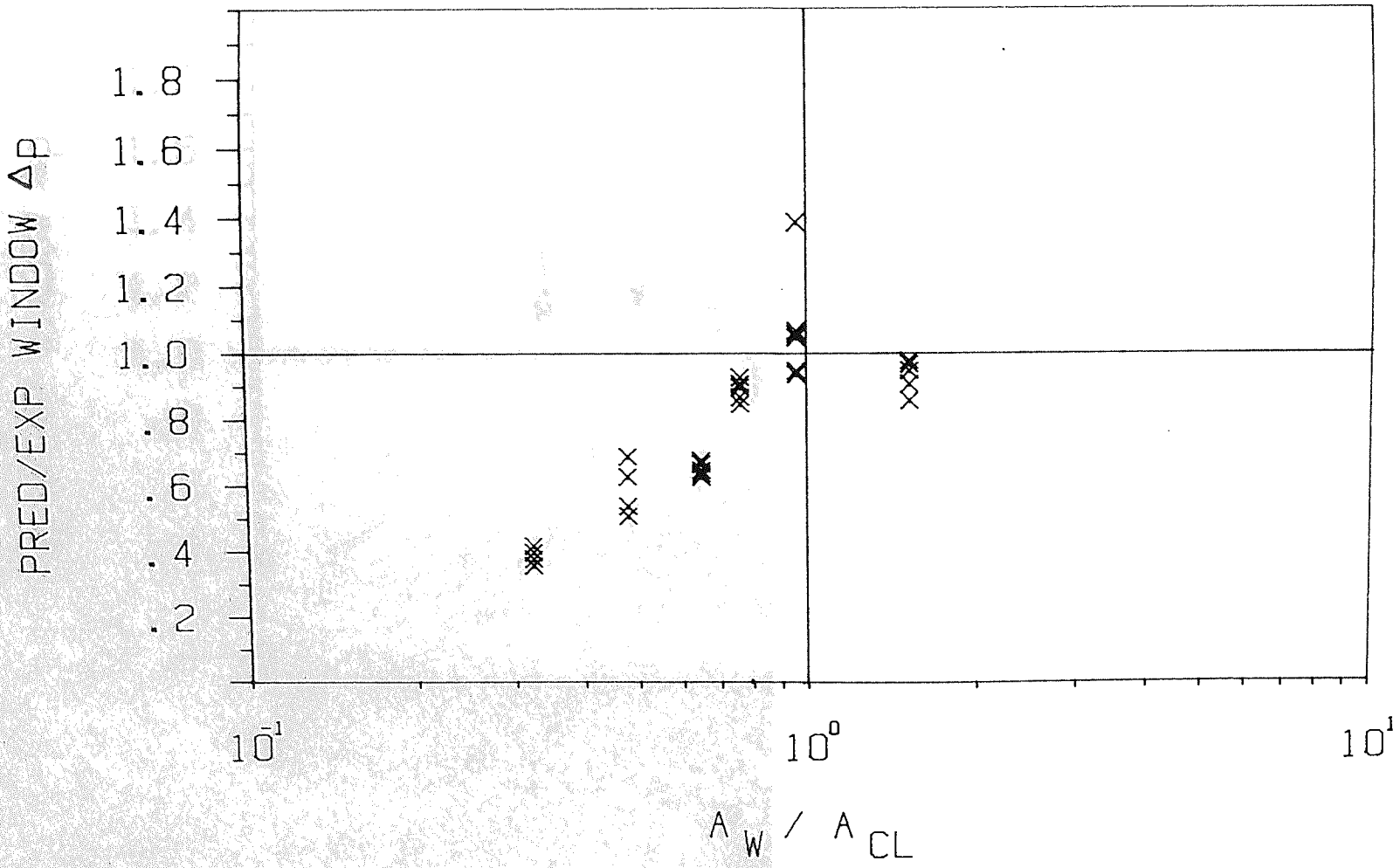

FIGURE 6.2 PREDICTIONS OF MACBETH WINDOWFLOW PRESSURE DROP DATA : ISHIGAI METHOD

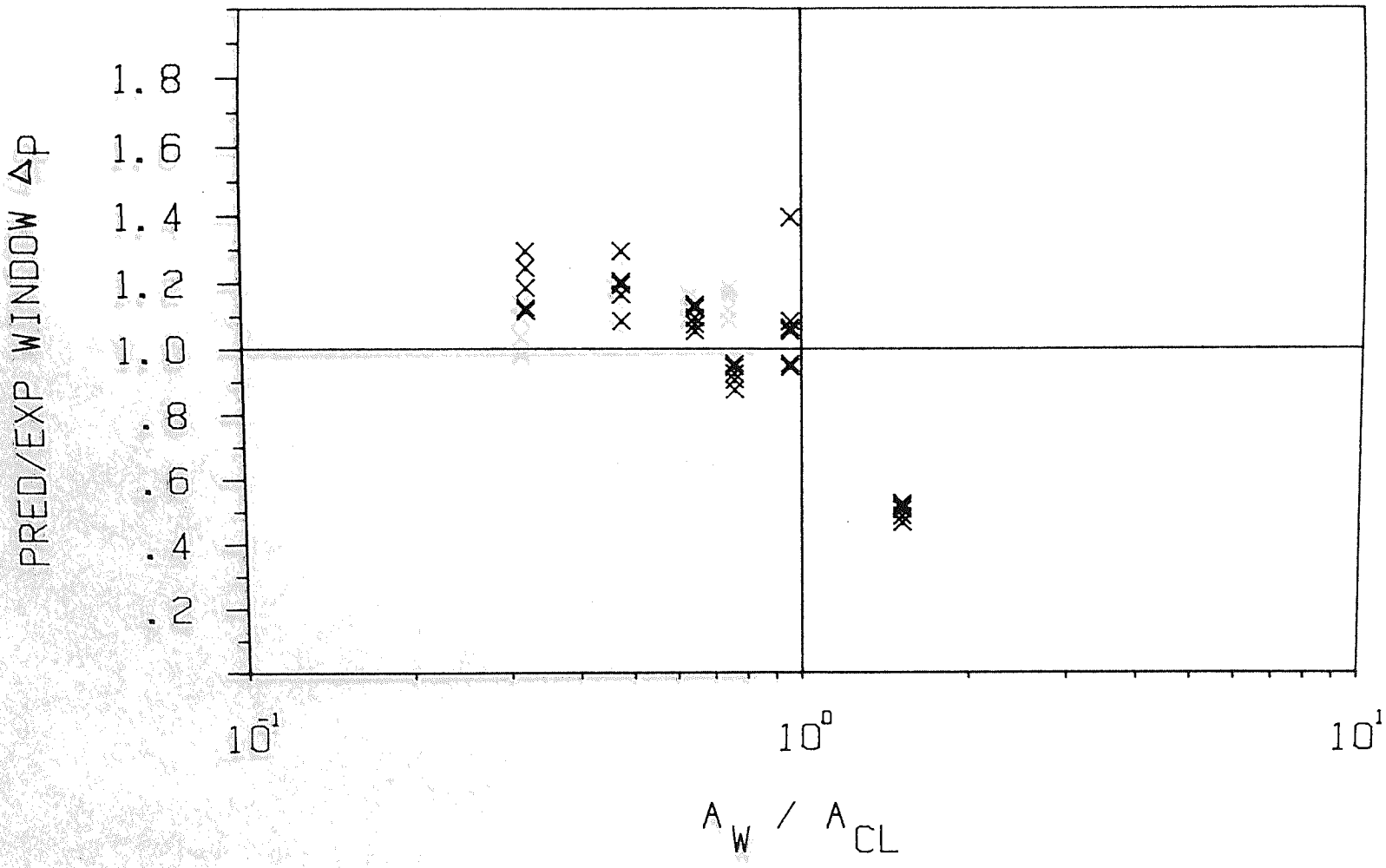

FIGURE 6.3 PREDICTIONS OF MACBETH WINDOWFLOW PRESSURE DROP DATA : GRANT METHOD

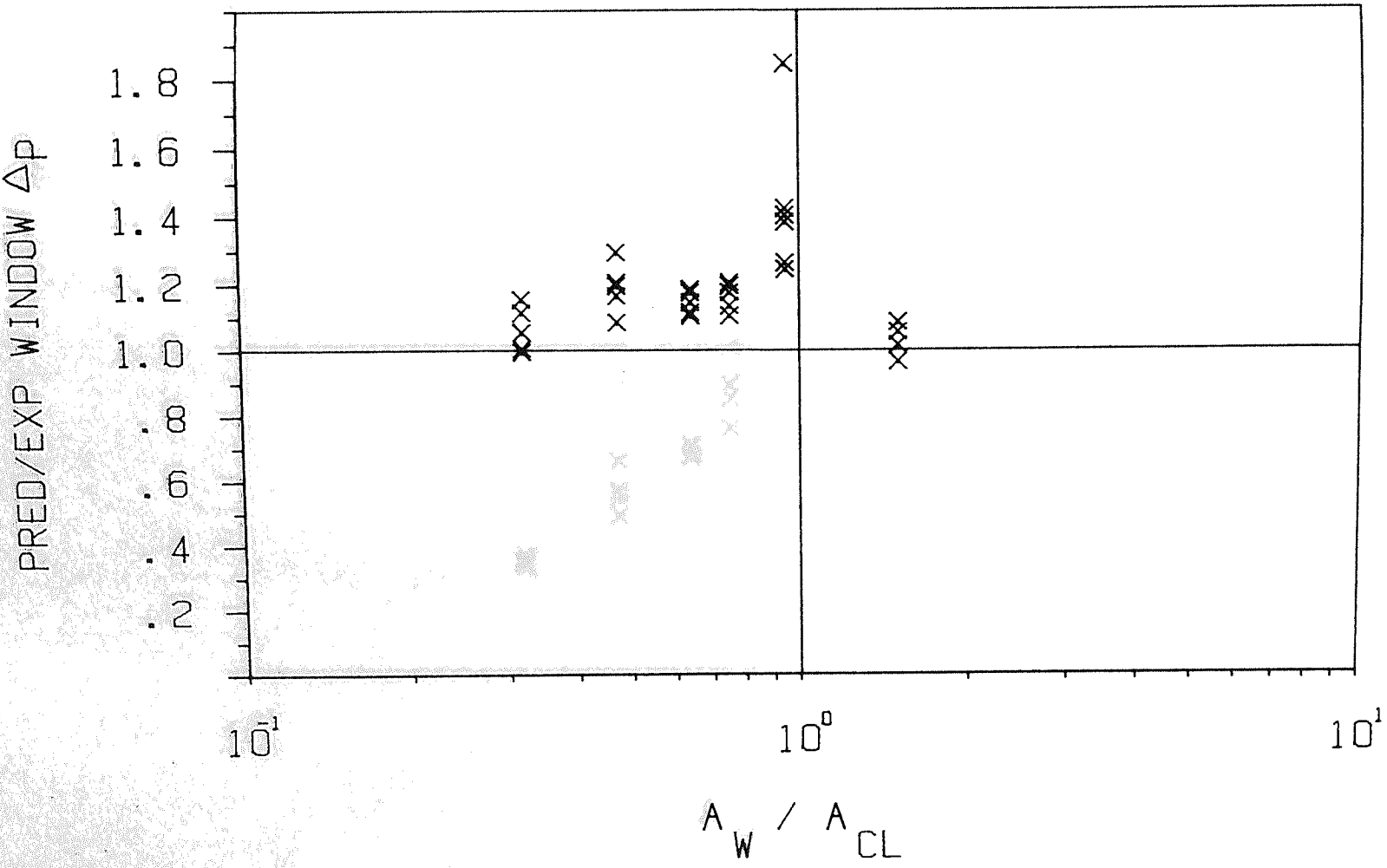

FIGURE 6.4 PREDICTIONS OF MACBETH WINDOWFLOW PRESSURE DROP DATA : MOORE METHOD

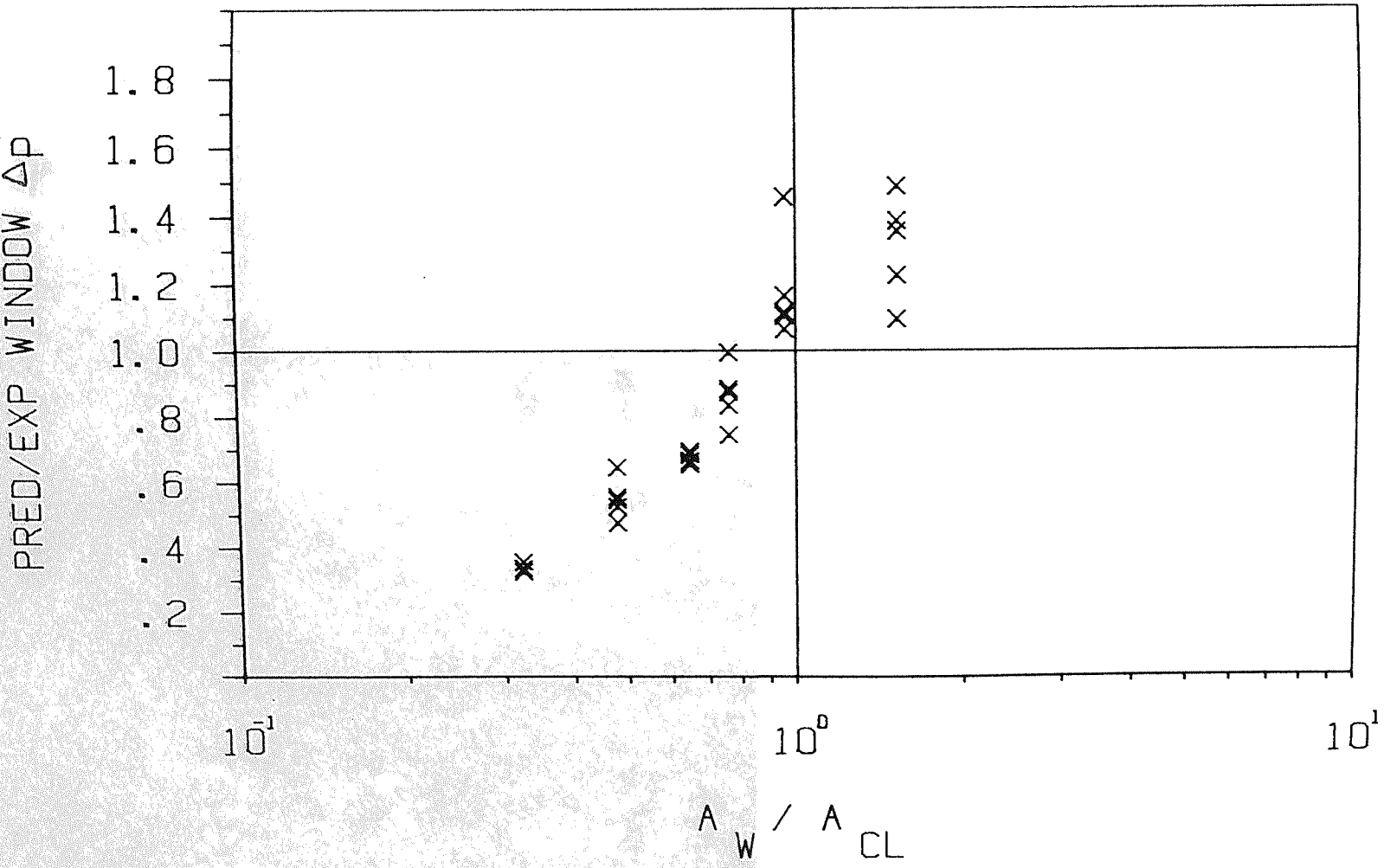

FIGURE 6.5 PREDICTIONS OF MACBETH WINDOWFLOW PRESSURE DROP DATA : WILLS METHOD

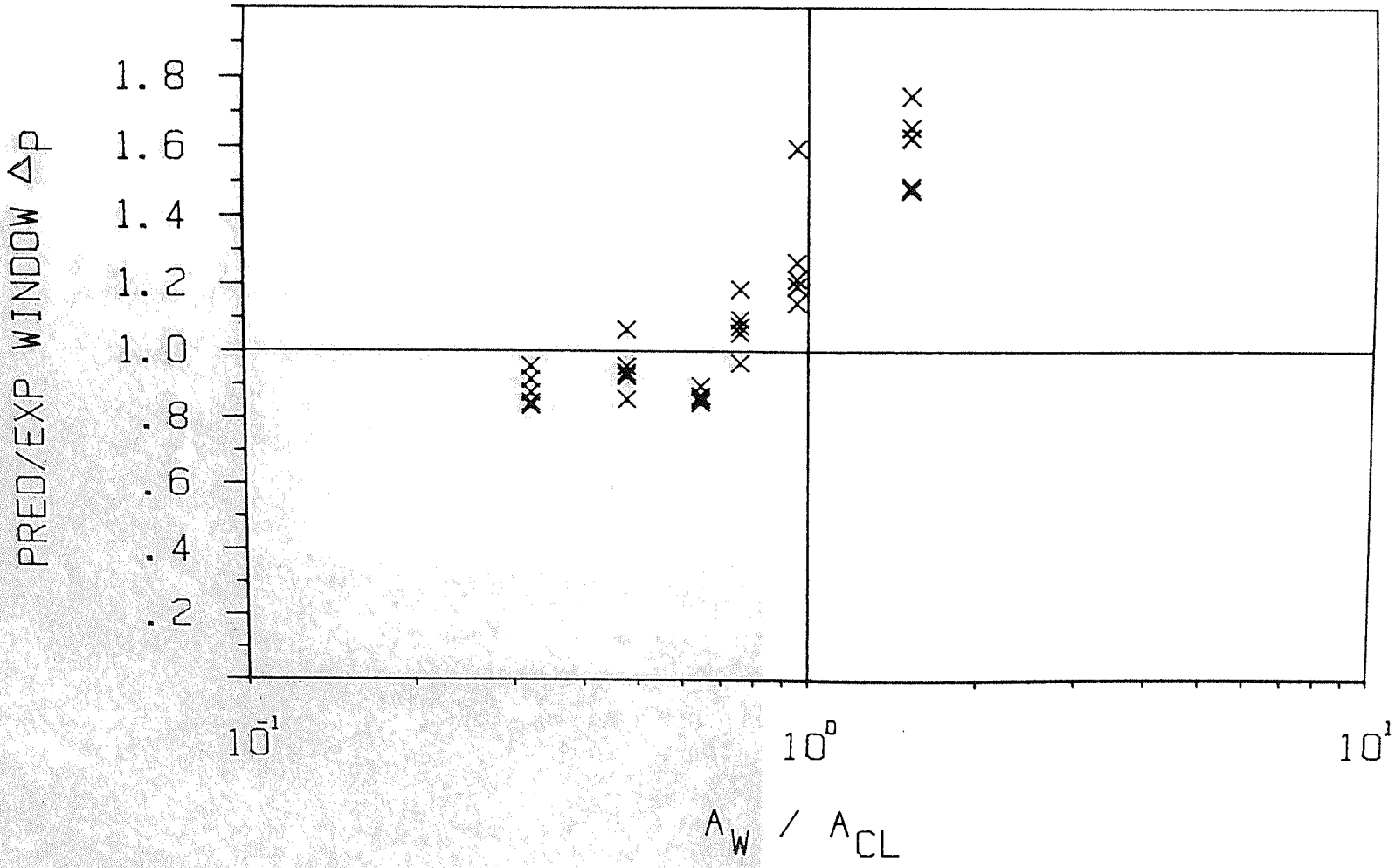

FIGURE 6.6a EFFECT OF CONSTANT CROSSFLOW PENETRATION ON WILLS MODEL FOR MACBETH DATA

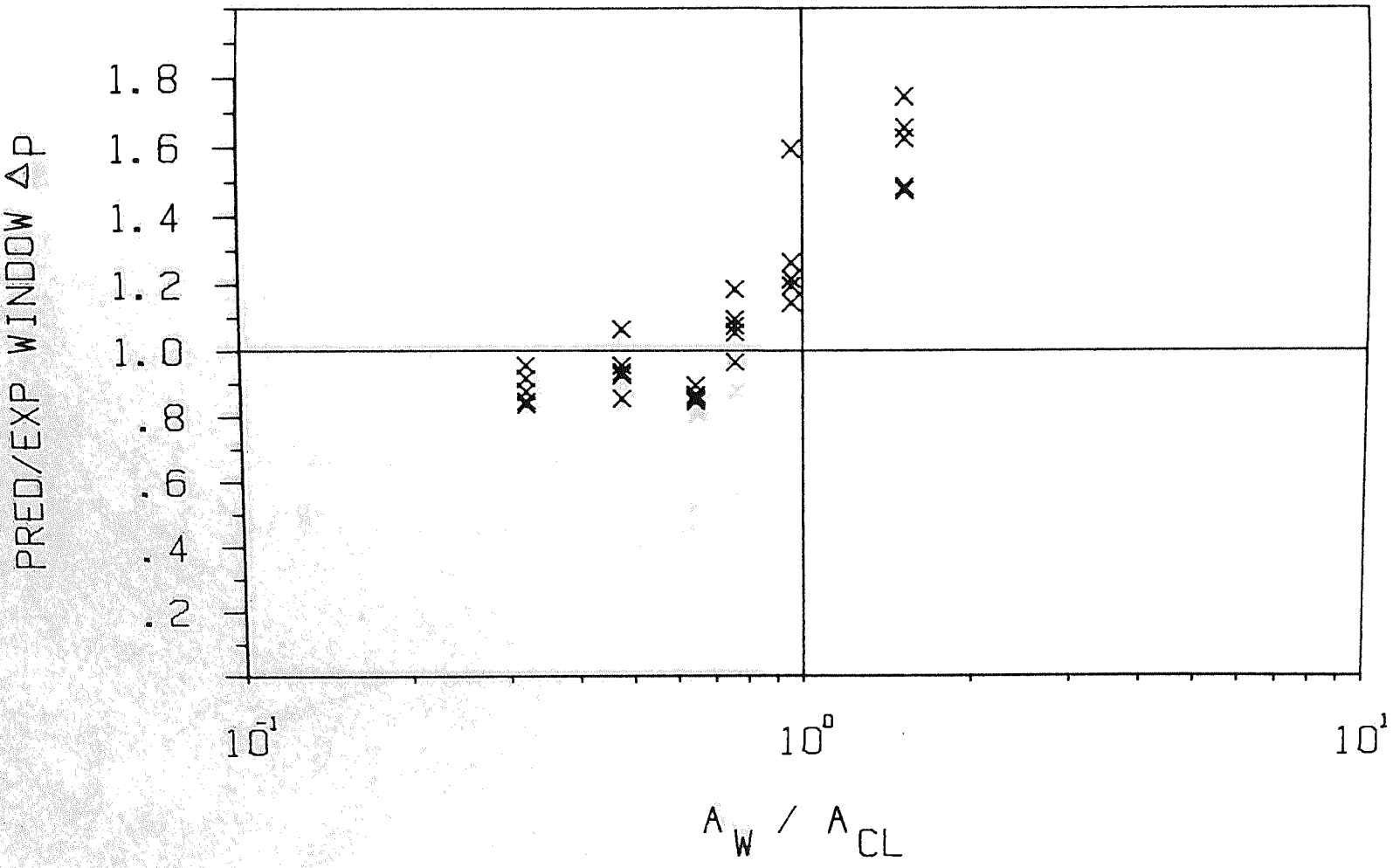

FIGURE 6.6b EFFECT OF VARIABLE CROSSFLOW PENETRATION ON WILLS MODEL FOR MACBETH DATA

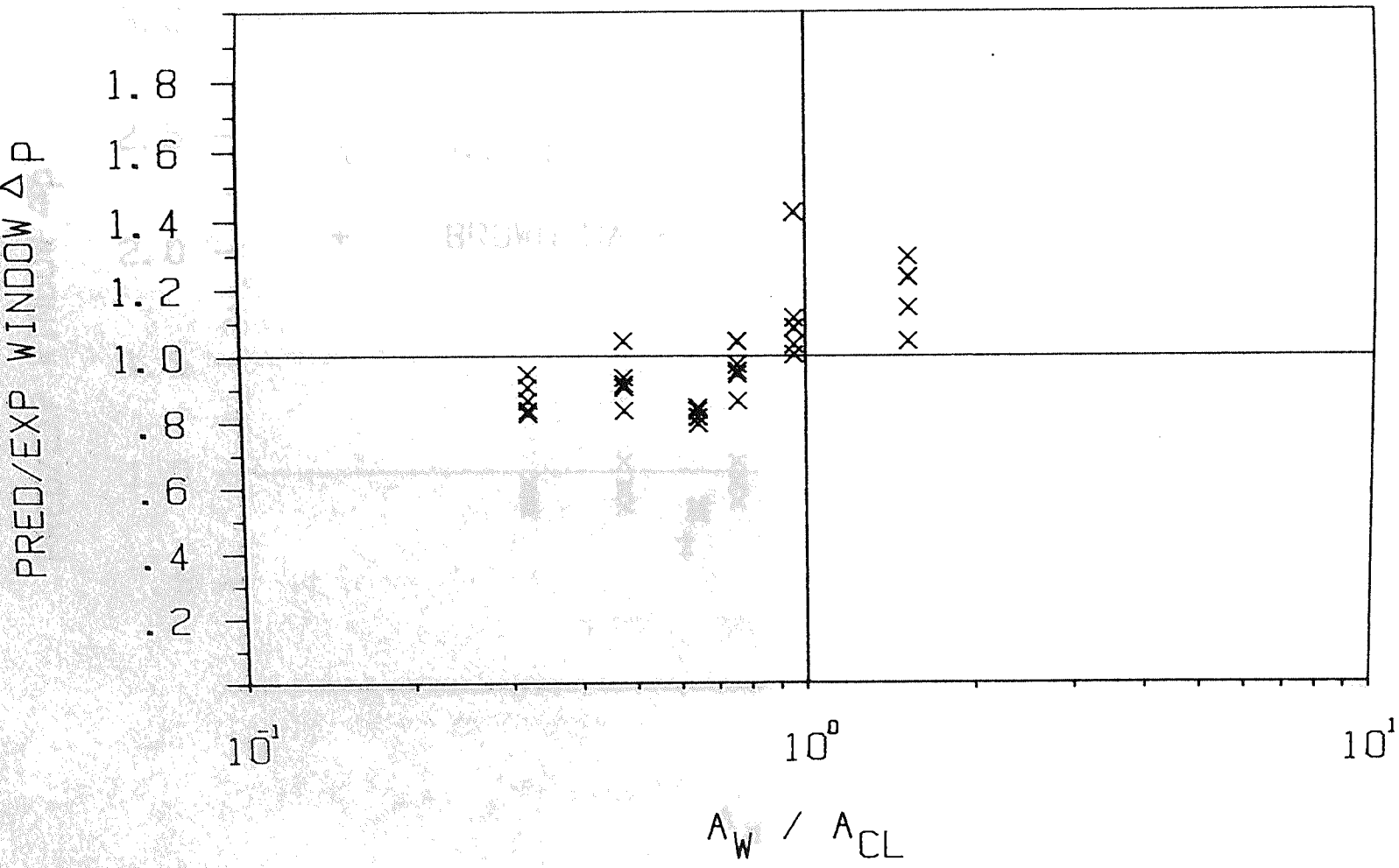

FIGURE 6.7 PREDICTIONS OF BROWN AND MACBETH DATA BY WILLS METHOD WITH VARIABLE CROSSFLOW PENETRATION

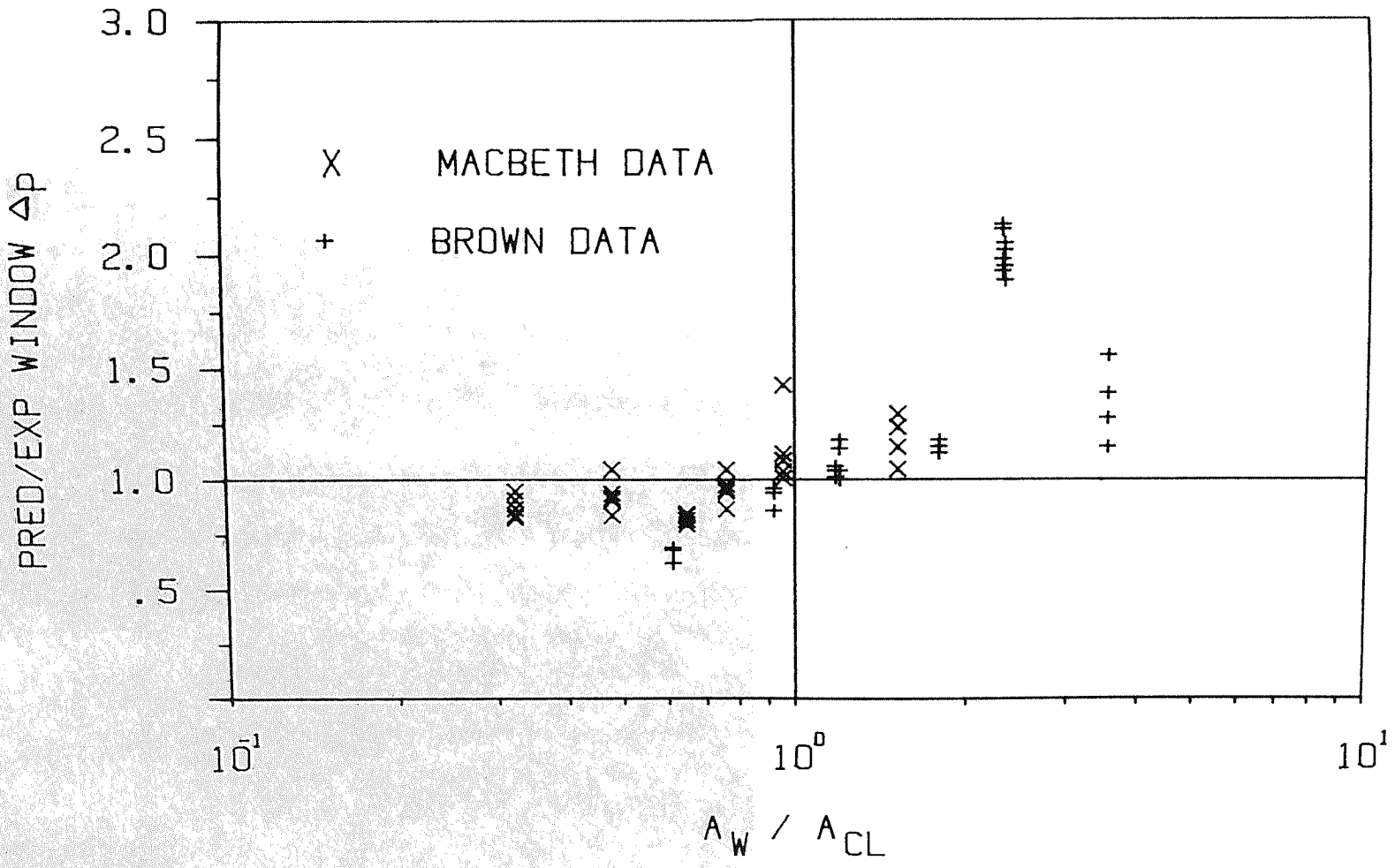

TABLE 6.1: PREDICTIONS OF MACBETH DATA

FLOWRATE Kg/s	BAFFLE CUT, PITCH	PREDICTED/EXPERIMENTAL WINDOWFLOW PRESSURE DROP				
		BELL	ISHIGAI	GRANT	MOORE	WILLS*
1.11	18.4%	0.63	1.07	1.11	0.68	0.86
1.58		0.62	1.05	1.10	0.66	0.84
2.37	48.5mm	0.67	1.13	1.18	0.69	0.89
3.16		0.64	1.09	1.14	0.65	0.85
3.96		0.66	1.12	1.17	0.66	0.86
4.74		0.66	1.13	1.18	0.66	0.86
1.11	18.4%	0.35	1.12	1.00	0.33	0.84
1.58		0.35	1.11	0.99	0.32	0.83
2.37	97.0%	0.39	1.24	1.11	0.35	0.91
3.16		0.37	1.18	1.05	0.33	0.87
3.96		0.41	1.29	1.15	0.35	0.95
1.11	25.0%	0.94	0.95	1.26	1.11	1.19
1.58		0.93	0.94	1.24	1.06	1.14
2.37	48.5mm	1.05	1.06	1.40	1.16	1.26
3.16		1.04	1.05	1.38	1.11	1.21
3.96		1.38	1.39	1.84	1.45	1.59
4.74		1.06	1.08	1.42	1.10	1.21
1.11	25.0%	0.68	1.29	1.29	0.64	1.06
1.58		0.62	1.20	1.20	0.54	0.93
2.37	97.0mm	0.62	1.19	1.19	0.55	0.95
3.11		0.50	1.16	1.16	0.52	0.92
4.74		0.53	1.08	1.08	0.47	0.85
1.11	37.5%	0.96	0.51	1.08	1.48	1.74
1.58		0.94	0.50	1.05	1.38	1.65
2.37	48.5mm	0.97	0.52	1.08	1.35	1.62
3.16		0.90	0.48	1.01	1.22	1.48
4.74		0.85	0.46	0.96	1.09	1.47
1.11	37.5%	0.92	0.95	1.20	0.99	1.18
1.58		0.86	0.90	1.13	0.88	1.07
2.37	97.0mm	0.90	0.94	1.19	0.87	1.09
3.16		0.89	0.92	1.17	0.83	1.05
4.74		0.84	0.87	1.10	0.74	0.96

*Fractional penetration constant at 0.5

TABLE 6.2: EFFECT OF CROSSFLOW PENETRATION MODEL ON PREDICTIONS OF WILLS MODEL FOR THE MACBETH DATA

FLOWRATE Kg/s	BAFFLE CUT PITCH	PREDICTED/EXPERIMENTAL WINDOWFLOW PRESSURE DROP		
		FRACTIONAL PENETRATION CONSTANT AT 0.5 *	FRACTIONAL PENETRATION VARIABLE	
		RATIO	FRACTIONAL PENETRATION	RATIO
1.11	18.4%	0.86		0.81
1.58		0.84		0.79
2.37	48.5mm	0.89		0.84
3.16		0.85	0.31	0.81
3.96		0.86		0.83
4.74		0.86		0.83
1.11	18.4%	0.84		0.83
1.58		0.83		0.82
2.37	97.0mm	0.91	0.39	0.90
3.16		0.87		0.86
3.96		0.95		0.94
1.11	25.0%	1.19		1.03
1.58		1.14		1.00
2.37	48.5%	1.26	0.27	1.11
3.16		1.21		1.08
3.96		1.59		1.42
4.74		1.21		1.08
1.11	25.0%	1.06		1.04
1.58		0.93		0.95
2.37	97.0mm	0.95	0.36	0.93
3.16		0.92		0.90
4.74		0.85		0.83
1.11	37.5%	1.74		1.29
1.58		1.65		1.23
3.37	48.5mm	1.62	0.21	1.23
3.16		1.48		1.14
4.74		1.47		1.04
1.11	37.5%	1.18		1.04
1.58		1.07		0.95
2.37	97.0mm	1.09	0.30	0.97
3.16		1.05		0.94
4.74		0.96		0.86

* Actually taken as 0.4 for a circular bundle. The variable penetration model assumes the free crossflow area is approximately constant because there are less tubes at the edge of the shell

TABLE 6.3: PREDICTIONS OF WILLS MODEL FOR BROWN DATA*

PITCH (in) CUT % PENETRATION Sw/Sc	FLOWRATE lb/hr	PREDICTED Δp lb/ft^2	EXPERIMENTAL Δp lb/ft^2
1.91 18.4 0.3159 0.61	23800 14550 8780 5240	170 65 24 8.7	276 95.5 35.0 12.7
0.976 18.4 0.2254 1.20	15050 6970 3510 1800 1000	158 35 9.1 2.5 0.8	138 29.7 7.7 2.4 0.8
0.50 18.4 0.1423 2.33	6200 3630 1790 760	108.9 37.8 9.3 1.7	55.9 18.4 4.6 0.9
1.91 31.0 0.2458 1.18	32300 14900 6300 2990	174.6 39.1 7.4 1.8	173.5 37.7 7.0 1.7
0.976 31.0 0.1590 2.31	18350 8890 4220 2050	192.8 46.7 10.9 2.7	90.5 22.1 5.5 1.4
3.72 43.7 .2899 0.92	32820 13450 5170	60.8 11.1 1.8	63.5 11.8 2.1
1.91 43.7 .1996 1.79	32360 13450 5130	160.4 29.6 4.7	143 25.1 4.1
0.976 43.7 0.1221 3.53	20450 9550 4310 2040	224 50.5 10.7 2.5	194.2 39.3 7.7 1.6

* The data for a cut of 31% and a pitch of 0.5" is not included as the data is extremely suspect.

6.6 Results and Discussion of Validation

Taking each of the models in turn then it is seen that

1) The Bell model is fairly reasonable when $A_w/A_{cl} \approx 1$ but underpredicts seriously outside this range. As A_w should equal A_{cl} for a "well designed" exchanger, then the above model is not too bad. However, commercial exchangers are often designed with substantially different crossflow and windowflow areas and hence caution is required in using this model.

2) The Ishigai model (1967) is fairly good if $A_w/A_{cl} < 1$ but seriously underpredicts if $A_w/A_c > 1$. In view of the fact that this model is developed by a very dubious curve fitting and data analysis, it is surprising any agreement is achieved at all. The method is not recommended as a design method unless $A_w/A_{cl} < 1$.

3) The Grant and Murray correlation (proprietary to HTFS) gives very good predictions but this is not entirely surprising as these data are the very data from which the correlation was obtained. This correlation represents the best predictions that can be obtained by a mechanistic model and hence this correlation is the "yard-stick" by which the model developed in this work is compared.

4) The Moore model (1979) underpredicts when $A_w/A_{cl} < 1$ but overpredicts when $A_w/A_{cl} > 1$ with the results being reasonable at $A_w/A_{cl} = 1$. When $A_w/A_{cl} < 1$ the model does not allow for the expansion contraction losses and when $A_w/A_{cl} > 1$ the model significantly overpredicts the frictional losses.

5) The model developed in this work (Wills) also gives good results for $A_w/A_{cl} < 1$ but overpredicts for $A_w/A_{cl} > 1$. This overprediction is because initially the fractional penetration of the crossflow is taken as 0.5 in these comparisons. Figures 6.6 (a) and 6.6 (b) show the effect of allowing for crossflow penetration, with the results being substantially improved.

Finally Figure 6.7 shows the predictions for the data of Brown along with that of Macbeth. Overall the model performs quite satisfactorily except for two strange sets of predictions at $A_w/A_{cl} \approx 2.3$ where the model overpredicts by a factor of 2. The reason for this is not known, and no explanation is offered, save that is is felt that the experimental values may be in error. Until more experimental data are obtained, it is unlikely that any satisfactory explanation can be offered for these anomolous data points.

The Grant and Murray correlation gives an average ratio of predicted/ experimental pressure drop of 1.17 with a standard deviation of 17%,

whereas the model developed here (including the crossflow penetration model) gives an average ratio of 0.97 with a standard deviation of 13%.

6.7 Conclusions

It is concluded that the windowflow pressure drop model developed in this work gives good predictions of the experimental data, and is the best of all the models known in detail. It has the great advantage of being applicable to a wide range of exchanger geometries and, furthermore, can be applied to geometries not considered in this work with confidence and, hence, is recommended as a design method.

7.0 BAFFLE LEAKAGE IN THE WINDOW ZONE

This chapter describes how the multi-stream methods overpredict by not allowing for baffle leakage in the window zone. A model is presented to allow for this effect, and it is validated against experimental data.

7.1 Baffle Leakage in Multi-Stream Methods

Multi-stream methods generally assume that the window flowrate equals the total crossflow flowrate i.e.

$$\dot{M}_w = \dot{M}_c + \dot{M}_b \qquad (7.1)$$

Parker and Mok presented their model for leakage (Chapter 3) which treats the baffle leakage as two parallel sets of streams i.e. baffle leakage in the overlap and leakage in the window zone. Within their method it can be seen from Figure 7.1 that equation 7.1 is incorrect i.e.

$$\dot{M}_w = \dot{M}_c + \dot{M}_b + \dot{M}_1 \qquad (7.2)$$

where

$$\dot{M}_1 = \dot{M}_{s1} + \dot{M}_{t1} \qquad (7.3)$$

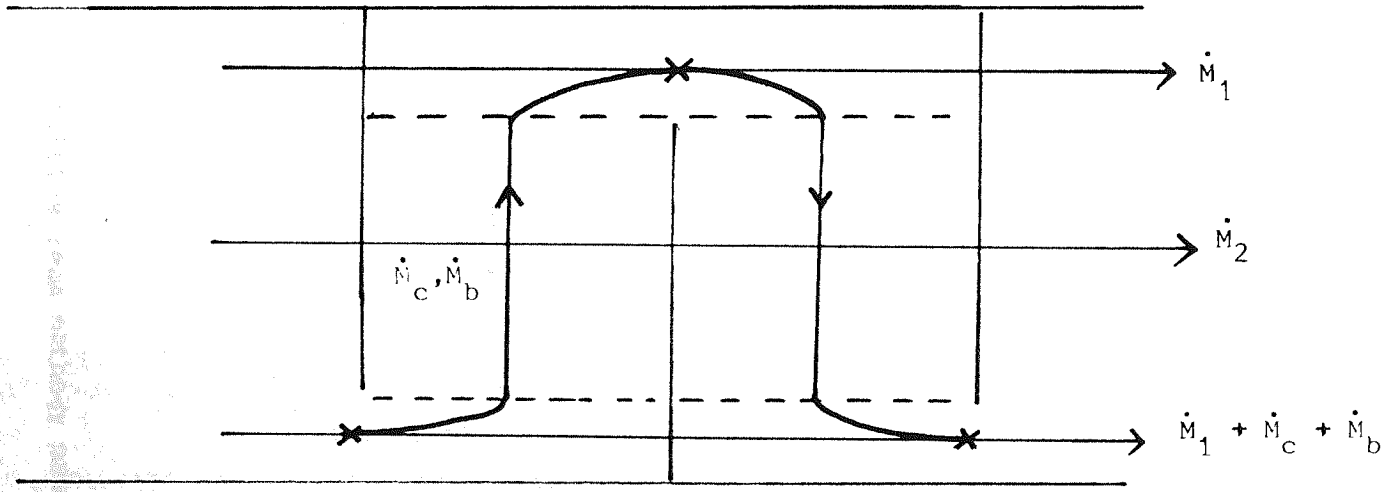

Figure 7.1 : SCHEMATIC OF PARKER AND MOK FLOW MODEL

Further consideration shows that the crossflow flowrate is over-predicted by ignoring the effect of baffle leakage in the window as a mass balance is usally written

$$\dot{M}_T = \dot{M}_w + \dot{M}_s + \dot{M}_t \qquad (7.4)$$

Compare this with the method of Parker and Mok who would obtain

$$\dot{M}_T = \dot{M}_c + \dot{M}_b + \dot{M}_s + \dot{M}_t \qquad (7.5)$$

where $$\dot{M}_s = 2\dot{M}_{s1} + \dot{M}_{s_2} \qquad (7.6a)$$

and $$\dot{M}_t = 2\dot{M}_{t1} + \dot{M}_{t2} \qquad (7.6b)$$

The multi-stream models define

$$\dot{M}_s = \dot{M}_{s1} + \dot{M}_{s2} \qquad (7.8)$$

$$\dot{M}_t = \dot{M}_{t1} + \dot{M}_{t2} \qquad (7.9)$$

hence the existing multi-stream methods predict less baffle leakage and consequently more crossflow than actually occurs.

From Equation 7.2 it is seen that the equations used to solve a multi-stream baffle space model are not truly valid as conditions of total

flow do not exist at the inlet to the crossflow. Each baffle space cannot be solved independently of the next since the downstream conditions depend on the upstream conditions i.e. the calculations need to know the leakage 'history' to be able to predict the pressure drop. The immediate and somewhat startling conclusion is that baffle-space multi-stream models are not valid!

The effect of baffle leakage in the window is well illustrated by considering the predictions of the Moore method, and the Grant and Murray method in Table 7.1 as plotted in Figure 7.2. For low baffle cuts, they give quite good results (where leakage in the window is low) but overpredict significantly for high baffle cuts. This effect is not observed in the no-leakage cases.

Having shown that baffle leakage in the window is a serious problem which is not taken into account by the multi-stream (baffle-space) methods, then it is necessary to be able to predict this effect without knowing the upstream conditions. Within the framework of the present one dimensional models it is possible to do this since at any point in the exchanger the sum of the flowrate in the vertical direction and the flow in the horizontal direction equals the total flowrate because of mass conservation, then equations 7.5,

TABLE 7.1: EFFECT OF BAFFLE CUT AND BAFFLE LEAKAGE ON PREDICTIONS OF BAFFLE SPACE PRESSURE DROP BY GRANT AND MURRAY METHOD, AND MOORE METHOD.

BAFFLE CUT	FLOWRATE Kg/s	PREDICTED/EXPERIMENTAL PRESSURE DROP	
		GRANT AND MURRAY	MOORE
	1.11	0.803	1.049
18.4%	1.58	0.828	1.064
	2.37	0.917	1.148
	3.96	0.949	1.144
NO LEAKAGE	4.75	1.006	1.196
37.5%	1.11	0.734	0.963
	1.58	0.726	0.923
	2.37	0.790	0.957
	3.16	0.786	0.917
NO LEAKAGE	4.75	0.791	0.878
	1.11	1.071	1.224
	1.58	1.132	1.309
18.4%	2.37	1.262	1.374
	3.16	1.286	1.397
	4.74	1.279	1.387
LEAKAGE	6.32	1.310	1.457
	7.90	1.249	1.350
37.5%	1.11	1.423	1.691
	1.58	1.401	1.645
	2.37	1.480	1.692
LEAKAGE	3.16	1.613	1.799
	4.75	1.511	1.645
	7.91	1.437	1.520

FIGURE 7.2 PREDICTIONS OF BAFFLE-SPACE PRESSURE DROP FOR 18.4% AND 37.5% CUT EXCHANGERS WITH AND WITHOUT BAFFLE LEAKAGE

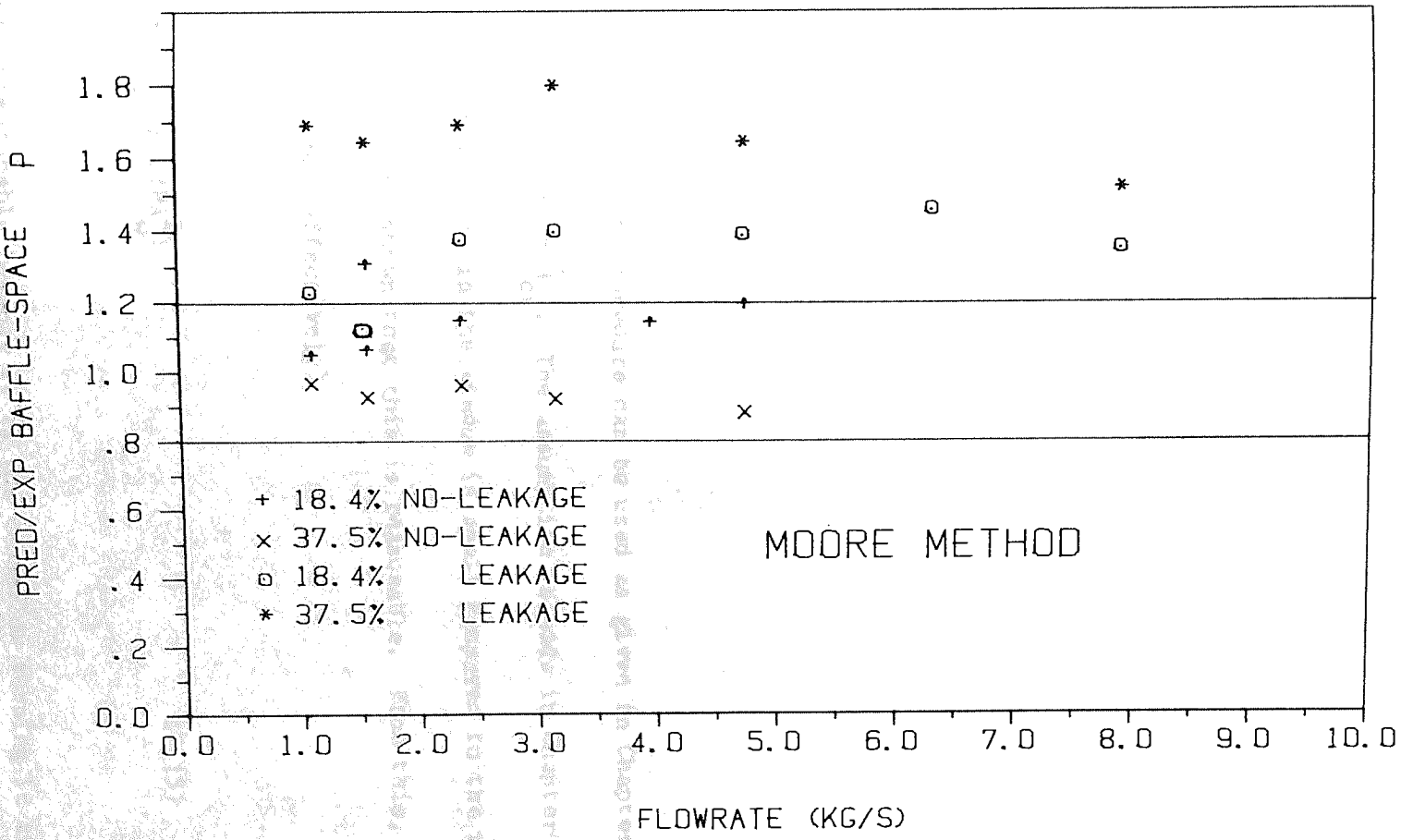

7.6, and 7.7, are written more simply as

$$\dot{M}_T = \dot{M}_c + \dot{M}_b + 2\dot{M}_1 + \dot{M}_2 \qquad (7.10)$$

where

$$\dot{M}_1 = \dot{M}_{s1} + \dot{M}_{t1} \qquad (7.11)$$

$$\dot{M}_2 = \dot{M}_{s2} + \dot{M}_{t2} \qquad (7.12)$$

Defining

$$\dot{M}_{cr} = \dot{M}_c + \dot{M}_b \quad \text{and} \qquad (7.13)$$

$$\dot{M}_L = 2\,\dot{M}_1 + \dot{M}_2 \qquad (7.14)$$

then the general solution procedure can be used as given in Chapter 3. This presupposes that $\dot{M}_w = \dot{M}_{cr}$. The assumption is made in Chapter4 that the effect of leakage in the window is small compared to the total losses, and it has been shown that this is reasonable. From this, the model is solved using (effectively)

$$\Delta p_w = K_w \dot{M}_{cr}^2 / (2\rho A_w^2) \qquad (7.15)$$

which is not unreasonable because it is the crossflow turning in the window that gives the major losses.

The important point to understand is that it is necessary to predict $\dot{M}_c$ correctly and less important to predict $\dot{M}_w$ correctly rather than the other way round. All that is required is a method for predicting $\dot{M}_L$. This is done by defining an effective baffle leakage area which is larger than the actual baffle leakage area. The development of this model is shown in the next section.

7.2 Development of an Effective Leakage Area to Allow for Leakage in the Window

Consider an exchanger of sufficient length as in Figure 7.1. Over this length, the leakage profile will have been set up; it is assumed that the leakage model is of Parker and Mok (1968) is the most realistic.

They define the pressure drop of the leakage in the window as

$$\Delta p_1 = \frac{N_B}{2} K_1 \frac{\dot{M}_1^2}{2 \rho A_1^2} + \frac{N_B}{2} \Delta p_w \qquad (7.16)$$

and the leakage pressure drop in the overlap as

$$\Delta p_2 = N_B K_2 \frac{\dot{M}_2^2}{2 \rho A_2^2} \qquad (7.17)$$

From Chapters 4 and 6 it has been assumed that the leakage in the window only undergoes axial losses and hence equation 7.1 should be written as

$$\Delta p_1 = \frac{N_B}{2} K_1 \frac{\dot{M}_1^2}{2 \rho A_1^2} + \Delta p_{wa} \qquad (7.18)$$

It is assumed here that these axial losses are small compared to the total losses i.e.

$$\Delta p_1 = \frac{N_B}{2} K_1 \frac{\dot{M}_1^2}{2 \rho A_1^2} \tag{7.19}$$

Furthermore K_i is only a weak function of $\dot{M}_i$ and hence

$$K = K_1 = K_2 \tag{7.20}$$

From equations 7.17, 7.19 and 7.20, assuming $\Delta p_1 = \Delta p_2$,

$$\left(\frac{\dot{M}_1}{A_1}\right)^2 = 2 \left(\frac{\dot{M}_2}{A_2}\right)^2 \tag{7.21}$$

The total flowrate of the leakage , $\dot{M}_L$, through the plane of the baffle including the leakage in the window is

$$\dot{M}_L = \dot{M}_2 + 2\dot{M}_1 \tag{7.22}$$

It is wished to define an effective leakage area, A_e such that

$$\Delta p_T = N_B K \frac{\dot{M}_L^2}{2 \rho A_e^2} \tag{7.23}$$

As $\Delta p_T = \Delta p_1 = \Delta p_2$, then

$$2 \left(\frac{\dot{M}_L}{A_e}\right)^2 = 2 \left(\frac{\dot{M}_2}{A_2}\right)^2 = \left(\frac{\dot{M}_1}{A_1}\right)^2 \tag{7.24}$$

hence

$$\dot{M}_L = \frac{A_e}{A_2} \dot{M}_2 \tag{7.25}$$

and

$$\dot{M}_1 = 2^{\frac{1}{2}} \frac{A_1}{A_2} \dot{M}_2 \tag{7.26}$$

Substituting equations 7.25 and 7.26 into 7.22 gives

$$\frac{A_e}{A_2}\dot{M}_2 = \dot{M}_2 + 2^{\frac{3}{2}}\frac{A_1}{A_2}\dot{M}_2 \qquad (7.27)$$

and hence the final equation defining effective leakage area is

$$A_e = A_2 + 2^{\frac{3}{2}} A_1 \qquad (7.28)$$

Compare this equation with the usual equation used in multi-stream methods,

$$A_L = A_2 + A_1 \qquad (7.29)$$

It is clear from equation 7.28 why the multi-stream methods overpredict for large baffle cuts, but give reasonable answers to small baffle cuts. When the baffle cut tends to zero then

$$A_L = A_2 = A_e \qquad (7.30)$$

and when the baffle cut tends to 50 % then

$$A_L = A_1 \qquad (7.31)$$

and

$$A_e = 2^{\frac{3}{2}} A_1 \qquad (7.32)$$

This limit may not seem plausible but consider an exchanger as in Figure 7.3 with N_B (even) 50% cut baffles where $A_2 = 0$. It is convenient to consider the leakage into two halves for the top and bottom of the shell (as parallel paths have the same pressure drop) hence

$$\Delta p_T = K\frac{N_B}{2}\frac{\dot{M}_1^2}{2\,\rho\,A_1^2} \qquad (7.33)$$

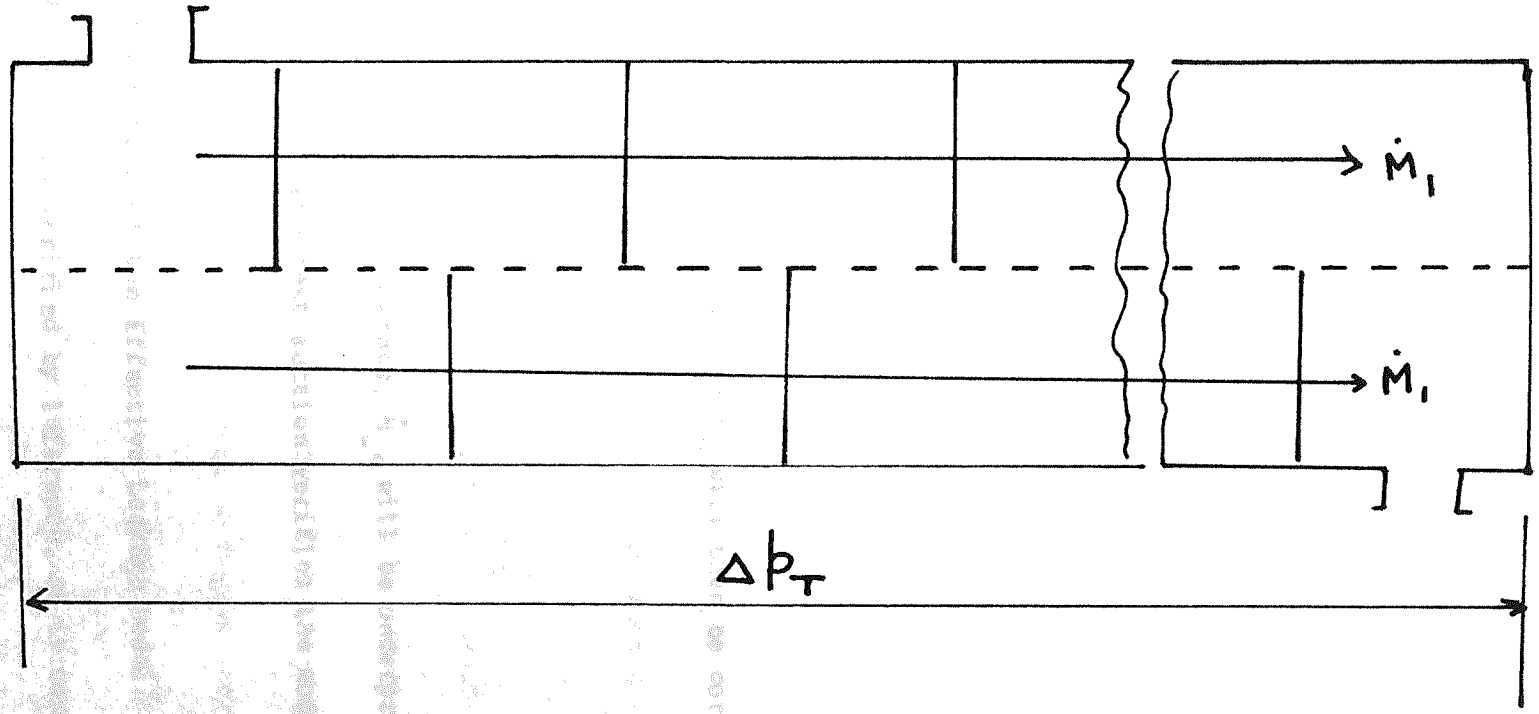

Figure 7.3 : AN EXCHANGER WITH 50% CUT BAFFLES

As we defined

$$\Delta p_T = K N_B \frac{\dot{M}_L^2}{2 \rho A_e^2} \qquad (7.34)$$

and as $A_2 = 0$, $\dot{M}_2 = 0$ and hence

$$\dot{M}_L = 2\dot{M}_1 \qquad (7.35)$$

From equations 7.33, 7.34 and 7.35 then

$$A_e = 2^{\frac{3}{2}} A_1 \qquad (7.36)$$

Obviously using an equation such as equation 7.36 will greatly increase the axial leakage predicted. As shown in section 7.1, the total crossflow flowrate, $\dot{M}_c + \dot{M}_b$ will then be correct as

$$\dot{M}_b + \dot{M}_c = \dot{M}_T - \dot{M}_L \qquad (7.37)$$

Of course the window flowrate, $\dot{M}_w$, will be underpredicted but this is less important. The next section verifies the model presented here.

7.3 Verification of the Effective Leakage Model

The model is verified by inference, as it cannot be truly tested. The next chapter outlines the full features of the 'STREAM-INTERACTION' method. Equation 7.24 is modified to allow for the parallel streams i.e.

$$A_{te} = A_{t2} + 2^{3/2} A_{t1} \qquad (7.38)$$

$$A_{se} = A_{s2} + 2^{3/2} A_{s1} \qquad (7.39)$$

Of course if the effect of baffle leakage in the window is not taken into account then

$$A_t = A_{t2} + A_{t1} \qquad (7.40)$$

$$A_s = A_{s2} + A_{s1} \qquad (7.41)$$

The method is tested against the data of Macbeth for four geometries,

1) No-leakage: baffle cut = 18.4%

2) No-leakage: Baffle cut = 37.5%

3) Leakage : baffle cut = 18.4%

4) Leakage : baffle cut = 37.5%

with results being given in Table 7.2 and plotted in Figure 7.4.

Comparing Figures 7.2 and 7.4, it is remarkable how the predictions are improved by this simple model. Also Figures 9.6 and 9.7 in Chapter 9 show how well the method predicts for the NEL boiler single-phase data and the NEL condenser single-phase data. The good predictions stem predominantly from this effective leakage area model, which enables virtually all the shellside drop data in turbulent flow to be predicted within +30% to -30%.

It is appreciated that the model presented in this chapter is a very simplistic model, ignoring effects such as interaction between the

TABLE 7.2: PREDICTIONS OF BAFFLE-SPACE PRESSURE DROP BY THE 'STREAM-INTERACTION' METHOD ALLOWING FOR LEAKAGE IN THE WINDOW

BAFFLE CUT	FLOWRATE Kg/s	PREDICTED/EXPERIMENTAL PRESSURE DROP
	1.11	0.89
18.4%	1.58	0.90
	2.37	0.99
	3.17	0.95
NO LEAKAGE	3.96	0.97
	4.75	1.11
37.5%	1.11	1.18
	1.58	1.15
	2.37	1.22
NO LEAKAGE	3.16	1.19
	4.75	1.33
	1.11	0.75
18.4%	1.58	0.76
	2.37	0.87
	3.16	0.91
LEAKAGE	4.74	0.93
	6.32	-
	7.90	0.93
37.5%	1.11	1.03
	1.58	1.04
	2.37	1.11
	3.16	1.21
LEAKAGE	4.75	1.13
	7.91	1.07

FIGURE 7.4 PREDICTIONS OF STREAM-INTERACTION METHOD FOR 18.4% AND 37.5% CUT EXCHANGERS WITH AND WITHOUT BAFFLE LEAKAGE

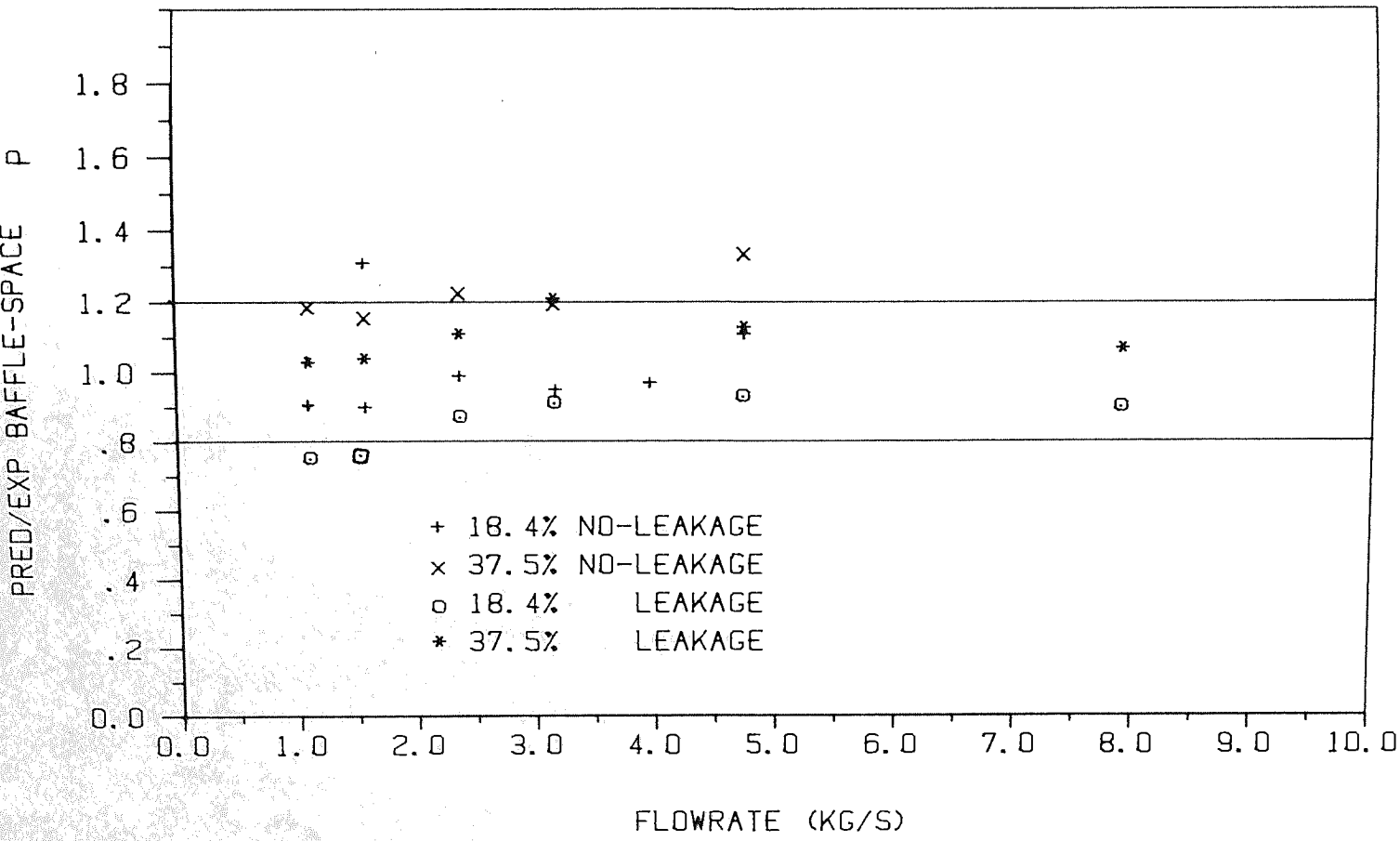

crossflow and leakage, mixing of the leakage with the crossflow in the window and so on, but this model enables surprisingly good predictions to be obtained indicating that the model has gone a long way to overcoming the major deficiency of the multi-stream models, and can only be regarded as a major success within the 'STREAM-INTERACTION' model which is defined in the next chapter.

8.0 THE STREAM-INTERACTION METHOD

This chapter describes the new method developed in this work which encompasses all the models developed in Chapters 4 to 7. It is called the 'Stream-Interaction' method as it allows for the interactions between the various streams.

8.1 The Features of the Stream-Interaction Method

The basic model consists of five flowstreams (six if an inline pass-partition lane is included) these being

1) the crossflow stream,
2) the crossflow bypass stream,
3) the windowflow stream,
4) the shell-baffle leakage stream,
5) the tube-baffle leakage stream,

and possibly

6) the inline pass-partition stream.

A schematic representation of this model is given in Figure 8.1.

The pressure drop/mass flowrate relationships for each path are calculated using either the new models developed in this work, or the best available HTFS correlations. Under no circumstance, has any new

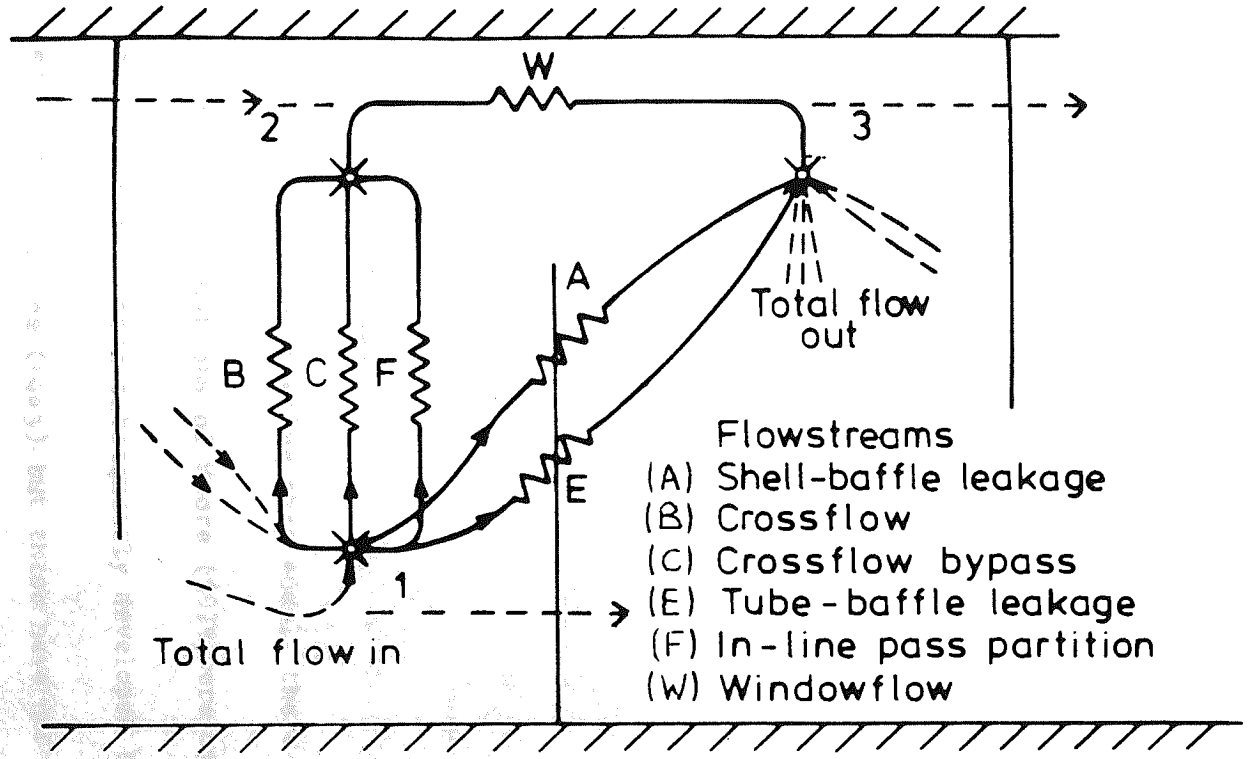

- - - - → DENOTES LEAKAGE IN WINDOW ALLOWED FOR BY THE EFFECTIVE LEAKAGE AREA

Figure 8.1 : A SCHEMATIC REPRESENTATION OF THE 'STREAM-INTERACTION' METHOD

correlation been used which is empirically based, the emphasis in the development of this model being on understanding the mechanics of shellside flow. The pressure drop/mass flowrate relationships are briefly described in the next section.

8.2 Pressure Drop/Mass Flowrate Relationships of the Stream-Interaction Method.

8.2.1 Crossflow

The equations of Moore (1979)are used. The crossflow pressure drop is defined as

$$\Delta p_c = 4 f_c N_c \frac{\dot{M}_c^2}{2 \rho A_c^2} \qquad (8.1)$$

where $f_c = a Re_c^b$, a, b depend on tube layout (8.2)

and

$$Re_c = \frac{\dot{M}_c (P_t - D_0)}{\eta A_c} \qquad (8.3)$$

8.2.2 Crossflow Bypass

At the time of testing this model, there were little data available and the bypass equations of Moore (1979)were used. Since then some new correlations have been subsequently developed by Russell and Wills (1983) based on data of Lee (1983) but these have not been tested in the Stream-Interaction method. However, testing has shown the Moore correlation gives similar results to the new correlations in the range over which it is applied.

The bypass pressure drop is defined by

$$\Delta p_b = 4 f_b N_b \frac{\dot{M}_b^2}{2 \rho A_b^2} \qquad (8.4)$$

where $f_b = aR_{e_b}^{b}$ (8.5)

and $Re_b = \frac{M_b D_e}{\eta A_b}$ (8.6)

where D_e is the hydraulic diameter of the bypass lane.

An important point to note here is that Moore assumed the crossflow extended to a distance of half the minimum tube clearance outside the outer tube limit as proposed by Bell. This is not to be necessarily true but since the crossflow and bypass correlations are based on this premise, it is necessary to apply this arbitrary limit in order to be able to use the correlations validly.

8.2.3 Windowflow

The model used is that developed in Chapter 6. The effect of crossflow penetration into the window as described in Chapter 5 is also included in the model.

8.2.4 Baffle Leakage

The baffle leakage losses are based on the eccentric orifice data of Bell (1958). The pressure drop is correlated in the form (i = shell/baffle or tube/baffle).

$$\Delta p_i = \left(C_i + 4 f_i \frac{B_t}{t_i}\right) \frac{M_i^2}{2 \rho A_i^2} \quad (8.7)$$

where the first term in brackets accounts for the frictional losses as the fluid leaks through the baffle and the second term allows for the discharge losses. The geometric discharge loss coefficient, C_i, is correlated as a function of the baffle geometry,

$$C_i = a \left(\frac{B_t}{t_i}\right)^b \tag{8.8}$$

and the friction factor, f_i, is given by the equivalent in-tube relationship of Wilson (1922)

$$f_i = 0.0035 + 0.264\ Re_i^{-0.42} \tag{8.9}$$

where the characteristic length in the Reynolds number is the diametral clearance of the shell or tube and baffle i.e. $2t_i$.

In addition the model for the 'Effective Leakage Area' as described in Chapter 7 is used to allow for baffle leakage in the window zone. Furthermore, the model for crossflow/leakage interaction is also included.

8.3 Solution Procedure

The solution procedure of Moore (1974) is used as it is quick and very simple. Appendix 2 shows another similar method which could easily be used in preference. As stated earlier solution procedures are interchangeable and hence it is clearly best to use the simplest available which at the time of developing this model was the Moore procedure.

8.4 The Strengths of the Stream-Interaction Method.

The Stream-Interaction method has been developed by studying various shellside phenomena, in isolation and/or together, leading to a number of improvements based on the physics of the phenomena. Overall the model has

1) A new and accurate windowflow model.

2) It allows for the effect of crossflow/leakage interaction.

3) The penetration of crossflow into the window is taken into account.

4) The model allows for the effect of baffle leakage in the window zone.

5) The model has less reliance on empirical correlations based directly on shellside flow.

The method is presently implemented in the HTFS TASC2 computer program which is used to design and/or rate shell-and-tube heat exchangers. The program is used over 1000 times a week throughout the world.

Chapter 9 describes the validation of 'Stream-Interaction' method.

9.0 THE EXPERIMENTAL VALIDATION OF THE 'STREAM-INTERACTION' METHOD

This chapter outlines the experimental validation of the 'Stream-Interaction' method showing it to be a reliable method. It is also compared with other shellside pressure drop methods, and is shown to be the most consistent method predicting virtually all the available shellside pressure drop data to within ± 30%.

9.1 The Experimental Data

9.1.1 Availability of Data

In order to test the 'Stream-Interaction' method, suitable data are required, namely baffle-space pressure drop data. There are rather more data available for overall pressure drop measurement i.e. where end-spaces and nozzles are included but these are not suitable. There are only three sources of baffle-space pressure drop measurements available in this work

1) The Co-operative Research Program at Delaware University

2) The HTFS Research Programme at UKAEA Winfrith

3) The HTFS Research Programme at the National Engineering Laboratory

The data from the HTFS Research Programmes are proprietary and hence are only presented in a non-dimensional form.

9.1.2 Categories of the Data

The experimental data may be divided into four main types, the first three for small-scale models.

1) No-Leakage data.

2) Single-Leakage data (i.e. only shell-baffle or tube-baffle leakage present).

3) Combined-Leakage data (i.e. both shell-baffle and tube-baffle leakage present).

4) Combined-Leakage data for large-scale exchangers.

The no-leakage data are obtained from small-scale model exchangers where the baffle leakage has been eliminated as shown in Figure 4.2 A variety of baffle cuts and baffle pitches have been tested covering the range that is typically found in commercial heat exchangers.

The Single-Leakage data, are from the same small-scale exchangers except that baffle leakage has been introduced in either the shell-baffle leakage stream or the tube baffle leakage stream.

The combined leakage data, where both leakage streams are present (the real situation),are split into two types i.e. small-scale data and large-scale data.

Although there are not many data available they do follow a logical sequence, with shell diameters ranging from 133.5 mm (small-scale) to over 456 mm (large-scale). The baffle cuts considered range from 18.4% of the shell diameter to 43.7% of the shell diameter (covering adequately the range found in commercial practices) and the baffle pitches range from 10% to 100% of the shell diameter. The leakage flowrates also cover a wide range from 0% (no-leakage) to over 60% of the total flow in some cases.

Altogether the data cover a wide enough range to validate, at least superficially, the 'Stream-Interaction' method.

9.1.3 Shellside Fluids Used

All the data available are for single-phase liquids, there being no data available for single-phase gases.

The Delaware experiments used oil as the shellside fluid, the Winfrith experiments used water (plus a quantity of sodium hydroxide), and the NEL experiments used refrigerant 12. The physical properties at $20^{o}C$ are as follows:

	Density Kgm^{-3}	Viscosity $N sm^{-2}$
oil	785	1.86×10^{-3}
water (+ Na OH)	1040	1.00×10^{-3}
refrigerant 12	1325	2.09×10^{-4}

showing that the physical properties cover a reasonable range.

9.2 Potential Accuracy of Shellside Pressure Drop Predictions

In order to validate any method it is necessary to examine the experimental data and the correlations used to assess an acceptable error band that may be expected.

Firstly consider the experimental data. For each of the various geometries tested, there are mass flowrate versus pressure drop measurements. For any individual geometry, the pressure drop can be expressed as a power law of flowrate i.e.

$$\Delta p = a M_T^b \qquad (9.1)$$

In general b is between 1.6 and 2.0. There are two types of error in the measurement i.e. systematic and random errors. It has to be assumed here that the systematic errors are zero (although this is by no means certain). A simple way of assessing the random fluctuations is to correlate each individual set of pressure drop mass flowrate measurements to obtain mean values for a, b for any given geometry. In all the experiments, the flowrate, $\mathring{M}_i$, is the independent (controlled) variable and the pressure drop, Δp_i, is the dependent (measured) variable. It is assumed here that the flowrates can be measured to an accuracy of $\pm$ 2% (a typical accuracy for rotameters). From equation 9.1 (where b = 2) gives a maximum expected error of 4% in the pressure drop. Having obtained mean values for a, b for any given geometry, equation 9.1 is used where the flowrate is the measured value to obtain an expected pressure drop.

This can be compared with the actual pressure drop to give the deviation from the best 'least-squares' fit of the data.

Performing this analysis for the experimental data revealed that the random fluctuations were usually between 0 to 10% (and sometimes greater). Since a fluctuation of 10% cannot be explained by variation in the flowrate (where it is expected a maximum error of 4% would occur) then it is clear that the measurement of pressure drop is much more prone to error than flowrate and hence is the critical measurement.

Secondly, the correlations used in any method must also be considered, as these will reflect in the overall accuracy of any method. Palen and Taborek state that the best possible crossflow correlations are accurate to $\pm$ 15%. It has already been shown in Chapter 6 that windowflow pressure drop is predicted to within $\pm$ 13% (standard deviation). Overall, it is considered that the accuracy of the correlations in the 'Stream-Interaction' method have a maximum error of about $\pm$ 20%.

In the worst case, the 'Stream-Interaction' method may underpredict by 20%, and the measured value may be overestimated by 10% leading to a maximum error of 30% at which the prediction is still reasonable. Any predictions within $\pm$ 30% will be considered to be good predictions and any outside $\pm$ 30% will be progressively considered poor depending on their magnitude.

9.3 The Comparisons with Experimental Data

Tables 9.1 and 9.2 give the predictions of the 'Stream-Interaction' method and the Bell (HEDH (1983)) method for the no-leakage data of Brown (1956) and Macbeth (1973) respectively.

Table 9.3 gives the predictions of the above two methods for the single-leakage data of Bell and Fusco (1958) whilst tables 9.4 and 9.5 give the predictions for the combined-leakage data of Holzman (1958) and Macbeth (1973) respectively.

Tables 9.6 and 9.7 give the predictions of the large-scale exchanger data of NEL (1980) for the following methods :-

1) the 'Stream-Interaction' method,

2) the 'Divided-Flow' method,

3) the 'Moore' method,

4) the 'Bell' method,

and

5) the 'Kern' method.

All the predictions in tables 9.1 to 9.7 are plotted in Figures 9.1 to 9.7 respectively with the exception of the Kern method, which is clearly shown in tables 9.6 and 9.7 to be totally inadequate.

TABLE 9.1: NO LEAKAGE DATA OF BROWN (1956)

Cut/ Pitch	Flowrate lb/hr	Δp EXP lb_f/ft^2	Δp STR-INT lb_f/ft^2	Δp HEDH lb_f/ft^2
1.91" 18.4%	23800 14500 8780 5240	393 154 59 22	339 134 52 20	226 86 32 12
0.976" 18.4%	15050 6970 3510 1600 1000	355 86 24 7.2 2.4	367 87 24 5.6 2.3	229 52 14 3.1 1.4
0.5" 18.4%	6200 3630 1790 760	210 79 21 4.5	174 63 17 3.3	113 41 11 2.2
1.91" 31%	32300 14900 6300 2990	309 72 14 3.4	303 71 14 3.6	276 61 11 2.7
0.976" 31%	18350 8890 4220 2050	244 67 17 4.5	342 87 22 5.6	224 55 13 3.3
3.72/ 43.7%	32820 13450 5170	81 15 2.5	71 13 2.2	93 16 2.4
1.91/ 43.7%	32360 13450 5130	194 36.0 5.7	198 37 6.0	187 33 4.9
0.976 43.7%	20450 9550 4310 2040	237 52 11 2.5	276 64 14 3.3	165 37 7.8 1.8

TABLE 9.2: NO LEAKAGE DATA OF MACBETH (1973)

Cut/ Pitch	Flowrate kg/s	Predicted/ Experimental $\Delta p_{STR-INT}$	Predicted/ Experimental Δp_{HEDH}
48.5mm 18.4%	1.11	0.89	0.62
	1.58	0.90	0.66
	2.37	0.97	0.72
	3.17	0.95	0.72
	3.96	0.97	0.75
	4.75	1.11	0.77
97.0mm 18.4%	1.11	0.94	0.45
	1.58	0.95	0.46
	2.38	1.04	0.51
	3.17	1.01	0.50
	3.96	1.09	0.54
48.5mm 25.0%	1.11	1.06	0.89
	1.58	0.99	0.85
	2.37	1.09	0.97
	3.16	1.06	0.97
	3.96	1.24	1.14
	4.75	1.06	0.99
97.0mm 25.0%	1.11	0.99	-
	1.58	0.95	0.70
	2.37	1.02	0.68
	3.16	0.84	0.74
	4.75	1.01	0.62
			0.76
48.5mm 37.5%	1.11	1.18	1.04
	1.58	1.15	1.04
	2.37	1.22	1.14
	3.17	1.19	1.14
	4.75	1.33	1.15
97.0mm 37.5%	1.11	0.93	0.98
	1.58	0.92	1.00
	2.37	0.98	1.10
	3.17	1.00	1.14
	4.75	0.95	1.12
	6.33	0.93	1.12

TABLE 9.3: SINGLE LEAKAGE DATA OF BELL AND FUSCO (1958)

Leakage Type/ Tolerance	Flowrate lb/hr.	Δp_{EXP} lb_f/ft^2	$\Delta p_{STR-INT}$ lb_f/ft^2	Δp_{HEDH} lb_f/ft^2
S/B 0.133"	30600	124	148	96
	14400	30	34	22
	6500	6.7	7.4	4.7
	3010	1.6	1.7	1.1
	1590	0.7	0.5	0.3
T/B 0.006"	27600	330	314	223
	14900	103	100	67
	6500	22	21	13
	3190	6.3	5.8	3.4
	1590	2.1	1.6	1.0
T/B 0.013"	27900	287	205	192
	15000	88	64	57
	6490	19	14	11
	3180	5.1	3.6	2.8
	1590	1.3	1.0	0.8
S/B 0.063"	28200	218	217	125
	15000	65	65	37
	6500	14	13	7.2
S/B 0.021"	26300	270	300	161
	14500	88	98	51
	6500	21	22	11
	3010	4.3	5.1	2.4
	1600	1.5	1.6	0.8

S = SHELL-BAFFLE

T = TUBE-BAFFLE

TABLE 9.4: COMBINED LEAKAGE STUDIES OF HOLZMAN (1958)

S/B tol./ T/B tol.	Flowrate lb/hr.	Δp_{EXP} lb_f/ft^2	$\Delta p_{STR-INT}$ lb_f/ft^2	Δp_{HEDH} lb_f/ft^2
	31500	170	118	152
0.063"	14400	39	27	33
	6500	9.5	6.0	7.0
0.013"	4400	4.6	2.7	3.3
	3020	2.3	1.5	1.6
	1590	0.8	0.44	0.5
0.133"	30460	111	97	96
	14400	28	23	22
0.013"	6500	7.0	5.1	4.7
	3020	1.8	1.2	1.1
	1590	0.6	0.4	0.3
0.021"	31820	247	221	209
	14400	65	50	44
0.013"	6500	15	11.4	9.5
	5480	11	8.3	6.8
	3620	4.8	3.9	3.0
	3620	5.6	3.9	3.0
	3190	4.6	3.1	2.4
	1590	1.4	0.9	0.7

TABLE 9.5: LEAKAGE DATA OF MACBETH (1973)

Cut% S/B tol T/B tol	Flowrate kg/s	Predicted/ Experimental $\Delta p_{STR-INT}$	Predicted/ Experimental Δp_{HEDH}
18.4 2.668mm 0. 66mm	1.11	0.75	0.97
	1.58	0.76	1.13
	2.37	0.87	1.31
	3.16	0.91	1.35
	4.74	0.93	1.28
	7.91	0.93	1.25
18.4 1.334mm 0. 33mm	1.11	0.70	0.67
	1.58	0.71	0.69
	2.37	0.77	0.77
	3.16	0.72	0.73
	4.74	0.70	0.72
25.0 2.668mm 0. 66mm	1.11	1.01	1.35
	1.58	1.14	1.54
	2.37	1.14	1.57
	3.16	1.17	1.62
	4.74	1.15	1.62
	7.91	1.14	1.63
37.5 2.668mm 0. 66mm	1.11	1.03	1.34
	1.58	1.04	1.38
	2.37	1.11	1.50
	3.16	1.21	1.66
	4.75	1.13	1.58
	7.91	1.07	1.53

TABLE 9.6: NEL BOILER SINGLE-PHASE TRIALS (1980)

Flowrate Kg/s	Predicted/Experimental Δp				
	KERN	HEDH	MOORE	DIV-FLO	STR - INT
A					
8.77	9.37	1.61	1.49	1.43	1.10
19.69	8.09	1.59	1.39	1.36	1.05
29.63	7.98	1.68	1.43	1.43	1.09
13.56	8.83	1.63	1.47	1.41	1.09
24.72	8.16	1.66	1.44	1.43	1.09
5.65	10.33	1.65	1.58	1.51	1.16
B					
9.85	7.45	1.31	1.21	1.16	0.90
12.56	7.48	1.37	1.24	1.19	0.92
15.59	7.14	1.35	1.21	1.16	0.91
18.35	7.82	1.52	1.32	1.28	0.99
20.10	6.89	1.36	1.20	1.18	0.90
23.97	7.43	1.50	1.29	1.27	0.97
25.77	7.47	1.53	1.34	1.33	1.01
29.81	7.09	1.49	1.26	1.26	0.96
31.62	6.98	1.48	1.25	1.25	0.95

TABLE 9.7: NEL CONDENSER SINGLE-PHASE TRIALS (1980)

Flowrate Kg/s	Predicted/Experimental Δp				
	KERN	HEDH	MOORE	DIV-FLO	STR-INT
9.2	22.2	1.87	3.09	1.73	1.15
15.0	19.3	1.73	2.52	1.55	1.09
13.1	19.1	1.66	2.67	1.50	1.04
6.7	16.6	1.33	2.29	1.33	0.86
9.3	20.1	1.72	2.74	1.53	1.08
11.8	19.1	1.65	2.64	1.50	1.02
13.6	18.6	1.63	2.57	1.45	1.01
15.6	18.5	1.66	2.51	1.43	1.04
28.7	16.7	1.53	2.25	1.29	0.94
25.8	16.9	1.58	2.46	1.40	0.97
20.0	17.5	1.55	2.40	1.36	0.95
17.0	17.7	1.64	2.53	1.43	1.03
14.4	18.3	1.65	2.53	1.44	1.01
11.0	18.6	1.63	2.51	1.41	1.01
7.9	19.6	1.48	2.50	1.41	0.94
18.8	17.7	1.64	2.49	1.40	1.01

FIGURE 9.1 : PREDICTIONS OF BROWN NO-LEAKAGE BAFFLE-SPACE DATA

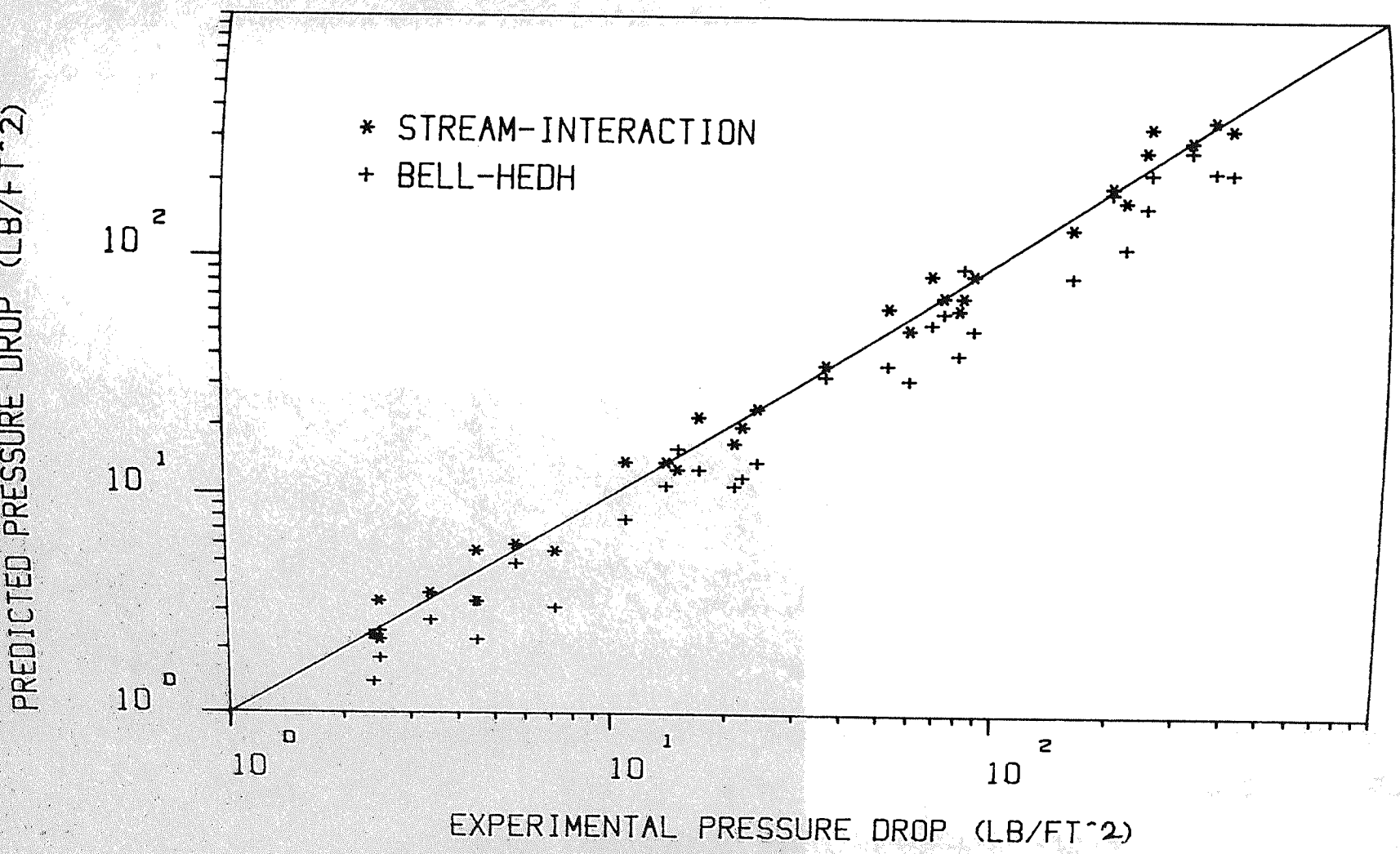

FIGURE 9.2 : PREDICTIONS OF MACBETH NO-LEAKAGE BAFFLE-SPACE DATA

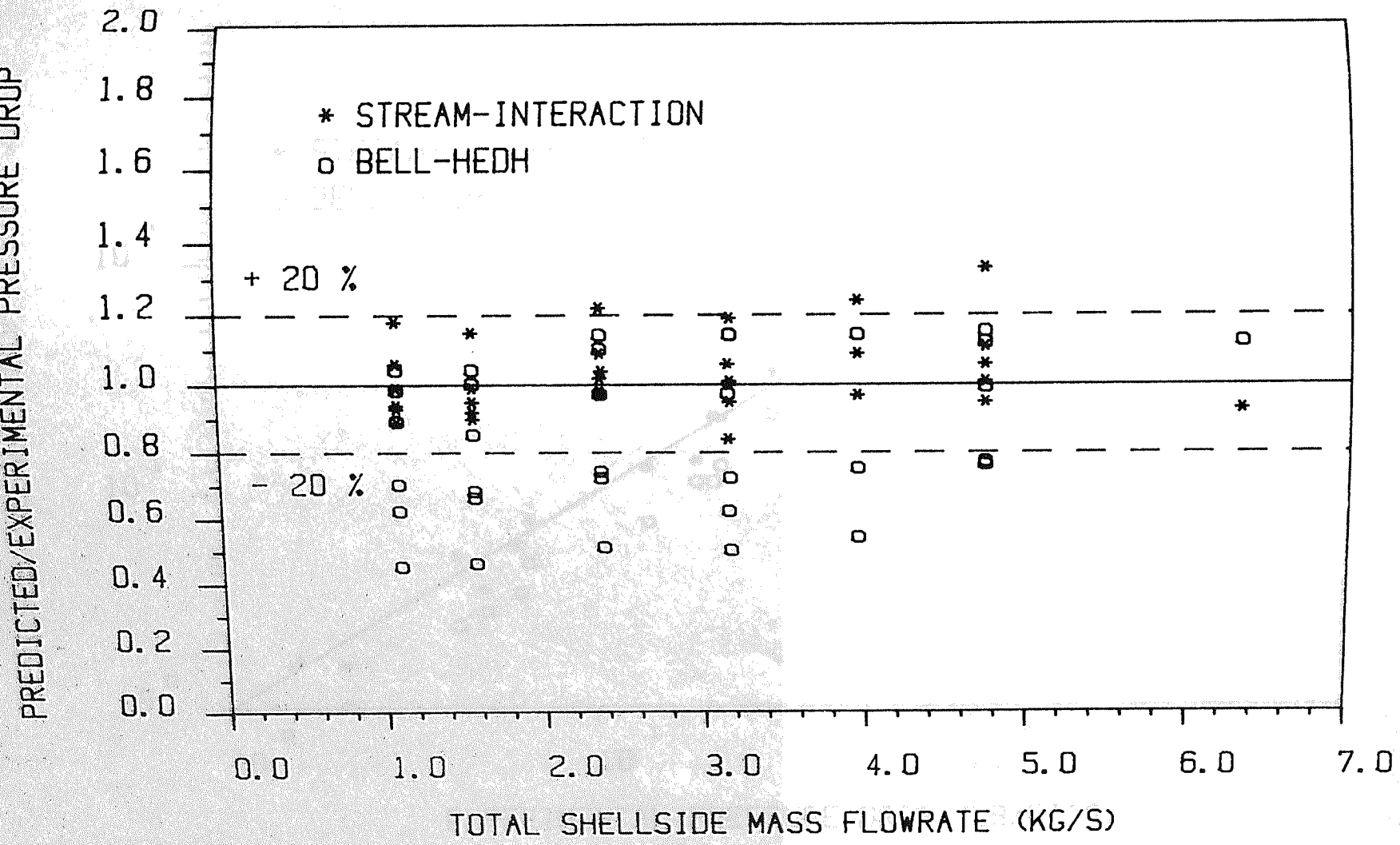

FIGURE 9.3 : PREDICTIONS OF SINGLE-LEAKAGE DATA OF BELL AND FUSCO

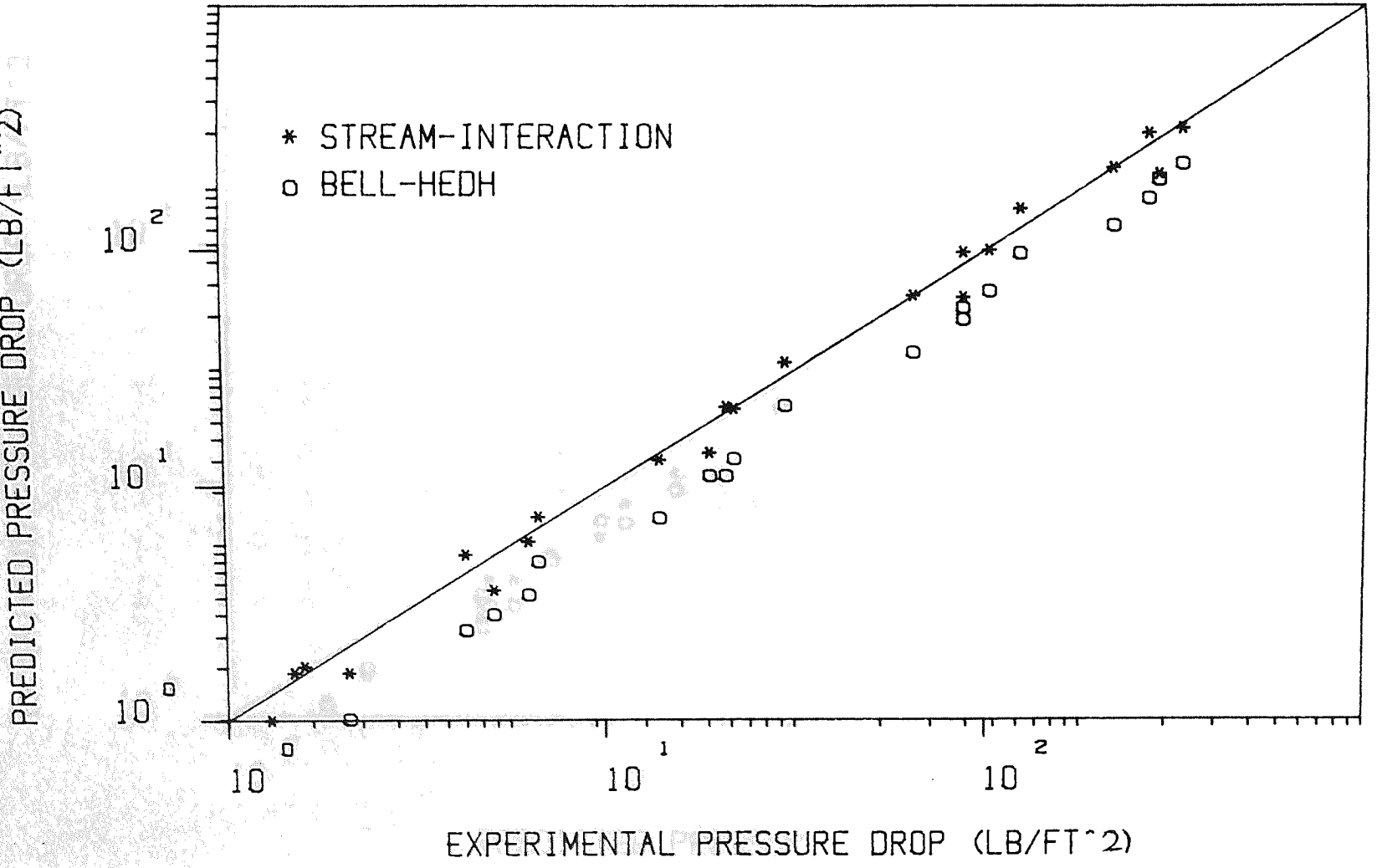

FIGURE 9.4 : PREDICTIONS OF COMBINED LEAKAGE DATA OF HOLZMAN

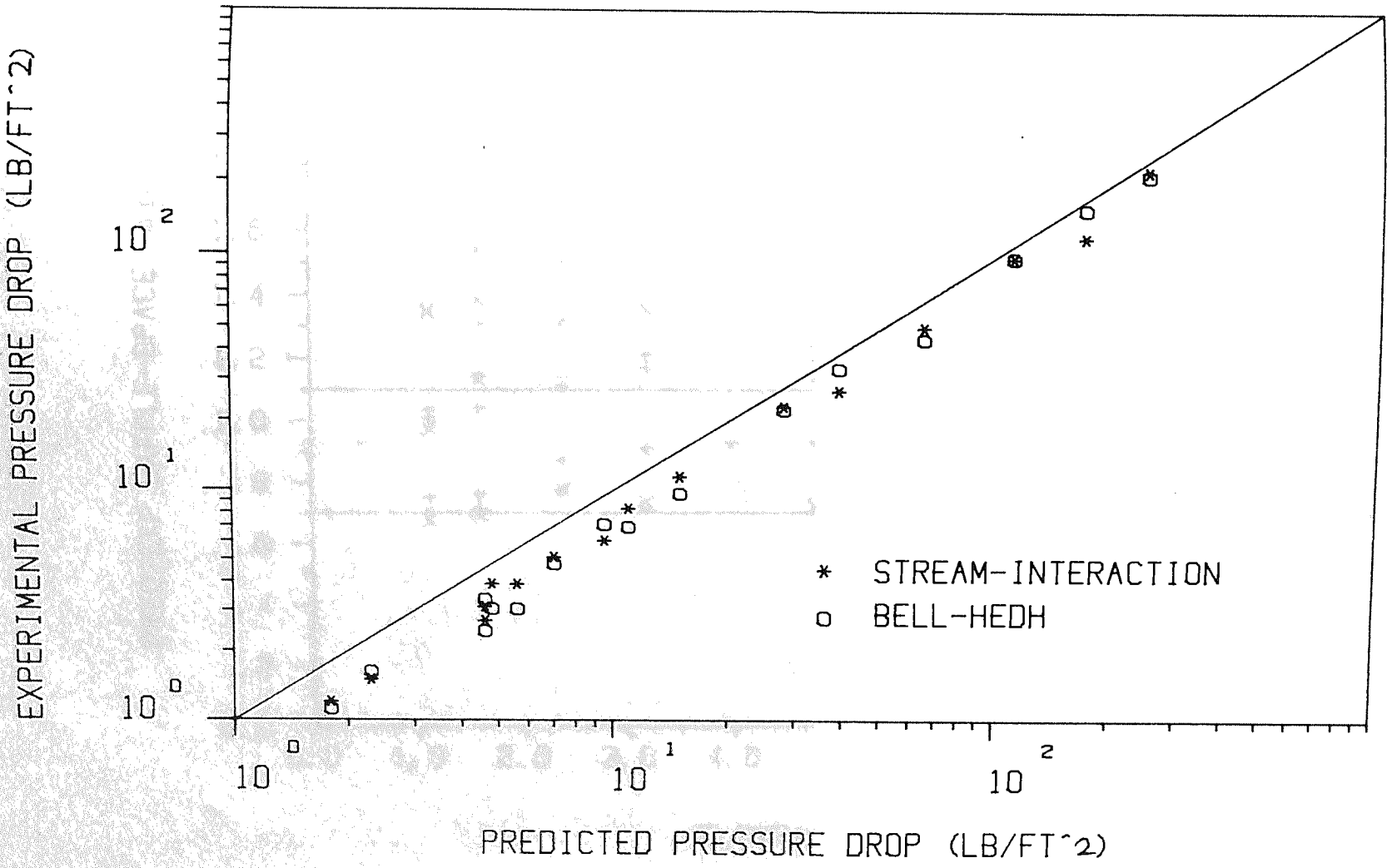

FIGURE 9.5 : PREDICTIONS OF COMBINED LEAKAGE DATA OF MACBETH

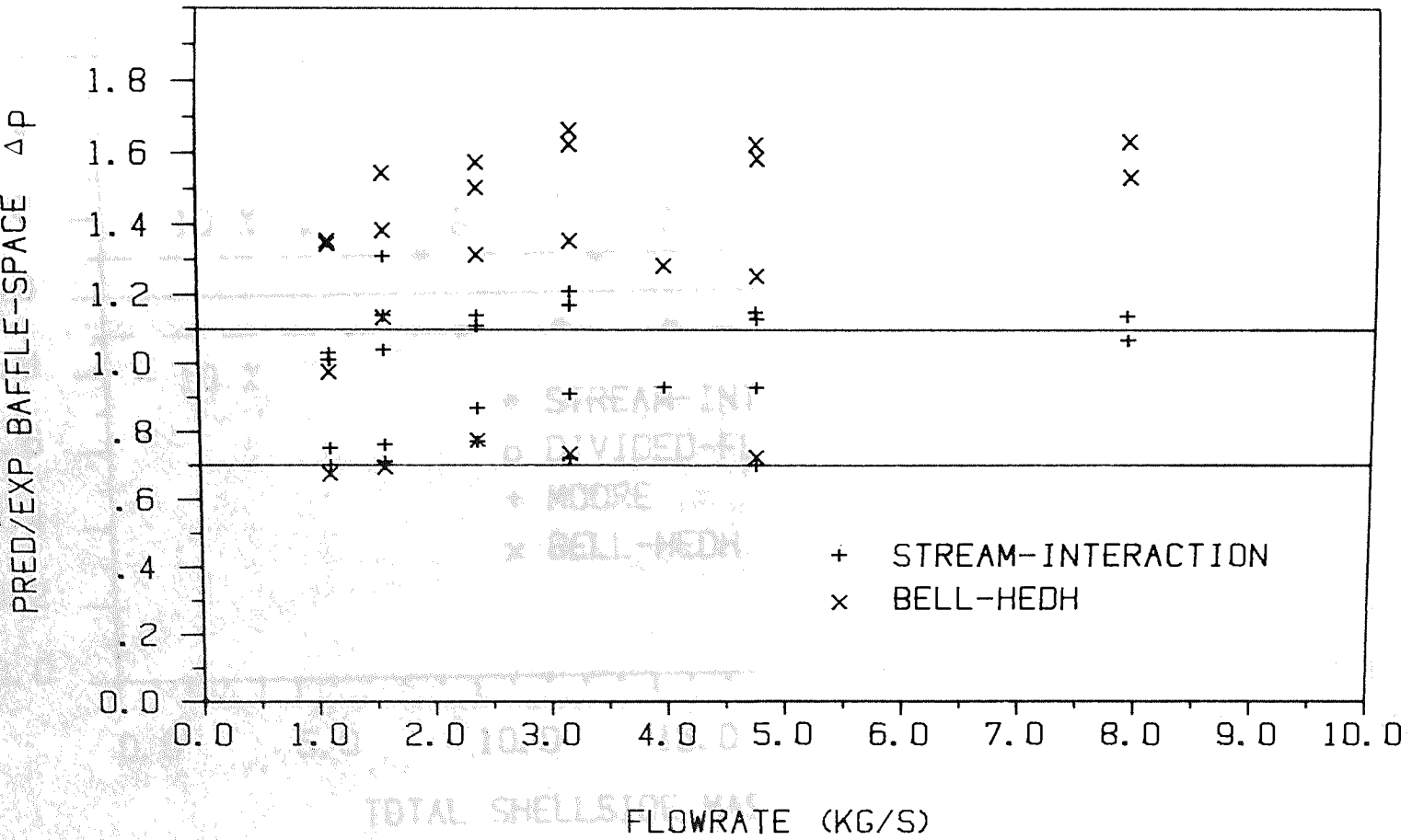

FIGURE 9.6 : PREDICTIONS OF NEL BOILER SINGLE-PHASE TRIALS

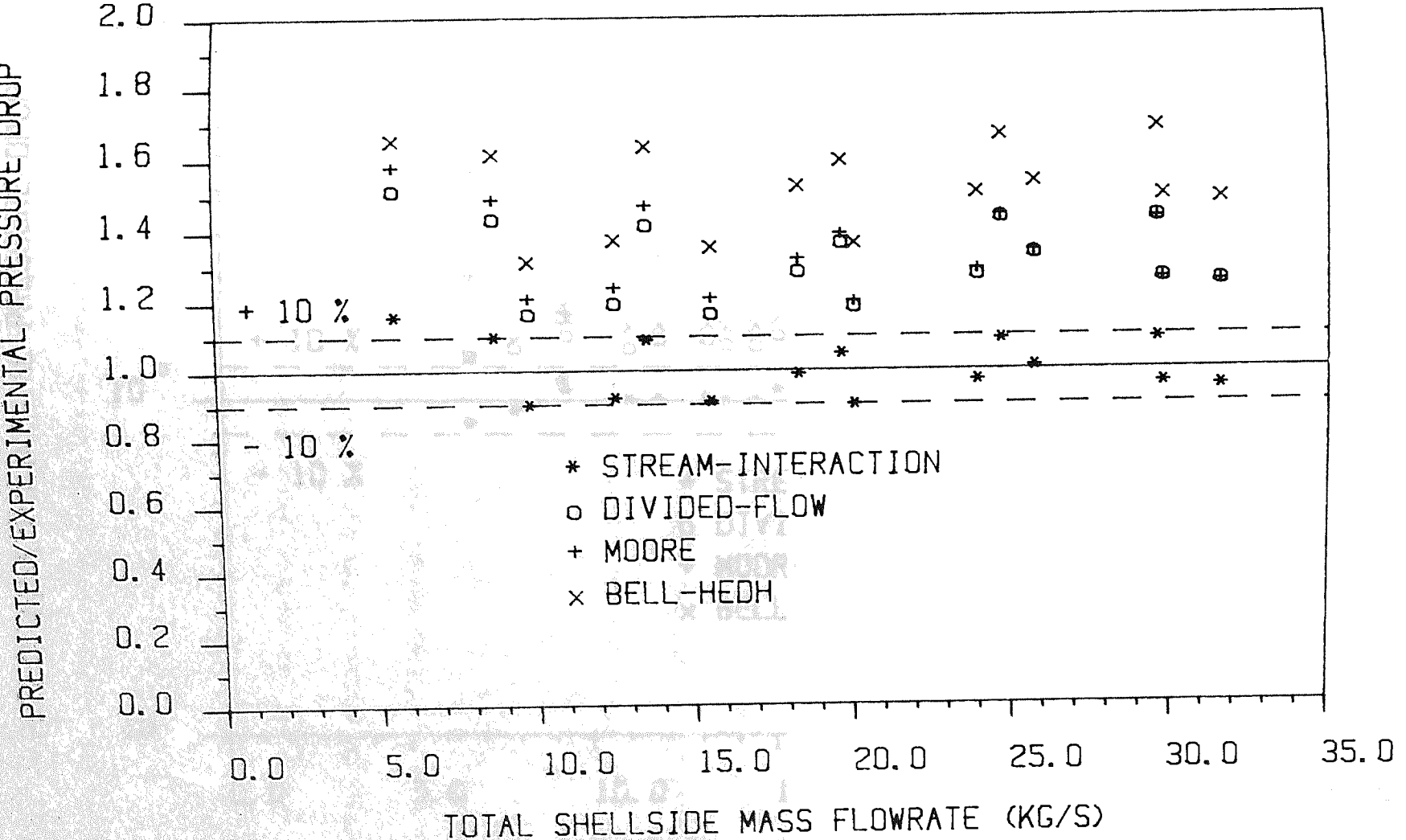

FIGURE 9.7 : PREDICTIONS OF NEL CONDENSER SINGLE-PHASE TRIALS

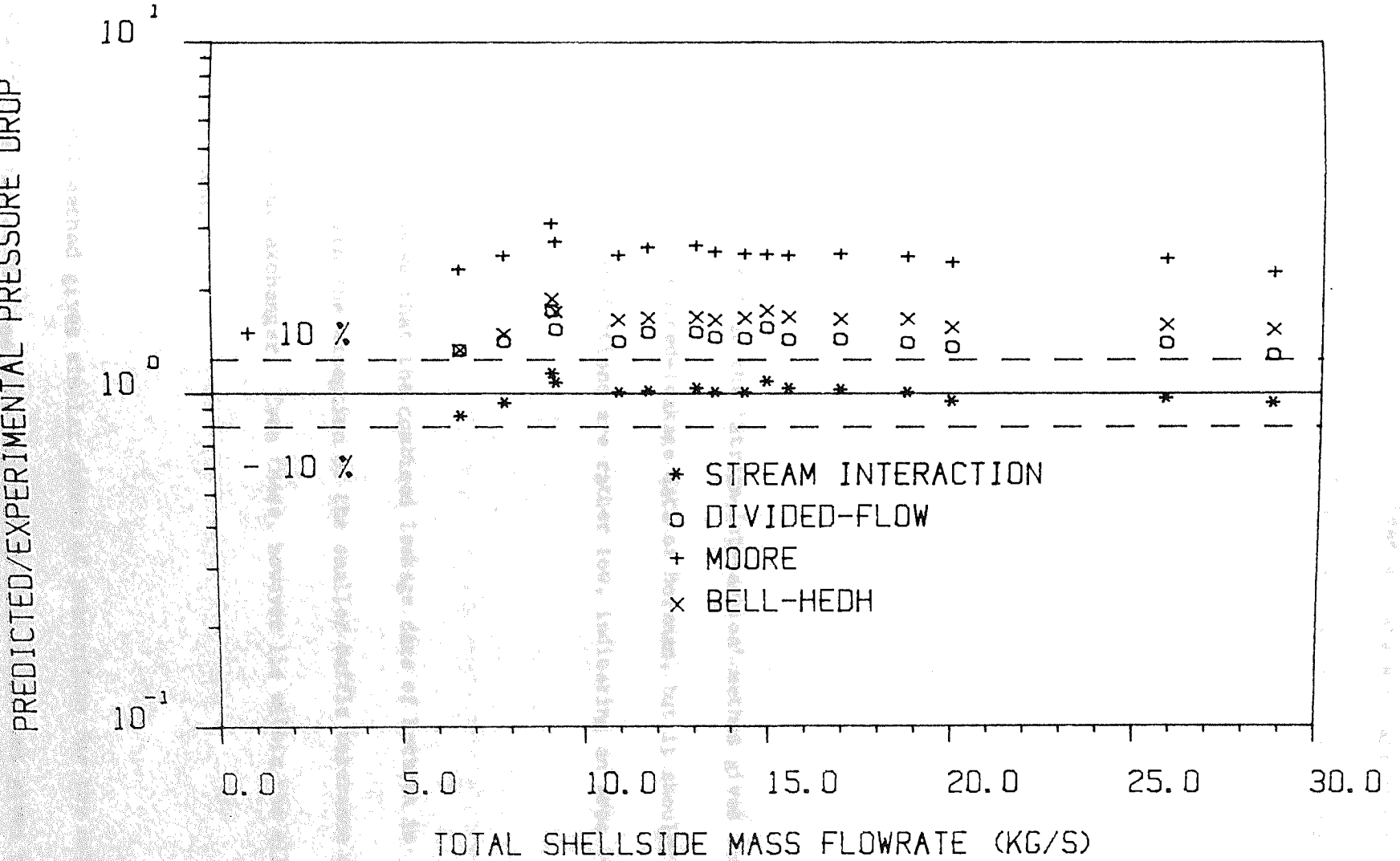

9.4 Results

Figures 9.1 and 9.2 show that the 'Stream-Interaction' method gives very good predictions of the no-leakage data with all the results falling within an error band of ± 20% and hence within the allowable ± 30% error band. Contrast this with the Bell method which underpredicts by up to 60% in some cases!

Figure 9.3 shows that the 'Stream-Interaction' method also gives good predictions of the single-leakage data with all the predictions lying withing a ± 30% error band. Again the Bell method seriously underpredicts by 40-50% in some cases.

Figure 9.4 shows that the 'Stream-Interaction' method gives fair predictions of the combined-leakage data of Holzman, but it should be noted that all the predictions are rather low, indicating an area of weakness.

Figure 9.5 shows that the combined leakage data of Macbeth is predicted well, with the exception of the smaller baffle tolerance data for the 18.4% cut exchanger. Even these, however lie within the allowable ± 30% error band.

The Bell method gives similar orders of predictions for the Holzman data (faring better for one case but this is fortuitous) but gives predictions

ranging from -30% to + 60% for the Macbeth data.

Figure 9.6 shows that the 'Stream-Interaction' method gives exceptionally good predictions of the single-phase trials of the NEL boiler with all results within ± 10%. The Moore and 'Divided-Flow' methods both give fair results with predictions ranging from + 20% to + 40%. The Bell method significantly overpredicts with predictions ranging from + 30% to + 70%.

Finally figure 9.7 shows that, again, the 'Stream-Interaction' method gives exceptionally good predictions of the single-phase trials of the NEL condenser, with all the results within ± 10%. The 'Divided-Flow' method also gives fair results ranging from + 40%to + 50%. The Bell method overpredicts by 50% - 80%, and the Moore method overpredicts by 150%.

Note from tables 9.6 and 9.7 that the Kern method overpredicts by a factor of 7-8 and 17-20 respectively.

9.5 Discussion

The most striking result from the validation exercise is that the 'Stream-Interaction' method predicts virtually all the shellside pressure drop data to within ± 30%, a claim which cannot be made of any other method tested, and as such, the method represents a significant improvement in shellside pressure drop prediction.

There are still areas in which the 'Stream-Interaction' method may be improved i.e. small baffle cuts with small baffle tolerances. It would appear in these cases (Figure 9.4 and Figure 9.5 for one dataset) that the 'Stream-Interaction' method tends to underpredict. The reasons for this are not clear but is is believed that the correlations for baffle leakage are inadequate, causing the leakage to be overpredicted. It is quite possible that the resistance to baffle leakage flow is much higher than predicted for tight tolerances, possibly due to a laminar sub-layer occupying a significant portion of the leakage annuli, but the leakage correlations assume fully turbulent flow. Clearly this is an area for future research from both an experimental and theoretical standpoint. Although not shown, the 'Divided-Flow' method actually gives better predictions for these cases, but it is believed this is fortuitous, the better predictions stemming from the fact that the 'Divided-Flow' method ignores leakage in the window, this being apparent by the relatively large overpredictions for other geometries.

The most exciting predictions are for the large-scale exchangers, with the 'Stream-Interaction' method giving exceptionally good results. This is very important as it gives confidence to the use of the method for commercial sized exchangers.

Contrast the results of the 'Stream-Interaction' method with the other methods. Firstly, the Bell method gives erratic predictions ranging from -60% to +80% with no obvious trend as to which way a prediction is likely to be, although it would appear the method tends to underpredict no-leakage data, in general, but overpredicts leakage data, i.e. the correction factors for leakage tend to "save" the Bell method.

The other HTFS methods, i.e. the 'Divided-Flow' method and the 'Moore' method tend to be rather conservative in general overpredicting by up to 60%. Also the Moore method can seriously overpredict for an unusual geometry e.g. the NEL condenser.

9.6 Conclusions

It is concluded the 'Stream-Interaction' method is the best of all the methods tested, being capable of predicting shellside pressure drop to within $\pm$ 30%. Most importantly the method gives good predictions of large-scale exchanger data, demonstrating its extrapolation capabilities. Overall the method is very reliable and is strongly recommended as a design method.

10.0 FUTURE WORK

This chapter discusses future work which may be performed to extend the development of shellside pressure drop prediction techniques.

10.1 Theoretical Work

This thesis has concentrated entirely on shellside pressure drop in the middle portion of a baffled exchanger and has not made any attempt to study the effect of end-spaces and nozzles. Clearly these are a very important part of shellside pressure drop prediction.

End-space pressure drop prediction is very different from mid-space pressure drop prediction because the flowrates for each path are not constant i.e. the method needs to take account of the varying flowrate in crossflow which occurs because of the setting up of the baffle leakage. The flowrate in the end-space will vary from the total, $\dot{M}_T$, at the inlet to the mid-space windowflowrate, $\dot{M}_w$ at the first window. (Of course, this may not even be true!).

A single model may be defined where the pressure drop is based on the mean end-space flowrate e.g.

$$\dot{M}_e = \frac{\dot{M}_w + \dot{M}_T}{2} \qquad (10.1)$$

and

$$\Delta p_e = a \dot{M}_e^b + \tfrac{1}{2} n_{we} \dot{M}_w^2 \qquad (10.2)$$

where a, b allow for bypassing as well, and n_{we} allows for the windowflow pressure drop in the end-space.

A better method may be to define a pressure drop mean i.e.

$$\Delta p_e = \int_0^{h_e} a M_x^b + \tfrac{1}{2} n_{we} \dot{M}_w^2 \qquad (10.3)$$

Clearly there is an area in which further theoretical research may be applied to the development of shellside pressure drop prediction.

Consider exchangers that have different baffle arrangements e.g. double segmental baffles. Again this is yet another area in which theoretical research may be applied. Nozzle shellside pressure drop prediction is another area of great uncertainty with nozzle geometries varying greatly.

10.2 Experimental Work

This thesis has presented a method which has been validated against a rather limited set of data. It would be extremely useful to actually measure the flowrates in each of the various paths. Work into this area is already under way by UKAEA Harwell and Aston University.

More 'single-effect' experiments on baffle leakage, bundle bypassing, windowflow and so on, would prove immensely valuable to remove some of the uncertainties of shellside pressure drop prediction.

10.3 Other Shellside Work

Overall, there are many areas, both theoretical and practical, in which future research may be directed. One of the most important areas is heat transfer research. This thesis has concentrated on pressure drop in isothermal situations but in real exchangers the flow is not isothermal. How does heat transfer affect the pressure drop?

Moreover how can we predict the heat transfer? There are a number of correlations for heat transfer coefficients in ideal tube-banks. How can these be applied to real exchangers? Are the bypass and leakage streams totally ineffective in heat transfer? This last question is a very important one as it leads on to a whole new dimension of modelling in shellside flow e.g. if the bypass and leakage streams are ineffective, then the traditional logarithmic mean temperature difference used in exchanger design is not valid, because it assumes that the shellside fluid is in plug flow, which is not the case with bypassing present.

The scope for future research is immense and it is hoped that this thesis will stimulate future researchers to investigate new and unexplored directions.

NOMENCLATURE

A	Cross-sectional area of a tube	(m^2)
A_{cl}	Minimum centre-line flow area	(m^2)
A_e	Effective leakage are	(m^2)
A_i	Flow area of path i	(m^2)
A_{se}	Effective shell/baffle leakage area	(m^2)
A_{te}	Effective tube/baffle leakage area	(m^2)
B_t	Baffle thickness	(m)
C_i	Discharge coefficient for baffle leakage (i = s, t only)	(-)
D_c	Height of centroid of window from centreline	(m)
D_e	Hydraulic equivalent diameter	(m)
D_o	Tube diameter	(m)
D_s	Shell diameter	(m)
D_t	Tube bundle diameter	(m)
F	Geometric factor in Buthod's method	(-)
F_i	Flow fraction of path i	(-)
F_L	Leakage enhancement factor	(-)
F_{Lb}	Leakage enhancement factor for the bypass path	(-)
F_{Lc}	Leakage enhancement factor for the crossflow path	(-)
F_r	Windowflow pressure drop correction factor	(-)
f	Fractional penetration of crossflow into the window	(-)

f_i	Friction factor of path i	(-)
f_T	Total shellside friction factor	(-)
H	Height of overlap zone	(m)
h	Height of window zone	(m)
K	Number of velocity heads lost	(-)
K_i	Number of velocity heads lost in path i	(-)
L	Extent of the crossflow	(m)
L_B	Baffle spacing	(m)
$\dot{M}$	Mass flowrate	($kg\ s^{-1}$)
$\dot{M}_i$	Mass flowrate in path i	($kg\ s^{-1}$)
$\dot{M}_{ri}$	Relative flowrate in path i	(-)
$\dot{M}_T$	Total shellside mass flowrate	($kg\ s^{-1}$)
$\dot{m}$	mass velocity	($kg\ s^{-1}\ m^{-2}$)
$\dot{m}_i$	mass velocity in path i	($kg\ s^{-1}\ m^{-2}$)
$\dot{m}_T$	total mass velocity	($kg\ s^{-1}\ m^{-2}$)
N_i	Number of rows crossed in path i	(-)
N_p	Rating number (Tinker's method)	(-)
N_{ss}	Number of sealing strips	(-)
N_{tr}	Number of tie rods	(-)
N_{tw}	Number of rows crossed in the window (Bell's method)	(-)
n_i	Flow resistance of path i	($kg^{-1}\ m^{-1}$)
P_d	Baffle cut as % of shell diameter	(-)
P_t	Tube pitch	(m)

p_x	Longitudinal tube pitch	(m)
p	Pressure	(Nm^{-2})
Δp	Pressure drop	(Nm^{-2})
Δp_c	Ideal crossflow pressure drop (Bell's Method)	(Nm^{-2})
Δp_e	End-space pressure drop	(Nm^{-2})
Δp_i	Pressure drop across path i	(Nm^{-2})
Δp_N	Nozzle pressure drop	(Nm^{-2})
Δp_p	Baffle space pressure drop	(Nm^{-2})
Δp_T	Total shellside pressure drop	(Nm^{-2})
Δp_w	Ideal windowflow pressure drop (Bell's Method)	(Nm^{-2})
R_b	Bypass pressure drop correction factor f	(-)
R_e	End-space pressure drop correction factor	(-)
R_L	Leakage pressure drop correction factor	(-)
R_b	Mean permeability resistance in bypass	
R_c	Mean permeability resistance in crossflow	
R_x	Mean permeability resistance	
S_g	Specific gravity	(-)
S_m	Minimum centre-line flow area	(m^2)
S_p	Effective flow area per baffle space (Moore's Method)	(m^2)
S_s	Net cross-sectional area (Short's method)	(m^2)
S_w	Windowflow area (Short's Method)	(m^2)
t_b	Bypass clearance	(m)
t'_b	Effective bypass clearance	(m)

t_s	shell/baffle clearance (radial)	(m)
t_t	tube/baffle clearance (radial)	(m)
u	local superficial crossflow velocity	(ms^{-1})
$\bar{u}$	mean superficial crossflow velocity	(ms^{-1})
v	mean superficial leakage velocity	(ms^{-1})
v_i	velocity of shellside fluid in path i	(ms^{-1})
v_z	geometric mean velocity	(ms^{-1})
w	width of exchanger	(m)
x	ratio of windowflow/crossflow area	(-)
α	angle of direction of flow to axis of exchanger	(-)
ρ	density	(kgm^{-3})
ε	void fraction	(-)
η	viscosity	$(kg\ m^{-1}s^{-1})$
ϕ_i	shellside viscosity correction factor of path i	(-)
Θ	Flow vector	(-)

SUBSCRIPTS

Main Flow paths

a pass-partition path

b bypass path

c crossflow path

s shell/baffle leakage path

t tube/baffle leakage path

w windowflow path

Miscellaneous

cr combined crossflow plus bypass

L combined shell/baffle plus tube/baffle leakage

t1 , tw tube/baffle leakage in window region

t2 , to tube/baffle leakage in overlap region

s1 , sw shell/baffle leakage in window region

s2 , so shell/baffle leakage in overlap region

1 refers to leakage in window

2 refers to leakage in overlap

APPENDIX 1 : THE MULTI-STREAM METHOD ITERATION SCHEMES.

The iteration schemes of Tinker, Palen and Taborek, Grant and Murray, and Moore are shown in sections A1.1 to A1.4 respectively.

A1.1 Tinker (1948)

Tinker produced his, now, **classic** method before the age of computers. Figure 1.6 in the main text shows his flowstreams which are

1) crossflow,

2) bypass,

3) windowflow,

4) shell-baffle leakage, and

5) tube-baffle leakage.

The total flowrate, $\dot{M}_T$, is defined by

$$\dot{M}_T = \dot{M}_c + \dot{M}_b + \dot{M}_s + \dot{M}_t \qquad (A1.1)$$

where $\dot{M}_c$, $\dot{M}_b$ are **really** effective flowrates to be discussed later on.

A windowflow/crossflow pressure drop ratio, x, is defined as

$$x = \frac{\Delta p_w}{\Delta p_c} \qquad (A1.2)$$

and the baffle-space pressure drop is given by

$$\Delta p_p = \Delta p_c + \Delta p_w \qquad (A1.3)$$

From equations A1.2 and A1.3 then

$$\Delta p_p = \Delta p_c \, (1 + x) \qquad (A1.4)$$

The pressure drop driving force for each of the streams are

$$c : \Delta p_c \qquad (A1.5)$$

$$b : \Delta p_c \qquad (A1.6)$$

$$s : \Delta p_c \, (1 + x) \qquad (A1.7)$$

$$t : \Delta p_c \, (1 + x) \qquad (A1.8)$$

For each of the streams, a mass flowrate may be calculated by

$$\dot{M}_i = \left(\frac{\Delta p_i}{n_i}\right)^{\frac{1}{2}} \qquad \text{(A1.9)}$$

Equations A1.5 to A1.8 are substituted, in turn into A1.9 to give the flowrates of each stream as

$$c : \Delta p_c^{\frac{1}{2}} C_c \qquad \text{(A1.10)}$$

$$b : \Delta p_c^{\frac{1}{2}} C_b \qquad \text{(A1.11)}$$

$$s : \Delta p_c^{\frac{1}{2}} C_s (1 + x)^{\frac{1}{2}} \qquad \text{(A1.12)}$$

$$t : \Delta p_c^{\frac{1}{2}} C_t (1 + x)^{\frac{1}{2}} \qquad \text{(A1.13)}$$

where

$$C_i = n_i^{-\frac{1}{2}} \qquad \text{(A1.14)}$$

Dividing equations A1.10 to A1.13 by $\Delta p_c^{\frac{1}{2}}$ gives the flowrates as relative flowrates (to each other) i.e.

$$c : C_c \qquad \text{(A1.15)}$$

$$b : C_b \qquad \text{(A1.16)}$$

$$s : C_s (1 + x)^{\frac{1}{2}} \qquad \text{(A1.17)}$$

$$t : C_t (1 + x)^{\frac{1}{2}} \qquad \text{(A1.18)}$$

The flowrate in any stream, $\dot{M}_i$ is then obtained by

$$\dot{M}_i = \frac{\dot{M}_{ri}}{\dot{M}_{rc} + \dot{M}_{rb} + \dot{M}_{rs} + \dot{M}_{rt}} \dot{M}_T \qquad \text{(A1.19)}$$

Tinker then defined an effective area such that

$$\frac{\dot{M}_c}{A_c} = \frac{\dot{M}_T}{A_e} \qquad \text{(A1.20)}$$

and then combining equations A1.19 and A1.20 for the crossflow stream gives

$$A_e = \left(\frac{A_b}{\dot{M}_{rc}}\right) \dot{M}_{ri} \text{ for } i = c,b,s,t \qquad \text{(A1.21)}$$

The crossflow pressure drop is

$$\Delta p_c = n_c \dot{M}_c^2 = n'_c \left(\frac{\dot{M}_c}{A_c}\right)^2 \qquad (A1.22)$$

substituting equation A1.20 into A1.22 gives

$$\Delta p_c = n'_c \left(\frac{\dot{M}_T}{A_e}\right)^2 \qquad (A1.23)$$

The leakage flowrates, $\dot{M}_s$ and $\dot{M}_t$ are obtained by using equation A1.19 for i = s and i = t.

The windowflow flowrate is given by

$$\dot{M}_w = \dot{M}_T - \frac{2}{3}\dot{M}_t - \frac{1}{2}\dot{M}_s \qquad (A1.24)$$

Equation A1.24 arises because Tinker assumes that 25 % of the tube-baffle leakage is effectively in crossflow. Consider equation A1.1 rewritten as

$$\dot{M}_T = (\dot{M}'_c + \frac{1}{4}\dot{M}'_t) + \dot{M}_b + \dot{M}_s + \frac{3}{4}\dot{M}'_t \qquad (A1.25)$$

where $\dot{M}'_c$, $\dot{M}'_t$ are the actual flowrates in crossflow and tube-baffle leakage. The effective flowrates mentioned earlier are then

$$\dot{M}_c = \dot{M}'_c + \frac{1}{4}\dot{M}'_t \qquad (A1.26)$$

$$\dot{M}_t = \frac{3}{4}\dot{M}'_t \qquad (A1.27)$$

From Tinker's model in figure 1.6 of the main text, then it is seen that $\dot{M}_s/2$ and $\dot{M}'_t/2$ flow through either half of the exchanger giving the mass balance through the window as

$$\dot{M}_w = \dot{M}_T - \dot{M}_s/2 - \dot{M}'_t/2 \qquad (A1.28)$$

Substituting equation A1.27 into A1.28 gives equation A1.24.

The windowflow pressure drop can then be evaluated by

$$\Delta p_w = n_w \dot{M}_w^2 \qquad (A1.29)$$

and then finally, the baffle space pressure drop, Δp_p, is obtained by

$$\Delta p_p = \Delta p_c + \Delta p_w \qquad (A1.30)$$

Tinker assumes that the end-spaces are ignored and also, little error is introduced by ignoring the fact that there is one more crossflow zone to a windowflow zone, (i.e. the end-spaces are treated as mid-space crossflow zones) to give the shellside pressure drop as

$$\Delta p_T = (N_B + 1)\Delta p_p \qquad \text{(A1.31)}$$

In Tinker's paper, he states that x is obtained by experience but that it is possible to estimate x form the pressure drops. In fact an iterative solution is possible i.e

1) guess x

2) evaluate the relative flowrates, $\dot{M}_{ri}$, from A1.15 to A1.18

3) evaluate the effective area, A_e , from A1.21

4) evaluate Δp_c from A1.23

5) evaluate $\dot{M}_s$, $\dot{M}_t$ from A1.19

6) evaluate $\dot{M}_w$ from A1.28

7) evaluate Δp_w from A1.29

8) re-evaluate x from A1.2

9) check convergence and repeat from step 2 until achieved.

Actually in Tinker's method , the C values in equations A1.10 to A1.18 were taken to be constants. This means, that in principle, by rearranging these equations even further an analytical solution for the pressure drop should be obtained. The method need only be iterative if the C values, themselves, are a function of flowrate.

Tinker must have realised this, as later he produced a rather simpler non-iterative method described in section 3.3.2 of chapter 3 in the main text.

A1.2 Palen and Taborek (1969)

Palen and Taborek produced the first truly iterative flowstream method, the 'STREAM-ANALYSIS' method in 1969. The method is proprietary to HTRI and has only been published in qualitative form only. The method is strongly based on Tinker's ideas and is truly iterative as flow resistance variation with flowrate is taken into account. In addition to the five streams defined by Tinker, they included an inline pass-partition stream. A schematic of Palen and Taborek's model is given in figure A1.1. The solution is given below . Firstly the pressure drop and mass balances are defined :-

$$\Delta p_p = \Delta p_c + \Delta p_w \tag{A1.32}$$

$$\dot{M}_T = \dot{M}_c + \dot{M}_b + \dot{M}_a + \dot{M}_s + \dot{M}_t \tag{A1.33}$$

$$\dot{M}_w = \dot{M}_T - \dot{M}_s - \dot{M}_t \tag{A1.34}$$

The flow fractions are defined by

$$F_i = \frac{\dot{M}_{ri}}{\sum \dot{M}_{ri}} \qquad , i = a,b,c,s,t \tag{A1.35}$$

The pressure drop in any path may be defined as

$$\Delta p_i = C\, K_i \left(\frac{\dot{M}_i}{A_i}\right)^2 \tag{A1.36}$$

Defining

$$x = \frac{\Delta p_w}{\Delta p_c} \tag{A1.37}$$

then the relative flowrates are given by

$$\dot{M}_{ri} = A_i\, K_i^{\frac{1}{2}} \quad \text{for } i = a,b,c \tag{A1.38}$$

$$\dot{M}_{ri} = A_i\, K_i^{\frac{1}{2}}\, (1 + x)^{\frac{1}{2}} \quad \text{for } i = s,t \tag{A1.39}$$

and finally

$$\dot{M}_i = F_i\, \dot{M}_T \tag{A1.40}$$

As $K_i = f\left(\dot{M}_i\right)$, then the solution is necessarily iterative.

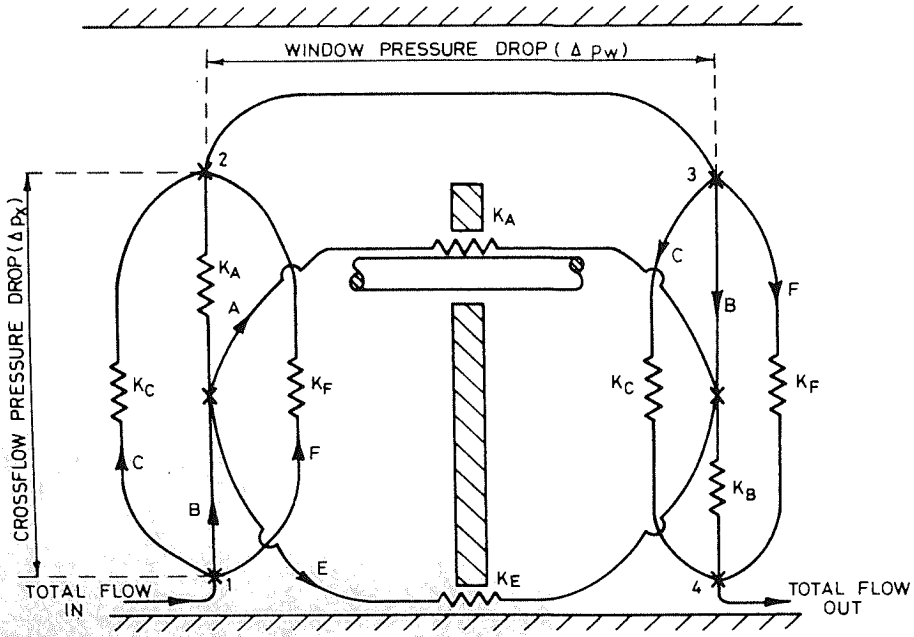

STREAMS		RESISTANCE
A	TUBE/BAFFLE LEAKAGE	(K_A)
B	CROSSFLOW	(K_B)
C	CROSSFLOW-BYPASS	(K_C)
E	SHELL/BAFFLE LEAKAGE	(K_E)
F	PASS PARTITION FLOW	(K_F)

Figure A1.1 : A Schematic of the Palen and Taborek Method

The iteration scheme is then

1) guess x and K_i's.

2) Calculate $\dot{M}_{ri}$'s from A1.38 and A1.39

3) Calculate F_i's from equation A1.35

4) Calculate $\dot{M}_i$'s from equation A1.40

5) Calculate $\dot{M}_w$ from equation A1.34

6) Calculate Δp_c, Δp_w from equation A1.36 (calculating K_w from M_w)

7) re-evaluate x from equation A 1.37

8) check convergence and stop if achieved.

9) Re-evaluate the K values from the relevant equations and continue from step 2.

Palen and Taborek state that the above scheme is fairly quick taking 3-5 iterations for turbulent flow.

A1.3 Grant and Murray (1972)

Grant and Murray produced the 'DIVIDED-FLOW' method for HTFS, recognising that the 'STREAM-ANALYSIS' method of Palne and Taborek was a considerable improvement in shellside pressure drop prediction. Their solution technique differs greatly from the forward substitution method of Palen and Taborek. They define the same streams as Palen and Taborek, as in figure A1.2. The relevant mass balance equations (in terms of flow fractions are

$$F_w = F_b + F_c + F_a \tag{A1.41}$$

$$1 = F_w + F_t + F_s \tag{A1.42}$$

The pressure drop/mass flowrate relationships for each path is defined as

$$\Delta p_i = K_i \frac{\dot{M}_i^2}{2\rho A_i^2} \tag{A1.43}$$

$$\text{As } \dot{M}_i = F_i \dot{M}_T \tag{A1.44}$$

then

$$\Delta p_i = K_i \frac{F_i^2 \dot{M}_T^2}{2\rho A_i^2} \tag{A1.45}$$

For any path the resistance, K_i is a function of flowrate and this is obtained in terms of a Blasius-type relationship

$$K_i = a_i \left(\frac{D_i \dot{M}_T F_i}{A_i}\right)^{b_i} \tag{A1.46}$$

Substituting A1.46 into A1.45 for each stream and rearranging where C_i' is constant
i being any path s, t, c, b, w, a

$$F_s = \left(C_s'(\Delta p_c + \Delta p_w)\right)^{\frac{1}{2-b_s}} \tag{A1.47}$$

$$F_t = \left(C_t'(\Delta p_c + \Delta p_w)\right)^{\frac{1}{2-b_t}} \tag{A1.48}$$

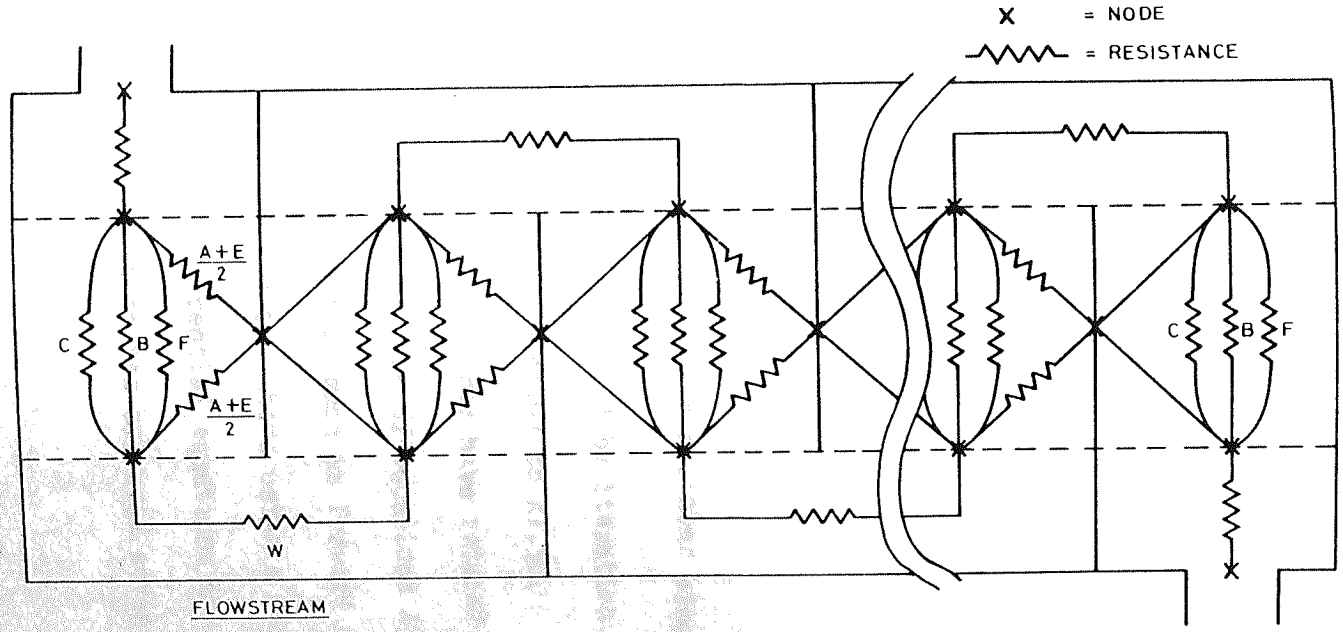

FLOWSTREAM

A = TUBE/BAFFLE LEAKAGE
B = CROSSFLOW
C = CROSSFLOW BYPASS
E = SHELL/BAFFLE LEAKAGE
F = PASS PARTITION FLOW
W = WINDOW FLOW

Figure A1.2 : The Divided-Flow Method of Grant and Murray

$$F_a = (C_a' \Delta p_c)^{\frac{1}{2-b_a}} \quad (A1.49)$$

$$F_b = (C_b' \Delta p_c)^{\frac{1}{2-b_b}} \quad (A1.50)$$

$$F_c = (C_c' \Delta p_c)^{\frac{1}{2-b_c}} \quad (A1.51)$$

$$F_w = (C_w' \Delta p_w)^{\frac{1}{2-b_w}} \quad (A1.52)$$

Equations A1.47 to A1.52 are then substituted into equations A1.41 and 1.42 to give

$$(C_w' \Delta p_w)^{\frac{1}{2-b_w}} = (C_c' \Delta p_c)^{\frac{1}{2-b_c}} + (C_b' \Delta p_c)^{\frac{1}{2-b_b}} + (C_a' \Delta p_c)^{\frac{1}{2-b_a}} \quad (A1.53)$$

$$(C_w' \Delta p_w)^{\frac{1}{2-b_w}} + (C_s'(\Delta p_c + \Delta p_w))^{\frac{1}{2-b_s}} + (C_t'(\Delta p_c + \Delta p_w))^{\frac{1}{2-b_t}} - 1 = 0 \quad (A1.54)$$

Equations A1.53 and A1.54 are non-linear **simultaneous** equations in Δp_c and Δp_w, which can be obtained by iteration. The flowsplits can then be determined using equations A1.47 to A1.52.

Althougth Grant and Murray have reduced the number of equations to be solved to a minimum, the form of equations A1.53 and A1.54 means that a simple iteration technique such as forward substitution cannot be used. Grant and Murray solved the above using a Newton-Raphson type of solution and the resultant differential equations are quite complicated, and as a result it is difficult to see any real advantage in this scheme.

A1.4 Moore (1974)

Moore also developed a multi-stream method for HTFS. Moore aimed to develop a more efficient solution technique than the method of Grant and Murray. The method is proprietary and can only be shown in a qualitative form. A schematic of the method is given in Figure A1.3. Moore did not define a pass-partition lane in his method but did include a windowflow bypass. The main equations are

$$\Delta p_p = \Delta p_c + \Delta p_w \tag{A1.55}$$

$$\dot{M}_T = \dot{M}_c + \dot{M}_b + \dot{M}_s + \dot{M}_t \tag{A1.56}$$

$$\dot{M}_w = \dot{M}_c + \dot{M}_b \tag{A1.57}$$

$$\dot{M}_w = \dot{M}_{w1} + \dot{M}_{w2} \tag{A1.58}$$

$$\dot{M}_{cr} = \dot{M}_c + \dot{M}_b \tag{A1.59}$$

$$\dot{M}_L = \dot{M}_s + \dot{M}_t \tag{A1.60}$$

An effective area is defined for each path such that

$$\Delta p_i = \frac{\dot{M}_i^2}{\rho S_i^2} \tag{A1.61}$$

where

$$S_i = f\{ A_i , \dot{M}_i \} \tag{A1.62}$$

Moore manipulates the equations to obtain

$$\Delta p_p = \frac{\dot{M}_T^2}{\rho S_p^2} \tag{A1.63}$$

where

$$S_p = f\{ S_c , S_b , S_{w1} , S_{w2} , S_s , S_t , N_{ss} , N_c \} \tag{A1.64}$$

where N_{ss} is the number of sealing strips and N_c is the number of rows crossed in crossflow. Moore's method is actually more complicated than the method of Grant and Murray as it includes a model for sealing strips, assuming that all the crossflow and bypass form a single stream in rows with sealing strips.

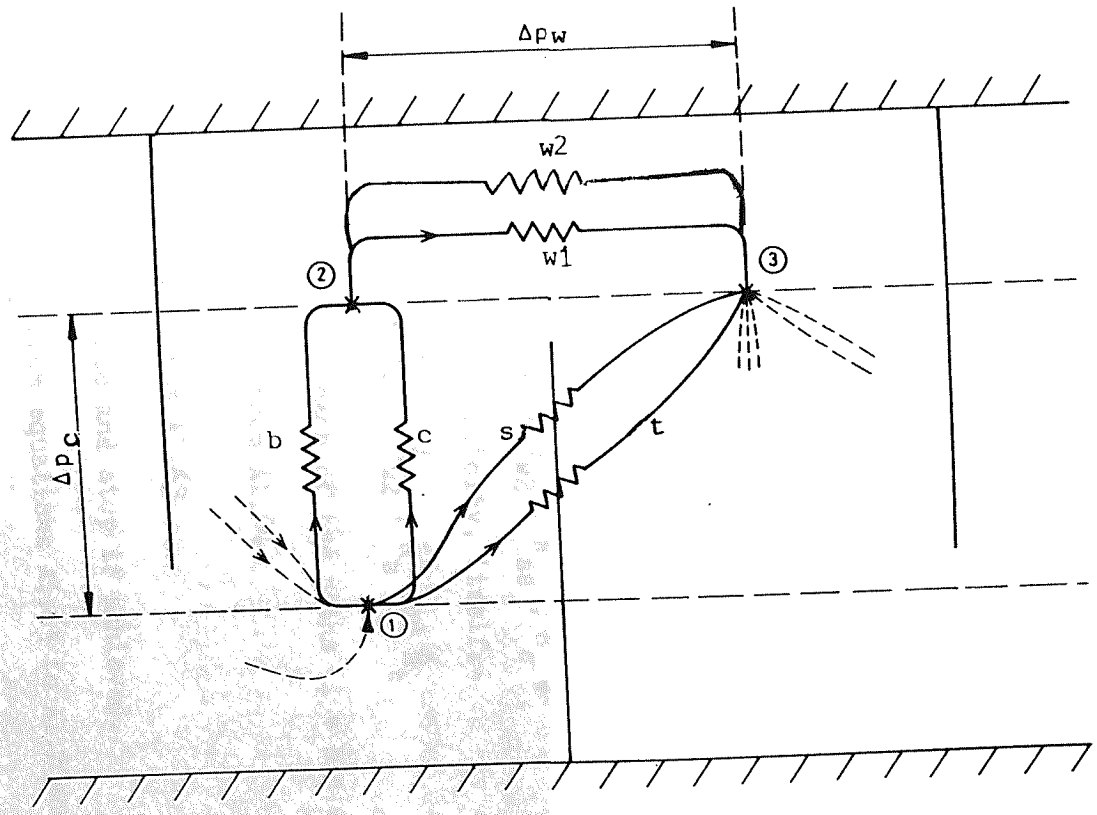

Figure A1.3 : The Moore Method

Finally the flowsplits are calculated by

$$\dot{M}_c = \frac{S_c}{S_p A_m} \left(\frac{S_{w1}+S_{w2}}{S_c + S_b}\right) \dot{M}_T \qquad (A1.65)$$

$$\dot{M}_b = \frac{S_b}{S_p A_m} \left(\frac{S_{w1}+S_{w2}}{S_c + S_b}\right) \dot{M}_T \qquad (A1.66)$$

$$\dot{M}_{w1} = \frac{S_{w1}}{S_p A_m} \dot{M}_T \qquad (A1.67)$$

$$\dot{M}_{w2} = \frac{S_{w2}}{S_p A_m} \dot{M}_T \qquad (A1.68)$$

$$\dot{M}_s = \frac{S_s}{S_p} \dot{M}_T \qquad (A1.69)$$

$$\dot{M}_t = \frac{S_s}{S_p} \dot{M}_T \qquad (A1.70)$$

where

$$A_m = f\left(S_c , S_b , S_{w1} , S_{w2} , N_{ss} , N_c\right) \qquad (A1.71)$$

The iteration scheme is simplicity, itself:-

1) Guess $\dot{M}_c$, $\dot{M}_b$, $\dot{M}_{w1}$, $\dot{M}_{w2}$, $\dot{M}_s$ and $\dot{M}_t$

2) Calculate S_i for each of the paths (i = b,c,w1,w2,s,t) (A1.72)

3) Evaluate A_m , S_p from A1.64

4) Calculate Δp_p from A1.63

5) check convergence and stop if achieved.

6) calculate $\dot{M}_i$ from equations A1.65 to A1.70and continue from step 2.

In fact it is not necessary to calculate Δp_p within the iteration loop, as the convergence check could be made on S_p, evaluating Δp_p at the end.

This solution technique is very fast, taking 3-5 iterations for turbulent flow. Overall, this is the most efficient of the solution methods shown in this appendix, requiring the least number of seperate calculations. As this method is proprietary, Appendix 2 gives a similar solution procedure, designed for hand-calculations

APPENDIX 2: A SIMPLIFIED ITERATION METHOD FOR CALCULATING THE FLOW DISTRIBUTION IN MULTI-STREAM MODELS

In Appendix 1, it is seen that there are as many different iteration techniques, as there are different multi-stream models. These schemes are, in fact, interchangeable because they do not influence the basic pressure drop and mass flowrate relationships. Unfortunately all the schemes (with the exception of the proprietary method of Moore (1974)) are unnecessarily complicated, and are not especially efficient.

A method is presented here which converges on one variable, the window flowrate. The method presented is very fast (usually 3-4 iterations for a difference of less than 1% in the window flowrate). Part of this rapid convergence is due to the scaling method for the initial guess of the flow distribution. Consider a simple multi-stream model as in Figure 3.1 of the main text, consisting of five streams

1) crossflow, (c)
2) bypass, (b)
3) windowflow, (w)
4) shell baffle leakage, and (s)
5) tube/baffle leakage (t)

The following pressure drop and mass flowrate relationships are written

$$\Delta p_p = \Delta p_c + \Delta p_w \qquad (A2.1)$$

$$\dot{M}_{cr} = \dot{M}_c + \dot{M}_b \qquad (A2.2)$$

$$\dot{M}_w = \dot{M}_{cr} \qquad (A2.3)$$

$$\dot{M}_L = \dot{M}_s + \dot{M}_t \qquad (A2.4)$$

$$\dot{M}_T = \dot{M}_w + \dot{M}_L \qquad (A2.5)$$

For any individual flowpath, i, a general pressure drop/mass flowrate relationship is defined as

$$\Delta p_i = n_i \dot{M}_i^2 \qquad (A2.6)$$

where the flow resistance, n_i, is a function of flowrate

$$n_i = f(\dot{M}_i) \qquad (A2.7)$$

Also the pressure drop between any two nodes is constant, regardless of the path taken, and hence

$$\Delta p_c = n_c \dot{M}_c^2 = n_b \dot{M}_b^2 \qquad (A2.8)$$

and

$$\Delta p_p = n_s \dot{M}_s^2 = n_t \dot{M}_t^2 \qquad (A2.9)$$

From Equation A2.2 and A2.8, then

$$\dot{M}_{cr} = (1 + (\frac{n_c}{n_b})^{\frac{1}{2}})\ \dot{M}_c \qquad (A2.10)$$

Using Equation A2.3. and rearranging gives

$$\dot{M}_c = \frac{n_b^{\frac{1}{2}}}{n_b^{\frac{1}{2}} + n_c^{\frac{1}{2}}}\ \dot{M}_w \qquad (A2.11)$$

Substituting A2.11 into A2.8 gives

$$\Delta p_c = n_c\ (\frac{n_b^{\frac{1}{2}}}{n_c^{\frac{1}{2}} + n_b^{\frac{1}{2}}})^2\ \dot{M}_w^2 \qquad (A2.12)$$

which is identical to

$$\Delta p_c = (n_c^{-\frac{1}{2}} + n_b^{-\frac{1}{2}})^{-2}\ \dot{M}_w^2 \qquad (A2.13)$$

Similarly solutions of Equations A2.4, A2.5 and A2.9 gives

$$\Delta p_p = (n_s^{-\frac{1}{2}} + n_t^{-\frac{1}{2}})^{-2}\ (\dot{M}_T - \dot{M}_w)^2 \qquad (A2.14)$$

As

$$\Delta p_w = n_w\ \dot{M}_w^2 \qquad (A2.15)$$

then substituting Equations A2.13, A2.14 and A2.15 into A2.1 gives

$$(n_s^{-\frac{1}{2}} + n_t^{-\frac{1}{2}})^{-2}(\dot{M}_T - \dot{M}_w)^2 = (n_c^{-\frac{1}{2}} + n_b^{-\frac{1}{2}})^{-2}\dot{M}_w^2 + n_w \dot{M}_w^2 \qquad (A2.16)$$

rearranging and isolating $\dot{M}_w$ gives

$$\dot{M}_w = \frac{\dot{M}_T}{1 + (n_s^{-\frac{1}{2}} + n_t^{-\frac{1}{2}})((n_c^{-\frac{1}{2}} + n_b^{-\frac{1}{2}})^{-2} + n_w)^{\frac{1}{2}}} \qquad (A2.17)$$

Having isolated $\dot{M}_w$ in terms of the total flowrate only and the five stream resistances, it is easy to set up a simple iteration scheme for obtaining the flow distribution and pressure drop.

Iteration Scheme

For any individual flow path define a flow fraction F_i, such that

$$\dot{M}_i = F_i \dot{M}_T \qquad \text{(A2.18)}$$

Equation A3.7 can usually be expressed in the form

$$n_i = C_i a \dot{M}_i^b \qquad \text{(A2.19)}$$

which leads to

$$n_i = C_i a \dot{M}_T^b F_i^b \qquad \text{(A2.20)}$$

A good first estimate is obtained for the flow resistance, n_i, for each path by assuming $F_i = 0.25$ for i = b, c, s, t and $F_i = 0.5$ for i = w in Equation A2.20.

Having obtained five reasonable values for the resistances, Equation A2.17 is used to obtain $\dot{M}_w$. The pressure drops (Δp_w, Δp_c, Δp_p) are obtained using Equations A2.15. A2.13 and A2.1 respectively.

The new flowsplits are then calculated by

$$\dot{M}_c = \left(\frac{\Delta p_c}{n_c}\right)^{\frac{1}{2}} \qquad \text{(A2.21)}$$

$$\dot{M}_b = \left(\frac{\Delta p_c}{n_b}\right)^{\frac{1}{2}} \qquad \text{(A2.22)}$$

$$\dot{M}_s = \left(\frac{\Delta p_p}{n_s}\right)^{\frac{1}{2}} \qquad \text{(A2.23)}$$

and finally

$$\dot{M}_t = \dot{M}_T - \dot{M}_w - \dot{M}_s \qquad \text{(A2.24)}$$

The process is then repeated using the new flowsplit to re-evaluate the resistances until convergence of $\dot{M}_w$ is achieved.

As a point of interest, it can be seen that the flow resistance, n_i, is largely insensitive to $\dot{M}_i$ for any stream i ($i = s, t, b, w, a$) except the crossflow, opening up the possibility of a hand-calculation because only n_c needs to be re-evaluated; n_w, n_s, n_t, n_w remaining constant. In this case, only Equations A2.1, A2.13, A2.15, A2.17, A2.20 and A2.22 are needed all of which are very simple expressions to evaluate. In fact, this method has been used by Wills and Johnston (1984), ESDU (1983) in a simplified hand calculation method. However, the iteration scheme is flexible enough to be able to allow for the variation of the resistance with flow in up to all of the five streams.

If the above analysis is repeated for laminar flow assuming

$$\Delta p_i = n_i \dot{M}_i \qquad \text{(A2.26)}$$

then the following will be obtained

$$\dot{M}_w = \frac{\dot{M}_T}{1 + (n_s^{-1} + n_t^{-1})(n_c^{-1} + n_b^{-1}) + n_w)^{-1}} \qquad \text{(A2.27)}$$

which is the laminar solution. As n_i is virtually constant for laminar flow ($\Delta p_i \propto \dot{M}_i$) then Equation A2.27 can be solved with little or no iteration.

APPENDIX 3 : THE CALCULATION OF BYPASS FRICTION FACTORS

There are no data on bypass friction factors available either in the literature* or, as far as is known, even in proprietary research. Bypass friction factors have been calculated by inference from data obtained from tube-banks with and without bypassing present.

The ideal tube-bank data is used to establish a crossflow relationship

e.g. $$\Delta p_c = K_c \frac{\dot{M}_c^2}{2 \rho A_c^2} \quad \text{where } \Delta p_c \text{ , } \dot{M}_c \text{ are obtained experimentally} \qquad (A3.1)$$

The tube-bank with bypassing is treated as a parallel resistance network, and the bypass pressure drop is given by (as $\Delta p_c = \Delta p_b$),

$$\Delta p_c = K_b \frac{\dot{M}_b^2}{2 \rho A_b^2} \qquad (A3.2)$$

Since M_b is not known, but the total flowrate ($\dot{M}_{cr}$) is known (as is Δp_c)

and $$\dot{M}_{cr} = \dot{M}_c + \dot{M}_b \qquad (A3.3)$$

then using Equation A3.1, it is possible to estimate the crossflow flowrate for the exchanger with bypassing, and hence the bypass flowrate.

A suitable definition for the bypass friction factor is defined as the usual form,

$$K_b = 4 f_b N_b \qquad (A3.4)$$

which combined with a suitable Reynolds number definition,

$$Re_b = f (\dot{M}_b) \qquad (A3.5)$$

leads to a bypass friction factor relationship

* At the time of writing this thesis, data have become available from Lee(1983)

APPENDIX 4: NUMERICAL SOLUTION PROCEDURE FOR CROSSFLOW/LEAKAGE INTERACTION

The resistance equation (Equation 4.22) is

$$\bar{R}_x = \frac{m\int_0^{L_B}\left(\frac{\Delta p_c}{\eta \bar{R}_x L}\left(1-\exp\left(\frac{-\varepsilon\eta\bar{R}_{xy}}{\rho v}\right)\right)\right)^n dy}{\int_0^{L_B} dy} \qquad (A4.1)$$

let $A = \frac{\rho v}{\varepsilon \eta \bar{R}_x}$, $B = \frac{\Delta p_c}{\eta \bar{R}_x L}$

i.e. $$\bar{R}_x = \frac{m B^n}{L_B}\int_0^{L_B}\left(1-\exp\left(\frac{-y}{A}\right)\right)^n dy \qquad (A4.2)$$

let $x = \exp(-y/A)$

The maximum value of x is 1 when $y = 0$

and the minimum is $x = 0$, when $y/A \to \infty$

Hence $|x|<1$ Substituting for gives

$$\bar{R}_x = \frac{m B^n}{L_B}\int_0^{L_B}(1-x)^n dy \qquad (A4.3)$$

Expanding equation A4.3 by the binomial theorem ie.

$$(1-x)^n = 1 - \frac{n}{1!}x + \frac{n(n-1)}{2!}x^2 - \frac{n(n-1)(n-2)}{3!}x^3 + \cdots \quad (A4.4)$$

hence

$$\frac{\overline{R_x}\, L_B}{m B^n} = \int_0^{L_B} \left(1 - \frac{n}{1!}\left(\exp\left(\frac{-y}{A}\right)\right) + \frac{n(n-1)}{2!}\left(\exp\left(\frac{-y}{A}\right)\right)^2 - \frac{n(n-1)(n-2)}{3!}\left(\exp\left(\frac{-y}{A}\right)\right)^3 + \cdots\right) dy \quad (A4.5)$$

but

$$\left(\exp\left(-\frac{y}{A}\right)\right)^2 = \exp\left(\frac{-2y}{A}\right) \quad (A4.6)$$

and the expression

$n(n-1)(n-2)\cdots(n-i)$ can be written in

mathematical notation as

$$n(n-1)(n-2)(n-3)\cdots(n-i) = \prod_{j=0}^{j=i}(n-j) \quad (A4.7)$$

hence

$$\frac{\overline{R_x}\, L_B}{m B^n} = \int_0^{L_B} \left(1 - \frac{\prod_{j=0}^{j=0}(n-j)}{1!}\exp\left(-\frac{y}{A}\right) + \frac{\prod_{j=0}^{j=1}(n-j)\exp\left(\frac{-2y}{A}\right)}{2!} - \frac{\prod_{j=0}^{j=2}(n-j)\exp\left(\frac{-3y}{A}\right)}{3!} + \cdots\right) dy \quad (A4.8)$$

Equation A4.8 may be expressed more concisely as:

$$\frac{\bar{R}_x L_B}{m B^n} = \int_0^{L_B} dy + \int_0^{L_B} \sum_{i=1}^{i=\infty} \left(\frac{(-1)^i \left(\prod_{j=0}^{j=i} (n-j) \right) \exp\left(\frac{-iy}{A}\right)}{i!} \right) dy \qquad (A4.9)$$

integrating

$$\frac{\bar{R}_x L_B}{m B^n} = L_B - \left[\sum_{i=1}^{i=\infty} \left(\frac{(-1)^i \left(\prod_{j=0}^{j=i} (n-j) \right) A \exp\left(\frac{-iy}{A}\right)}{i \cdot i!} \right) \right]_0^{L_B} \qquad (A4.10)$$

evaluating between limits

$$\frac{\bar{R}_x L_B}{m B^n} = L_B - A \sum_{i=1}^{i=\infty} \left((-1)^i \frac{\left(\prod_{j=0}^{j=i} (n-j) \right)}{i \cdot i!} \left(\exp\left(\frac{-i L_B}{A}\right) - 1 \right) \right) \qquad (A4.11)$$

hence

$$\frac{\bar{R}_x L_B}{m B^n} = L_B - \frac{\rho V}{\varepsilon \eta \bar{R}_x} \left(\sum_{i=1}^{i=\infty} \frac{(-1)^i \left(\prod_{j=0}^{j=i} (n-j) \right)}{i \cdot i!} \left(\exp\left(\frac{-\varepsilon \eta \bar{R}_x L_B}{\rho V}\right) - 1 \right) \right) \qquad (A4.12)$$

From equation 4.16 the pressure drop is defined as:

$$\Delta p_c = \frac{\eta \bar{u} \bar{R}_x L}{1 - \frac{\rho V}{\varepsilon \eta \bar{R}_x L_B} \left(1 - \exp\left(\frac{-\varepsilon \eta \bar{R}_x L_B}{\rho V}\right) \right)} \qquad (A4.13)$$

The required solution procedure is very lengthy as an iterative solution is required using both equations A4.12 and A4.13 i.e.

1) guess $\bar{R}_x$,

2) evaluate $\bar{R}_x$ from A4.12 (taking sufficient terms in the infinite series for accuracry.

3) Substitute new value of $\bar{R}_x$ into equation A4.13 to evaluate a new Δp_c .

4) repeat steps 2 and 3 with new values of $\bar{R}_x$, until convergence is achieved.

In practice, this solution procedure is sufficiently lengthy to be unsuitable for use as a design procedure.

REFERENCES

BELL, K. J. (1958)
See Bergelin et al (1958).

BELL, K. J. and Fusco (1958)
See Bergelin et al (1958).

BELL, K. J. (1960)
"Exchanger Design", Petro/Chem. Engineer, vol. 32,pp.C-26 - C-40, October.

BELL, K. J. (1963)
"Final Report of the Cooperative Research Program on Shell and Tube Heat Exchangers", University of Delaware, Engineering Experimental Station, Bulletin No. 5, June.

BERGELIN, O.P., Brown, G.A., Colburn, A.P. (1954)
"Heat Transfer and Fluid Friction During Flow Across Banks of Tubes - V ," A Study of a Cylindrical Baffled Exchanger Without Internal Leakage", Transactions of the American Society of Mechanical Engineers, vol. 76, pp. 841-855, July.

BERGELIN, O.P., Leighton, M.D., Lafferty, W.L. and Pigford, R.L. (1958)
"Heat Transfer and Pressure Drop During Viscous and Turbulent Flow Across Baffled and Unbaffled Tube Banks",University of Delaware, Engineering Experimental Station, Bulletin No. 4, April.

BOUCHER D.F. and LAPPLE C.E. (1948)
"Critical Comparison of Available Data and of Proposed Methods of Correlation, Chemical Engineering Progress, vol. 44, No. 2, February.

BROWN, G.A. (1956)
"Heat Transfer and Fluid Friction During Turbulent Flow Through a Baffled Shell-and-Tube Heat Exchanger", Ph.D Thesis, University of Delaware.

BUTHOD, A.P. (1960)
"How to Estimate Heat Exchangers", Oil and Gas Journal, 58, pp.67 - 82.

BUTTERWORTH, D. (1977)
"The Development of a Model for Three-Dimensional Flow in Tube Bundles", International Journal of Heat and Mass Transfer, vol. 21, pp.253 -256.

BUTTERWORTH, D. (1979)
"The Correlation of Crossflow Pressure Drop by Means of The Permeability Concept", U.K.A.E.A. Harwell report, A.E.R.E. - R.9435.

COULSON, J.M. and RICHARDSON, J. F. (1970)
"Chemical Engineering", vol. 1, Permagon Press, Oxford, 2nd. edition.

DONOHUE, D. A. (1949)
"Heat Transfer and Pressure Drop in Heat Exchangers", Industrial Engineering and Chemistry, vol.41, No. 11, pp.2499 - 2511 November.

E.S.D.U. (1979)
"Crossflow Pressure Loss Over Banks of Plain Tubes in Square and Triangular Arrays Including Effects of Flow Direction", Engineering Sciences Data Unit, Item No. 79034.,
251 - 259 Regent Street, London

E.S.D.U. (1983)
"Baffled Shell-and-Tube Heat Exchangers: Flow distribution pressure drop and heat transfer coefficient on the shellside", Engineering Sciences Data Unit, Item no. 83038,
251 - 159 Regent Street, London.

GRANT I. D. R. and MURRAY I. (1972)
Private Communication.

GRIMISON, E. D. (1937)
"Correlation and Utilisation of New Data on Flow Resistance and Heat Transfer for Cross-Flow of Gases Over Tube Banks",
Transactions of the American Society of Mechanical Engineers, vol. 59, No. 7,
pp.583-594.

HEDH (1983)
"Shell— and —Tube Heat Exchangers", Chapter 3,
The Heat Exchanger Design Handbook,
Hemisphere Publishing Corporation,
Washington D.C.

HOLLAND, F. A. (1973)
"Fluid Flow for Chemical Engineers",
Edward Arnold, 1st edition.

HOLZMAN
See Bergelin et al (1958).

ISHIGAI, S., NISHIKAWA, E., NAKAYAMA, Y. and FUKUDA, Y. (1967)
"Shellside Pressure Drop in Multi-Baffled Shell-and Tube Heat Exchangers", Japan Shipbuilding and Marine Engineering, vol. 2, No. 1. pp.29-35.

KERN, D. Q. (1950)
Process Heat Transfer, McGraw-Hill, London.

LEE, N. (1983)
Private Communication.

MACBETH, R. V. (1973)
Private Communication.

MOORE, M. J. C. (1974, 1979)
Private Communication.

NATIONAL ENGINEERING LABORATORY (1980)
Private Communication.

PALEN, J. W. and TABOREK, J. (1969)
"Solution of Shellside Flow Pressure Drop and Heat Transfer by Stream-Analysis Method", Chemical Engineering Progress Symposium Series, vol. 65, No. 92, pp.53 - 63.

PARKER, R.O., and MOK, Y. I. (1968)
"Shell-side Pressure Loss In Baffled Heat Exchangers",
British Chemical Engineering, vol. 3, pp.366-368, March.

PERRY, J.H. and CHILTON, C.H. (1963)
"Chemical Engineers Handbook", McGraw-Hill,
New York, 4th edition.

ROSENHOW, W.M. and HARTNETT (1973
"Handbook of Heat Transfer", McGraw-Hill,
New York, pp. 18 - 40 - 18 - 55.

RUSSELL and WILLS (1983)
Private Communication.

SHORT, B.E. (1947)
"The Effect of Baffle Height and Baffle Clearance on Heat Transfer and Pressure Drop in Heat Exchangers", Transactions of the American Society of Mechanical Engineers, no. 47 - A - 105.

SMALL, Y.M. and YOUNG, R.K. (1979)
"The ROD baffle Heat Exchanger", Heat Transfer Engineering, vol. 1. no. 2.

T.E.M.A. (1958)
Standards of Tubular Exchangers Manufacturers Association, 5th edition, New York, Tubular Exchangers Manufacturers Association Inc.

TABOREK, J.M. (1983)
SEE HEDH (1983)

TINKER, T. (1948)
"Shellside Characteristics of Shell and Tube Heat Exchangers", Transactions of the American Society of Mechanical Engineers, pp. 89 - 116.

TINKER, T. (1951)
"Shellside Characteristics of Shell-and Tube Heat Exchangers", Institution of Mechanical Engineers, "Proceedings of General Discussion on Heat Transfer", pp. 36 - 49, 11th - 13th Sept, London.

TINKER, T. (1958)
"Shellside Characteristics of Shell-and Tube Heat Exchangers - A Simplified Rating System for Commercial Heat Exchangers", Transactions of the American Society of Mechanical Engineers, January.

WHITLEY, D.L. (1961)
"Calculating Heat Exchanger Shellside Pressure Drop", Chemical Engineering Progress, vol.57 no. 9, September.

WILLIAMS, R.B. and KATZ, D. L. (1952)
"Performance of Finned Tubes in Shell-and Tube Heat Exchangers, Transactions of the American Society of Mechanical Engineers, vol. 74, pp.1307 - 1320.

WILLS, M. J. N. and JOHNSTON, D. (1984)
"A New and Accurate Hand-Calculation Method for Shellside Pressure Drop and Flow Distribution" to be presented at the 22nd ASME/AICHE National Heat Transfer Conference, August.

WILSON, R. E., McADAMS, W. H., and SELTZER, M. (1922)
Industrial Engineering and Chemistry, vol. 14, pp. 105 - 119.